T.C.
ISTANBUL UNIVERSITY-CERRAHPASA
INSTITUTE OF GRADUATE STUDIES

M.Sc. THESIS

INFLUENCE OF EQUIVALENT LINEAR MODELING OF SEISMIC ISOLATION SYSTEMS ON THE SEISMIC RESPONSE OF BUILDING CONTENTS

Mohamud Muhumed OSMAN

SUPERVISOR
Prof. Dr. Cenk ALHAN

Department of Civil Engineering

Civil Engineering Programme

ISTANBUL November, 2020

This study was accepted on 5/11/2020 as a M. Sc. thesis in Department of Civil Engineering, Civil Engineering Programme by the following Committee.

Examining Committee Members

Prof. Dr. Cenk ALHAN(Supervisor)
İstanbul University-Cerrahpaşa
Faculty of Engineering

Prof. Dr. Name SURNAME
UniversityUniversity
Faculty of Engineering

Assoc. Prof. Dr. Name SURNAME
UniversityUniversity
Faculty of Engineering

Assoc. Prof. Dr. Name SURNAME
UniversityUniversity
Faculty

Prof. Dr. Name SURNAME
UniversityUniversity
Faculty

As required by the 9/2 and 22/2 articles of the Graduate Education Regulation which was published in the Official Gazette on 20.04.2016, this graduate thesis is reported as in accordance with criteria determined by the Institute of Graduate Studies by using the plagiarism software to which Istanbul University-Cerrahpasa is a subscriber.

FOREWORD

I would like to extend my sincere thanks and appreciation to my supervisor Prof. Dr. Cenk Alhan for his guidance throughout my thesis. His invaluable feedback and support helped me to structure and improve this thesis.

I am thankful to my family for their encouragement and constant support. Special thanks to my mother Halima Sheikh Abdi for her constant believe in me and support and my father Muhumed Osman who worked hard tirelessly to give me opportunities that he couldn't dream of himself.

I would like to also thank my brother Hassan Osman for cheering me all along my academic journey.

November 2020 Mohamud Muhumed OSMAN

TABLE OF CONTENTS

Page

LIST OF FIGURES

Page

LIST OF TABLES

Page

LIST OF SYMBOLS AND ABBREVIATIONS

Symbol	Explanation
α	: Post to pre-yield stifness ratio
a	: Acceleration
a_g	: Ground acceleration
β_{eff}	: Effective viscous damping ratio
C_{eff}	: Effective viscous damping coefficient
c_{eff}	: Effective viscous damping coefficient per isolator
D	: Peak Isolation system displacement
D_y	: Yield displacement
F_y	: Yield force
f_y	: Yield force per isolator
g	: Gravitational acceleration
K_1	: Pre-yield stifness
K_2	: Post yield stiffness
K_{eff}	: Effective stiffness of the isolation system
k_{eff}	: Effective stiffness of the isolation system per isolator
kN	: Kilo Newton
M	: Mass
M_s	: Total mass of superstructure
M_W	: Earthquake magnitude
Q	: Characteristic force
q	: Yield displacement
Q/W	: Characteristic force weight ratio
R_{rup}	: Rupture distance
T	: Natural frequency
T_0	: Isolation system period
W	: Weight
ω_{eff}	: Effective angular frequency
T_{eff}	: Effective isolation system period

Abbreviation	Explanation
FPS	: Friction Pendulum System
FREI	: Fiber Reinforced Elastomeric Isolator
HDRB	: High Damped Rubber Bearing
LDRB	: Low Damped Rubber Bearing
LRB	: Lead-Rubber Bearing
PEER	: Pacific Earthquake Engineering Research Centre
PGA	: Peak Ground Acceleration
PGD	: Peak Ground Displacement
PGV	: Peak Ground Velocity
SREI	: Steel Reinforced Elastomeric Isolator
USC	: University of South California
NPP	: Nuclear Power Plant

ÖZET

YÜKSEK LİSANS TEZİYÜKSEK LİSANS TEZİ

SİSMİK İZOLASYON SİSTEMLERİNİN EŞDEĞER DOĞRUSAL MODELLENMESİNİN BİNA İÇERİKLERİNİN SİSMİK TEPKİLERİNE ETKİSİ

Mohamud Muhumed OSMAN

İstanbul Üniversitesi-Cerrahpasa

Lisansüstü Eğitim Enstitüsü

İnşaat Mühendisliği Anabilim Dalı

Danışman: Prof. Dr. Cenk ALHAN

Sismik izolasyon sistemlerinde kullanılan izolatörlerin davranışları, doğaları gereği doğrusal olmayan (Nonlineer) davranıştır. Ancak, yapısal analizlerde kolaylık sağlaması bakımından bu izolatörler uygun formülasyonlarla eşdeğer doğrusal özellikler elde edilmek suretiyle doğrusal olarak modellenebilirler. Bu sayede doğrusal analizler gerçekleştirilebilir ve bu da kolaylık sağlar. Ancak, eşdeğer doğrusal modelleme ve doğrusal analiz ile elde edilen yapısal tepkilerin doğrusal olmayan modelleme ve doğrusal olmayan analiz ile elde edilen yapısal tepkilerden farklılıklar içerdiği önceki çalışmalarda ortaya konmuştur. Öte yandan, özellikle sismik izolasyonlu yapıların içerisinde yer alan nesnelerin çoğu titreşime hassas kritik ekipman olup bu nesnelerin deprem güvenliği en az yapısal güvenlik kadar önemlidir. Dolayısıyla, yapının taban seviyesinde yer alan izolatörlerin eşdeğer doğrusal modellenmesi ve doğrusal analizler yapılması sonucunda bu ekipmanın sismik tepkilerinin doğrusal olmayan modelleme ve analizlere kıyasla nasıl değiştiğinin incelenmesi de büyük önem taşımaktadır. Bu tezin amacı, bu tür kritik ekipmanların hesaplanan sismik tepkilerinin yapıya ait izolasyon sisteminde yer alan izolatörlerin eşdeğer modellemesine bağlı olarak gerçek durumdan ne kadar saptığının belirlenmesidir.

Kasım 2020, 125. sayfa.

Anahtar kelimeler: Sismik İzolasyon, Zaman Tanım Alanı Analizi, Deprem Analizi

SUMMARY

M.Sc. THESIS

INFLUENCE OF EQUIVALENT LINEAR MODELING OF SEISMIC ISOLATION SYSTEMS ON THE SEISMIC RESPONSE OF BUILDING CONTENTS

Mohamud Muhumed OSMAN

Istanbul University-Cerrahpasa

Institute of Graduate Studies

Department of Civil Engineering

Supervisor: Prof. Dr. Cenk ALHAN

The behaviour of isolators used in seismic isolation systems is nonlinear by nature. However, for the convenience of structural analysis, these isolators can be linearly modelled by obtaining equivalent linear properties with appropriate formulations. In this way, linear analysis can be performed, which provides convenience. However, it has been demonstrated in previous studies that structural responses obtained by equivalent linear modelling and linear analysis differ from structural responses obtained by nonlinear modelling and nonlinear analysis. On the other hand, most of the contents in seismic isolated structures are critical equipment sensitive to vibration and earthquake safety of these contents is at least as important as structural safety. Therefore, it is of great importance to examine how the seismic responses of this equipment located at the floor level of the building change compared to nonlinear modelling and analysis as a result of equivalent linear modelling and linear analysis of the isolators. The aim of this thesis is to determine how much the calculated seismic responses of such critical equipment deviate from

the real situation due to the equivalent modelling of the isolators in the isolation system of the building.

November 2020, 125 pages.

Keywords: Seismic Isolation, Time History Analysis, Earthquake Engineering

1. INTRODUCTION

Every year across the world we face many types of natural disasters. Earthquake is one of these disasters and it has potential to cause considerable damage leading to severe social economic impact. The massive damaging potential of the earthquake can also cause major damage to structures and contents of the structures. There is approximately 11000 death reported every year due to earthquakes. Apart from the loss of life there is also impact on the economy of countries due to damage on properties (Saifullah and Alhan, 2017).

For instance, on 12th May 2008, China experienced Wenchuan earthquake with a magnitude of 7.9 on the eastern edge of Tibetan Plateau which resulted in more than 17,000 deaths, 374,643 injuries and many buildings were destroyed (Parsons, Ji and Kirby, 2008; (Chigira *et al.*, 2010). On January 12, 2010, Haiti experienced the largest earthquake ever recorded in the country and left parts of the country devastated. The earthquake had a 7.0 magnitude and cantered 15 miles southwest of Port-au- Prince which left according to experts $8 to $14 billion in damage. 3 million people (approximately one-third of the population) was affected. According to the government reports, 230,000 people died while 300,600 injured. Almost all structures in the country have been damaged or collapsed (Margesson and Taft-Morales, 2011).

Engineers are working hard to come up with solutions to prevent or keep the impact of the earthquake to the minimum. The main challenge for structural engineers is to reduce the impact of earthquakes on buildings. One of the effective ways of protecting structures from earthquake effect and obtaining desired performance is to reduce the seismic demand on the system (Chimamphant and Kasai, 2016).

Conventionally, seismic impact design approach was based on increasing the strength or ductility of the building. This leads to increase in stiffness of the structure resulting in higher floor accelerations, which causes damage to building contents. Past earthquakes have shown that structures collapse or become dysfunctional when the ductility capacity of the structure is consumed. Even in the case where the building has been designed with more strength and ductility, the vibration sensitive equipment in the structure may loose function due to high accelerations. In order to keep such equipment functional even after an earthquake, engineers have adopted an alternative approach called seismic isolation (Buckle and Mayes, 1990).

The aim of seismic isolation is to reduce seismic demand rather than increasing the capacity of the structure. In seismically base-isolated systems, the superstructure is decoupled from the earthquake ground motion by introducing a flexible interface between the foundation and the base of structure. Since earthquakes generally contain low period or high frequency waves, the isolation system increases the dominant period of the structure in order to decouple it from ground dominant shaking period and thereby protect the structure from heavy damage. During an earthquake, an isolation system makes large displacements and spends earthquake energy through damping resulting in reduced floor accelerations and relative floor displacements in the superstructure, thus preserves structural integrity (Alhan and Sürmeli, 2011).

The seismic isolation method is one of the practical ways to simultaneously reduce relative floor displacements and floor accelerations. A seismic isolated structure has the necessary flexibility to reduce floor accelerations with the isolation system, in which large displacements are focused; it also reduces relative floor displacements of the superstructure, which moves in an almost rigid manner. In the event of an earthquake, a structure with seismic isolation system produces substantially smaller accelerations and deformations when compared with structures that use other systems. Hence the seismic isolation system better protects the non-structural components and essential contents of the structure (Gandelli *et al.*, 2018).

This ability to protect building content from damage resulted in increased usage of seismic isolators in important buildings that are required to be functional after an earthquake or contain expensive equipment that are sensitive to vibration. While the study of seismic isolation has been overwhelmingly focused on the isolated structures, less attention has been paid to the seismic performance of non-structural components such as the building contents which cost more than 80% of the cost of the structure itself (Taghavi and Miranda, 2003).This is despite reports of damage to non-structural components in the past earthquakes that led to substantial economic loss (Miranda *et al.*, 2012).

On the other hand, the study of the modelling and analysis of isolation systems has been an important subject for some time. While the isolation system naturally exhibits nonlinear behaviour, they can be modelled linearly using an equivalent linear model via use of effective stiffness and effective damping. Previous studies conducted on the suitability of using equivalent linear model and analysis instead of the more accurate nonlinear model and analysis and have shown discrepancies (Dicleli and Buddaram, 2007; Mavronicola and Komodromos,

2011; Liu *et al.*, 2014; Alhan and Ozgur, 2015). However, these studies were limited to only the behaviour of the isolated structure and little focus was given to the structural contents such as the important equipment located within the structure. It is therefore equally important to study the accuracy of adopting equivalent linear modelling and analysis of the isolation system by investigating the response of the content of the structure.

1.1. OBJECTIVE OF STUDY

It has been demonstrated in previous studies that structural responses obtained by equivalent linear modelling of isolators and linear analysis differ from structural responses obtained by nonlinear modelling and nonlinear analysis (Dicleli and Buddaram, 2007; Mavronicola and Komodromos, 2011; Liu *et al.*, 2014; Alhan and Ozgur, 2015). On the other hand, most of the objects in seismic isolated structures are critical equipment sensitive to vibration and earthquake safety of these objects is at least as important as structural safety. Therefore, the aim of this thesis is to determine how much the calculated seismic responses of such critical equipment deviate from the realistic situation of nonlinear modelling and nonlinear analysis due to the equivalent modelling of the isolators in the isolation system of the building and linear analysis.

1.2. SCOPE AND STRUCTURE OF STUDY

Within the scope of this thesis, prototype seismic isolated buildings are analysed first by nonlinear modelling of isolators and nonlinear time history analysis and all the floor acceleration time history responses are obtained. The same process is repeated by modelling the isolation system as an equivalent linear one and analysing the model by linear time history analysis method. The floor acceleration time histories obtained for both equivalent linear and nonlinear cases are then applied at the base of different racks with different periods that are assumed to house vibration sensitive contents and located at floors of the base-isolated benchmark buildings. Racks are modelled independently by assuming that coupling between racks and the building are negligible. Time history responses of these racks are finally compared for both equivalent linear and nonlinear cases. Historical earthquake records are used in the analyses. Isolation systems with different isolation characteristics are taken into account.

2. GENERAL PARTS

2.1. LITERATURE REVIEW

The usage of seismic isolation as a solution to protect structures and their contents located in earthquake prone areas from the impact of earthquakes was first proposed in 1909 and has developed since then into important industry (Markou, Oliveto and Athanasiou, 2016). In 1969 the first rubber isolated reinforced concrete building was designed by a Swiss engineer in Skopje former Yugoslavia. At that time, reinforced rubber bearing was not common and instead nonreinforced rubber was used which was not only exhibiting same vertical and horizontal rigidity but also had characteristic of bouncing under force (Garevski, 2012).

The modern concept of seismic isolation first emerged in New Zealand in the early 1970s and used in bridges and buildings. At the time, the technology was essentially limited to buildings with special functional requirement and historic significance. (Mayes, Brown and Pietra, 2012). In Japan, which is one of the earthquake prone countries, the application of seismic isolation didn't start until 1980s. The first seismically isolated building was completed in 1983. The application of seismic isolation has since developed after two isolated buildings exhibited excellent behaviour during the Kobe earthquake of 1995. Similar behaviour was observed during the subsequent earthquakes in Japan for all isolated buildings (Martelli *et al.*, 2014).

During the 1994 Northridge earthquake, the seismically isolated USC (University of South California) University Hospital performed very well. According to the sensor records obtained in the aftermath of the earthquake, it was observed that the isolation system was able to reduce the accelerations by half and filtered the high frequency waves. While the hospital was left undamaged after the earthquake, another hospital on the USC Medical Campus faced severe structural damage that led to the evacuation of the hospital occupants and subsequently was destroyed. Also, a nearby fixed based steel structure building that served as a pharmacy was damaged (Nagarajaiah and Erazo, 2016).

In Turkey, seismic isolation was first used in Adana-Tarsus-Gaziantep Highway Project at the Ataturk viaduct. It was later on used in Bolu mountain viaducts and at Atatürk airport International Terminal where isolators were placed at the column connections with the roof of the Terminal Building. Antalya and Sabiha Gökçen Airports are the other examples where the

technology was applied in Turkey. In addition to airports and viaducts, seismic isolation technic was used in strengthening Trabya hotel, Kocaeli University Medical Faculty Hospital and Erzurum State Hospital; Seismic isolation system has been also used in the liquid natural gas depots in Ankara Metropolitan (Erişgen, 2010).

Seismic isolation further became popular in Turkey following the 2013 technical Memorandum of Ministry of health that obliged the design of hospitals with capacity of 100 and more and are located in the first and second seismic zone as seismic isolated. Numerous hospital buildings have been recently designed and constructed with seismic isolation (Özdemir, 2016). According to the Memorandum, there is no project-specific or site-specific technical criteria when deciding on the seismic isolation application to the intended hospital buildings. Turkish Earthquake Code started to cover the design considerations of seismically isolated buildings by 2018 (Turkey Building Earthquake Code, 2018).

Technological advancement and development of materials such as multi-layered elastomeric bearings have seen the base isolation technic gain widespread practical use. The elastomeric bearing consists of layers of rubber and thin steel plates which makes them rigid in vertical direction and flexible horizontally allowing large displacement during earthquakes. (Hu, 2015). The most commonly used rubber isolators are natural (synthetic) rubber isolator, lead core rubber isolator, high-damping rubber isolator (Naeim and Kelly, 1999). In the late 1970s, rubber isolators with lead core were used in New Zealand. Subsequently, high damping rubber isolators emerged and different compositions were used to increase the damping rate to the range of 10-20% and shear stress 100%. These high damping materials were first produced by the Malaysian Rubber Producers' Research Association and their first applications were made in 1985 for the Foothill Communities and Justice Center in California (de la Llera et al., 2015). The damping ratio of the low-damping rubber bearings is around 5% and exhibits linear behaviour. The damping ratio of the high damped rubber bearings has been increased (around 10%) and they display nonlinear behaviour that can be modelled in binary linear. In lead core bearings; unlike low and high damped rubber bearings, lead core is placed in the middle of the support to achieve high damping between 10% and 20% (Nagarajaiah, Reinhorn and Constantinou, 1991).

The analysis methods for seismically isolated structures are focused on, in various studies in literature. For example, in the work done by (Turkington et al., 1989), a method based on the

concepts of equivalent rigidity and equivalent damping has been developed in order to model and design bridges on lead core rubber isolators with nonlinear inelastic behaviour. Equivalent period was obtained by adding the period extension that will occur due to inelastic deformation to the period to be calculated due to the initial stiffness. Equivalent damping is obtained by adding extra damping that will occur with the flow of the lead core to the 5% damping that inherently exists. Seismic response values of the modelled equivalent single degree of freedom elastic superstructures were obtained by using elastic response spectra.

In a study by (Kikuchi and Aiken, 1997), an analytical hysteretic model is proposed to accurately predict the seismic behaviour of floor-isolated structures. The application was made using four types of seismic isolation bearings, namely two types of high-damping rubber bearings, one type of lead-rubber bearing and one type of silicon rubber bearing. The validity of the model used was proved by comparing the dynamic analysis with two isolated structures and the earthquake simulation experiment results. When the results were examined, it was determined that there was a good agreement between analytical and experimental results and the use of the model was appropriate.

In the work of Mavronicola and Komodromos (2011), the suitability of equivalent linear elastic analysis of seismically isolated multi-story buildings is assessed. In this study, the appropriateness of the linearized models was assessed through a parametric study on a 3-storey and a 5-storey seismically isolated building by using strong earthquake motion. According to the study, equivalent linear analysis procedure is found to be conservative regarding the total displacement at the isolation level and it was recommended that the use of equivalent linear analysis be limited to the preliminary stage of the design. In the case the building includes acceleration sensitive equipment, it recommends use of the more accurate bilinear models.

Curadelli (2013) studied the seismic performance of base isolated cylindrical liquid storage tanks with isolation system consisting of bilinear bearings. The bilinear behaviour is modelled as equivalent linear through effective damping and effective stiffness using a statistical linearization scheme. The influence of different design parameters (isolation period, yield strength and viscous damping ratio) and soil conditions are included and it is found out that soft soil conditions intensify the general response of the system, particularly the base displacements, along with the normalized base shear to a smaller extent.

Lee and Song (2015) investigated the seismic response of isolated nuclear power plant (NPP) containment structure by subjecting the structure to artificial acceleration and different site class earthquake. The isolation system was modelled both equivalent linearly and nonlinearly and the response was observed. The maximum displacement of the equivalent linear model is observed to be larger than the nonlinear model while the spectral acceleration for equivalent linear model was found to be 2-3 times more than equivalent linear model for a model of frequency of 0.5 Hz.

Dicleli and Buddaram (2007) studied the seismic response quantities from equivalent linear analyses compared with the response obtained from nonlinear time history analyses using 2-dimensional shear frame (no eccentricity considered). It was observed that equivalent linear analysis is affected by factors such as the post-elastic stiffness and yield strength of the isolator, distance of the structure from the fault and magnitude of the near-fault ground motion. Similarly, Alhan and Ozgur (2015) investigated the precision of equivalent linear modelling by conducting experiment on seismic-isolated buildings using three dimensional structure with eccentricity considered. It was observed that the peak seismic response of the seismically isolated building exhibited substantial errors in equivalent linear analysis. In both studies the isolated structure response for nonlinear and equivalent linear systems is investigated but the studies didn't investigate the response of the content of the isolated structures. It is therefore equally important to investigate the response of the isolated structures content.

2.2. PRINCIPLE OF SEISMIC ISOLATION

The aim of seismic isolation is to reduce seismic demand rather than increasing capacity of the structure. In seismically isolated systems, the superstructure is decoupled from the earthquake ground motion by introducing a flexible interface between the foundation and the base of structure. Thereby, the isolation system shifts the fundamental period of the structure to a large value and/or dissipates the energy in damping, limiting the amount of force transferred to the superstructure. As a result, inter-story drift and floor accelerations are reduced drastically as shown in Figure 2.1 and Figure 2.2. The matching of fundamental frequencies of base-isolated structures and the predominant frequency contents of earthquakes is also consequently avoided leading to a flexible structural system more suitable from earthquake resistance viewpoint (Tena-Colunga *et al.*, 2015).

Seismic isolation protects the structure together with the content of the structure by simultaneously reducing floor accelerations and relative floor displacements hence is accepted as an earthquake resistant design method. It is a highly preferred technology especially in strategic buildings such as schools, hospitals, industrial structures and places where sensitive equipment is intended to be protected from hazardous effects during earthquake (Clemente and Martelli, 2019). The performances of seismic isolated structures are generally evaluated by the base displacements, base accelerations, floor accelerations and relative floor displacements (Alhan and Sürmeli, 2011).

While a properly designed seismic isolation system can reduce floor accelerations and relative floor displacements in far fault earthquakes to acceptable limits without causing unacceptably large displacements, the effectiveness of isolation system in near-fault earthquakes is questionable due to potential of very large isolator displacements (Alhan and Öncü-Davas, 2016)

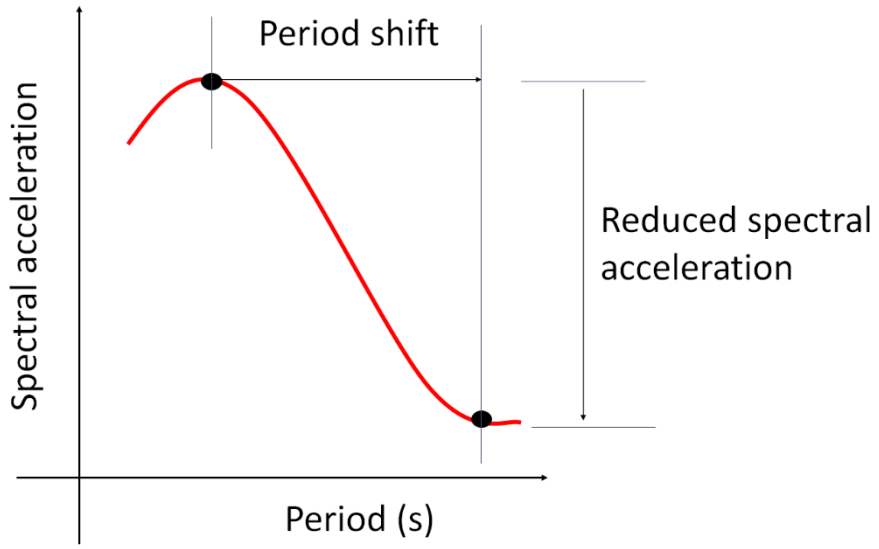

Figure 2.1: Effect of period shift in isolated structures on spectral accelerations

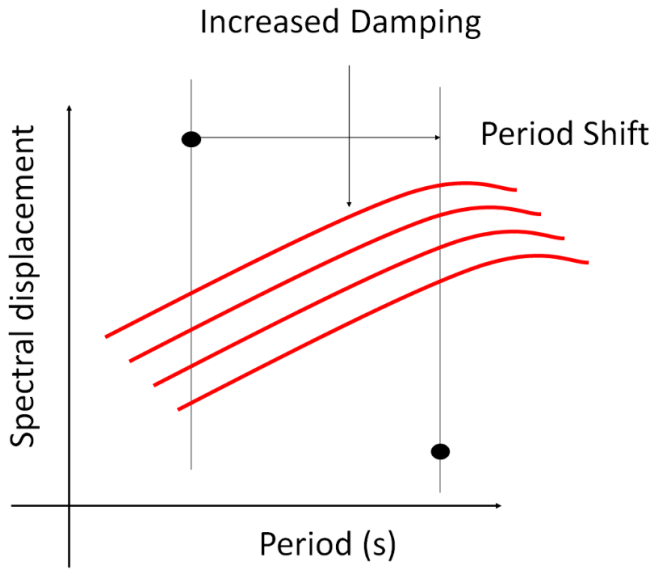

Figure 2.2: Effect of period shift in an isolated structure on Spectral displacements

2.3. TYPES OF ISOLATION SYSTEMS

In general, seismic isolation systems can be categorized into two main groups; elastomeric based systems and friction-based systems. As technology develops there is emergence of different isolation systems. However, in general isolation systems needs to satisfy some fundamental requirements (Alemdağ, 2016).

1. High lateral deformation capacity

The lateral rigidity of the isolation systems needs to be low (high lateral deformation capacity). This lowers the frequency of the base isolated structure significantly when compared to a similar structure with a fixed base. It also helps to shift the frequency of the structure from the dominant frequency of the severe earthquakes.

2. Adequate lateral rigidity for wind load and low-level earthquakes

Isolation systems need to have adequate lateral rigidity in order to avoid small movement of the structure under low level loads such as wind and minor earthquake and in order to satisfy the serviceability conditions.

3. High vertical rigidity

In order to support the total weight of the structure and avoid crushing or lateral bulging the isolation system needs to have high vertical rigidity.

4. Restoring force effect

After a large displacement due to earthquake loads isolation system must have a restoring force effect to return back to its original position.

5. Damping

An isolation system ought to have an adequate damping ratio (15 to 30%) more than the structure to prevent a potential resonance case and high displacements of the super structure. Furthermore, higher damping of the isolation system dissipates more energy coming from the earthquake.

2.3.1. Elastomeric-Based Systems

Elastomeric based systems were used for the first time as natural rubber bearing in Pestalozzi School, Macedonia in 1969 (Naeim and Kelly, 1999). The isolator design consisted of only rubber materials in block shape which caused the structure to display shaking motions during strong earthquakes. This is because the system displays less vertical rigidity compared to horizontal rigidity causing the natural rubber to laterally bulge under gravitational load of the structure.

This phenomenon of low vertical rigidity in the rubber bearings led to engineers developing laminated elastomeric bearings that are composed of rubber layers with a steel shim. Laminated elastomeric bearings are commercial products mainly developed for bridge sector. Lately there has been emergence of steel reinforced elastomeric isolator (SREI) bearings however, their weight and high price have mostly reduced their application to only huge and expensive structures.

On the other hand, fiber reinforced elastomeric isolators (FREIs) use fibers instead of steel plates, as a reinforcement sheet. Fiber reinforced elastomeric isolator~~s~~ (FREI) bearings can provide adequate levels of vertical and lateral stiffnesses as required in a base isolation device. Sufficient energy dissipation ability, low cost of manufacturing provides promising advantages for this type of bearing (Toopchi-Nezhad, Tait and Drysdale, 2008).

Another type of elastomeric bearing is the lead-rubber bearing~~s~~ (LRB) shown in Figure 2.3. It was invented in New Zealand in 1975. It is similar to steel reinforced elastomeric isolator (SREI) and Fiber reinforced elastomeric isolators (FREI) but have a cylindrical lead core

inserted into the center of the bearing. The system shows a bilinear response and dissipates energy, controls displacement and supports the weight of the structure (Naeim and Kelly, 1999).

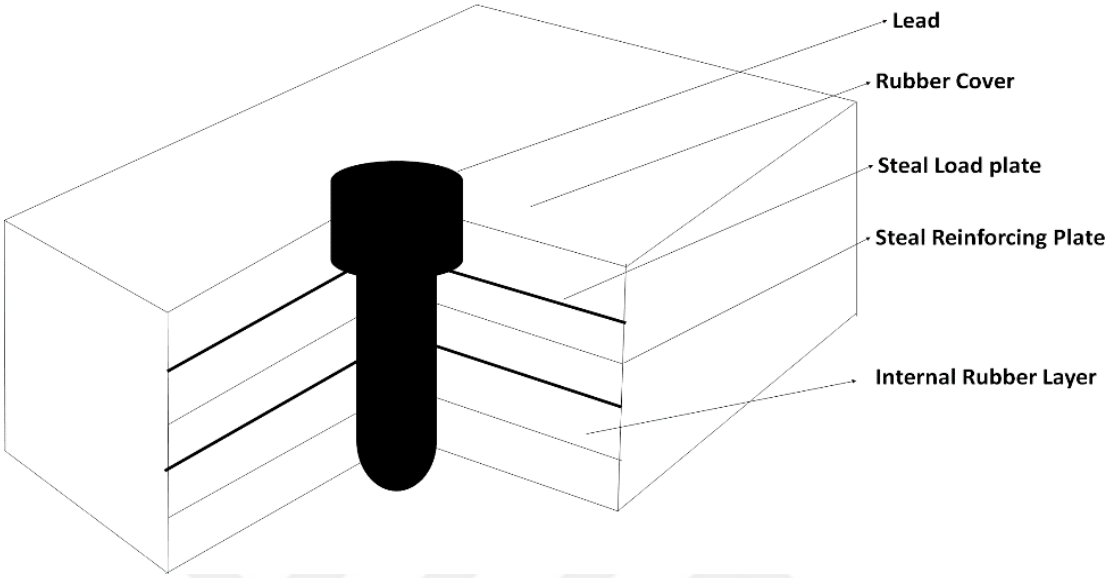

Figure 2.3: Lead Rubber Bearing

2.3.2. Sliding-Based Systems

The first idea of base isolation was based on sliding and proposed in 1909. The basic concept behind this type of isolator is to limit the transfer of shear force to the superstructure by means of friction. The articulated slider within the bearing travels along the concave surface during an earthquake causing the supported structure to move with gentle pendulum motions. The most preferred materials on sliding surfaces are stainless steel and Teflon as shown in Figure 2.4 (Komodromos, 2000). Friction at the interface is dependent on the contact between the Teflon-coated slider and the stainless-steel surface, which increases with pressure. Movement of the slider generates a dynamic frictional force that provides the required damping to absorb the earthquake energy. They are effective for a wide range of frequency ranging between 3% to 10% which is considered reasonable for a Friction Pendulum System (FPS) to be effective. The center of mass of the structure and the center of mass of the sliding support coincides. As a result, the torsional effects produced by the asymmetric building are diminished. It is possible that these systems can be designed to allow very low shear force by using low friction coefficients. These systems can be used efficiently in large earthquakes. It is relatively inexpensive and easy to apply. The system does not return to its original position since there is

no return force after the earthquake. For this reason, friction-based isolators are not used alone and an additional system must be used. Therefore, it may be considered to use additional elastomer isolators. The different section of the isolation system is shown is Figure 2.4.

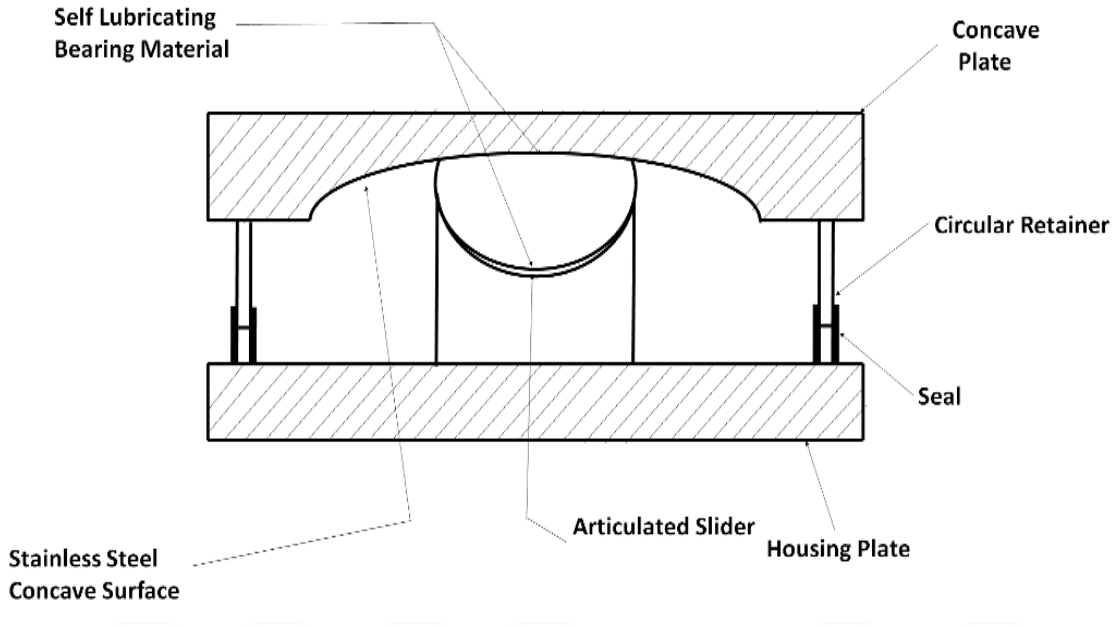

Figure 2.4: Friction Pendulum System

2.4. MODELING OF SEISMIC ISOLATORS

2.4.1. Nonlinear Model of Seismic Isolators

The nonlinear force-deformation behaviour of the isolation system can be modelled by use of the Bouc–Wen model of hysteresis (Mavronicola and Komodromos, 2012) and is characterized by the following parameters namely:

(i) Characteristic strength, Q
(ii) Post-yield stiffness, K_2
(iii) Yield displacement, D_y
(iv) Yield Force F_y

Although a bilinear model can be used for most popular isolation systems with appropriate parameters, it suits best for rubber isolators and will be used in this thesis to represent such systems. The post-yield stiffness of the isolation system, K_2 is generally designed in such a way

to provide the specific value of the isolation period (also known as rigid-body-mode period) which is one of the most important indicators of an isolated building. The isolation period T_0 is expressed as;

$$T_0 = 2\pi\sqrt{\frac{M}{K_2}} \tag{2.1}$$

where M is the total mass of the base-isolated structure and K_2 is the post yield stiffness. Thus, the bi-linear hysteretic model of the base isolation system can be characterized by specifying the three parameters namely T_0, Q and D_y. The characteristic strength, Q is normalized by the weight of the building, W = mg (where g is the gravitational acceleration) and is expected to be in the typical range of 5% to 15%.

In seismically isolated buildings, isolation systems are modelled with two main stiffness namely the pre-yield and the post-yield stiffness (stiffness in isolation mode). The post yield stiffness of the isolation system can be driven from equation (2.1).

$$K_2 = \frac{4\pi^2 \times W}{T_0^2 \times g} \tag{2.2}$$

The characteristic strength of the isolation system can be provided as a function of the yield displacement (D_y), pre-yield stiffness (K_1) and post-yield stiffness (K_2) using equation (2.2).

$$Q = (K_1 - K_2) \times D_y \tag{2.3}$$

The pre-yield stiffness, which represents the primary stiffness of the isolation system up to the yield displacement, depends on the post-yield stiffness (K_2), the characteristic strength (Q) and the yield displacement (D_y). From equation (2.3) we can derive the formula for pre-yield stiffness;

$$K_1 = \frac{Q}{D_y} + K_2 \tag{2.4}$$

All the formulas used above are adopted from work of Alhan and Ozgur (2015) who retrieved originally from (Matsagar and Jangid, 2004).

2.4.2. Modelling of Nonlinear Isolator Systems As An Equivalent Linear Model

Nonlinear force-deformation characteristic of the seismic isolator can be substituted with an equivalent linear model by means of effective elastic stiffness and effective viscous damping. The behaviour of isolation systems and the base isolated structures is now well established and codes are developed for designing the base-isolated structures (e.g. Uniform Building Code, 1997 and International Building Code, 2000). For nonlinear isolation systems, the codes may allow to use the equivalent linear model to permit the use of response spectrum method for designing the isolated structures. The linear force developed in the isolation system can be expressed as; (Matsagar and Jangid, 2004).

$$F_b = K_{eff}X_b + C_{eff}X'_b \tag{2.5}$$

where K_{eff} is the effective stiffness and C_{eff} the effective viscous damping constant. Here, X_b is the base displacement.

$$C_{eff} = 2\beta_{eff}M\omega_{eff} \tag{2.6}$$

where β_{eff} is the effective viscous damping ratio, M is the total mass of the structure and ω_{eff} is the effective isolation angular frequency.

$$\omega_{eff} = 2\pi/T_{eff} \tag{2.7}$$

where T_{eff} is the effective isolation period.

$$T_{eff} = 2\pi\sqrt{\frac{M}{K_{eff}}} \tag{2.8}$$

while the effective viscous damping β_{eff} can be calculated using;

$$\beta eff = \frac{4Q(D - D_y)}{2\pi K_{eff}D^2} \tag{2.9}$$

At a specified design isolation displacement and a specified characteristic strength, the effective stiffness of a bi-linear system is expressed as;

$$K_{eff} = K_2 + \frac{Q}{D} \tag{2.10}$$

All the formulations of the equivalent linear models are retrieved from (Alhan and Ozgur, 2015) who originally obtained from (Matsagar and Jangid, 2004).

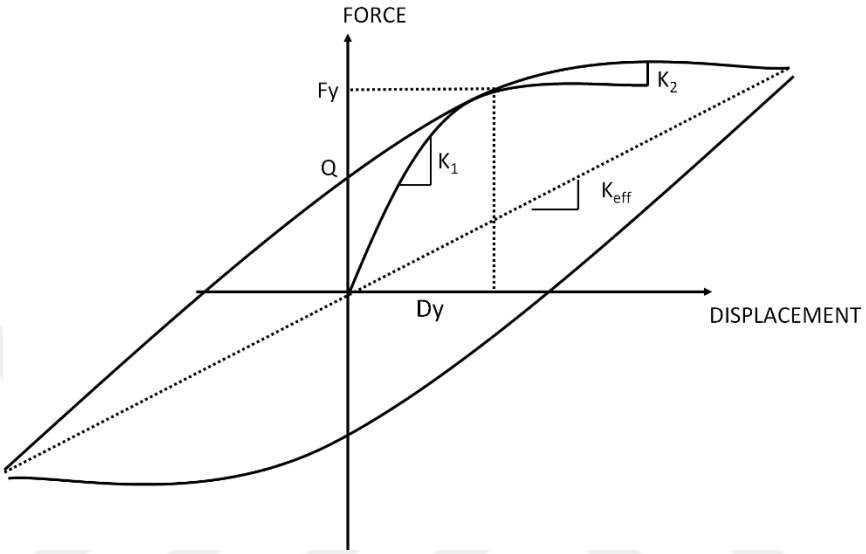

Figure 2.5: Graph force versus displacement for a hysteresis loop

3. MATERIALS AND METHODS

In the context of this thesis, a benchmark model of a three-story base-isolated building is used. Isolation systems with different isolation characteristics are taken into account. Details of the building are explained in sub-sequent section. The building is then exposed to historical earthquake (details of the earthquake is given in section 3.3. The building is then analysed in 3DBASIS (Nagarajaiah, Reinhorn and Constantinou, 1991) primarily by nonlinear modelling and nonlinear time history analysis method and all the floor acceleration time history responses are obtained. The same process is repeated by modelling the isolation system as equivalent linear and analysing by linear time history analysis method. The floor acceleration time histories are extracted from the top floor of the building and are applied at the base of the rack models. It should be noted here that, within the scope of this thesis, it is assumed that rack systems are housed on the top floor of the building and these racks are modelled independently by assuming that coupling between racks and the building are negligible. This is illustrated in Figure 3.1.

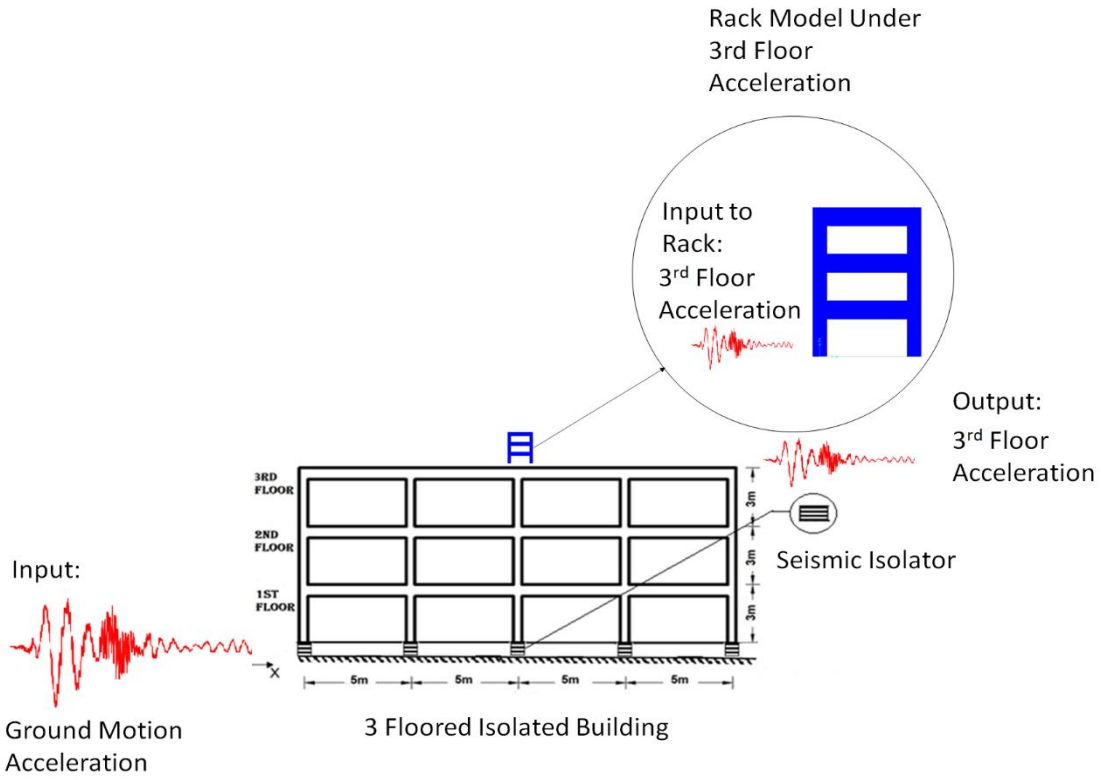

Figure 3.1: Illustration of how the ground motion impact on the superstructure and subsequently the rack through the 3rd floor motion.

Different racks with different periods that are assumed to house vibration sensitive contents are considered. Time history responses of these racks are finally compared for both equivalent linear and nonlinear cases.

3.1. MODELLING OF THE BASE-ISOLATED BUILDING

The base isolated building model used in this study was obtained from the study of Alhan and Sürmeli (2011). The structure consists of four floors including the base floor which lies on a symmetric plan of 20m x 20m and distance between the columns both in the x and y axis are equal and 5m each. The axis plan of the building is given in Figure 3.3. The structure consists of moment frames made of reinforced concrete C30 and modulus of elasticity of each frame element is 32,000MPa. All the columns of the building are 450 mm × 450 mm and all beams are 300 mm × 550 mm. Each floor has a mass of 320ton and the total mass of the building including the base floor is (4 x 320) M = 1280 ton corresponding to total building weight of 12557 kN. The mass moments of inertia of the floors are 21333 tm. Each floor of the building including the base floor has a height of 3m. The two-dimensional model of the base isolated building used in numerical experiments is given in Figure 3.2. There is no eccentricity since the center of mass of each floor coincides with the center of gravity of the corresponding floor. The base floor is made of a rigid slab and has an isolation bearing fixed below each column of the base floor. This makes the total number of isolators at the base to be 25. All floors are modelled as a rigid diaphragm with floor mass defined at the center of mass. Each floor of the building has three degrees of freedom, two horizontal and one rotational motion. Therefore, there are a total of 12 degrees of freedom.

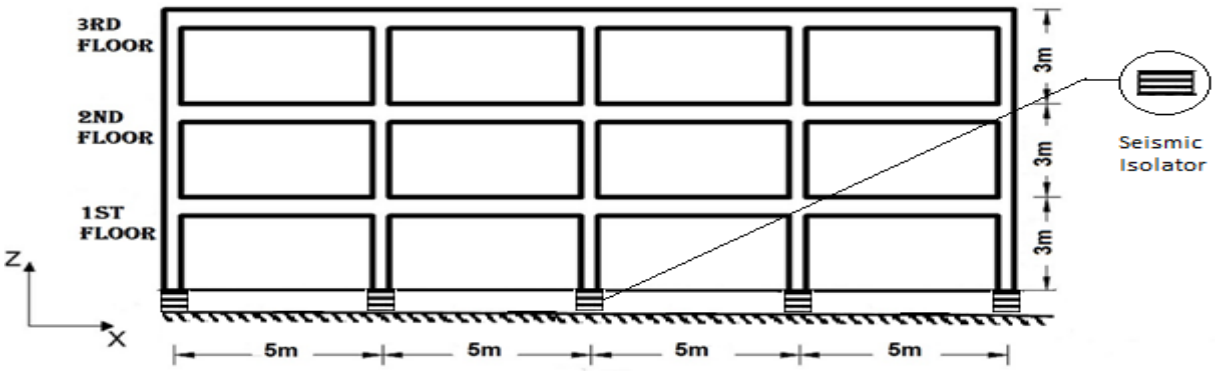

Figure 3.2: Two-dimensional views of the 3-story base isolated building modified from Alhan and Sürmeli (2011).

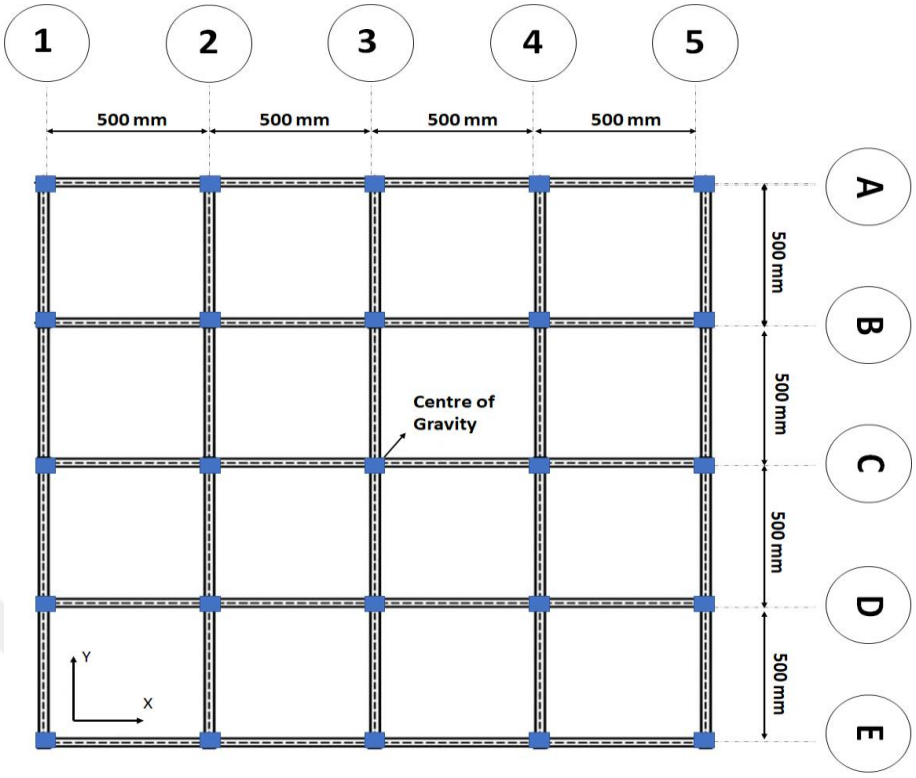

Figure 3.3: Floor plan for the 3-story base isolated building modified from Alhan and Sürmeli, (2011)

3.2. ISOLATION SYSTEMS MODELS

The seismic isolation system consists of rubber bearings placed under the base floor of the building between the base floor columns and the foundation. They are connected to each other and move together. In this study, types of nonlinear isolation systems and their equivalent linear counterparts are considered. All systems are modelled using 3DBASIS.

3.2.1. Nonlinear Isolation Systems

The effective isolation periods of seismically isolated buildings typically lie within a range of 2 to 3 s. The ratio of the post-yield stiffness to the pre-yield stiffness in nonlinear isolation system is typically between 0.1 and 0.2. Similarly, the yield displacements typically range from 6 mm to 25 mm (McVitty & Constantinou, 2015). Nonlinear isolation systems with four different post-yield isolation periods (T_0 = 2.0, 2.5, 3.0, 3.5) with a characteristic strength ratio Q/W of 7.5% were modelled in 3DBASIS (Nagarajaıah, Reınhorn, & Contantınou, 1991b) for the purpose of this study. All the isolation systems have the same yield displacement of 20 mm.

The isolation systems are named according to their periods as shown in Table 3.1. Pre yield stiffness, post-yield stiffness, and characteristic strengths of the isolation system were calculated using the equations (2.2-(2.4) and given in Table 3.2. Each of the nonlinear isolation system modelled was then analysed under 6 selected earthquakes (the details of the earthquakes are discussed in section 3.3).

Table 3.1: Nonlinear isolation system

NL20	Nonlinear isolation system with an isolation period 2.0 s
NL25	Nonlinear isolation system with an isolation period 2.5 s
NL30	Nonlinear isolation system with an isolation period 3.0 s
NL35	Nonlinear isolation system with an isolation period 3.5 s

In order to explain in detail, the calculation of an isolation system's (NL20) parameters are discussed step by step as an example here:

As given in section 3.1. the total weight of the superstructure with 3 Storey is 12557 kN

The characteristic strength normalized by the weight of the building is 0.075 for the whole isolation system. Therefore, the characteristic strength of the isolation system is;

$Q = 12557 \times 0.075 = 941.76$ kN

Post-yield isolation system stiffness K_2 (using equation (2.2));

$K_2 = \frac{4\pi^2 \times 12557}{2^2 \times 9.81} = 12633.09$ kN/m

As stated before; all the isolators have same yield displacement. $D_y = 0.02$ m

The pre-yield isolation stiffness is calculated using equation (2.4).

$K_1 = \frac{941.76}{0.02} + 12633.09 = 59721.09$ kN

The post-yield to pre-yield ratio α is;

$$\alpha = \frac{12633.09}{59721.09} = 0.21$$

Yield force (F_y) = $59721.09 \times 0.2 = 1194.422$ kN

Since there are 25 isolators the yield force for each isolator (f_y) is $= 47.78$ kN

Table 3.2: Properties of nonlinear isolation systems

Isolation System	T_0 (s)	Q/W	D_y (m)	K_2 (kN/m)	Q (kN)	K_1 (kN/m)	α	F_y	f_y Per isolator
NL20	2	0.075	0.02	12633.09	941.76	59721.09	0.21	1194.42	47.78
NL25	2.5	0.075	0.02	8085.18	941.76	55173.18	0.15	1103.46	44.14
NL30	3	0.075	0.02	5614.71	941.76	52702.71	0.11	1054.05	42.16
NL35	3.5	0.075	0.02	4125.09	941.76	51213.09	0.08	1024.26	40.97

3.2.2. Equivalent Linear Isolation Systems

Each of the nonlinear isolation system discussed in section 3.2.1 is then used to obtain equivalent linear isolation systems under each earthquake. The detail of the earthquakes is given in section 3.3. At first, the peak isolation system displacement (D) is obtained from the output of the nonlinear analysis for both x and y direction. The peak isolation displacement obtained for each isolation system and for each earthquake is then used to obtain the effective stiffness, effective isolation period and effective viscous damping ratio using Equations (2.10), (2.8) and (2.9), respectively. The effective stiffness, effective isolation period, and effective damping is calculated for both x and y direction. Since there are four main nonlinear isolation systems and 6 different earthquakes a total of 24 equivalent linear isolation systems are modelled. To

illustrate further how the equivalent linear isolation model is obtained, linearization of one nonlinear isolation system (NL20) under one earthquake (San Fernando earthquake) for x direction is shown here step by step:

From the nonlinear analysis conducted, the peak isolation system displacement obtained for x direction is; D = 0.42 m

The effective stiffness of the isolation system is given by equation (2.10);

$K_{eff} = 12633.09 + \frac{941.76}{0.42}$ = 14827.58 kN

Since there are 25 isolators the stiffness of each isolator is 14827.58/25 = 593.10 kN

The effective isolation period is given by equation (2.8);

$T_{eff} = 2\pi\sqrt{\frac{1280}{14827.58}}$ = 1.85 s

The effective angular frequency is given by equation (2.7);

$\omega_{eff} = \frac{2\pi}{1.85}$ = 3.40 rad/sec

The effective viscous damping ratio is then calculated using equation (2.9);

$\beta_{eff} = \frac{4\times(0.42-0.02)}{2\pi\times14827.58\times0.42^2}$ = 0.09

Finally, the effective viscous damping coefficient is calculated using equation (2.6);

$C_{eff} = 2 \times 0.09 \times 1280 \times 3.40 =$ 782.68 N s/m

Since there are 25 isolators, the effective viscous damping coefficient for each isolator

c_{eff}= 31.31 N s/m

In Table 3.3 and Table 3.4, the properties of the equivalent linear isolation system models are provided for all isolation systems and all earthquakes in x and y directions, respectively.

Table 3.3: properties of the equivalent linear isolation system models in x direction

Equivalent linear Isolation System	Earthquake Name	Dx (m)	K_{eff} (m)	T_{eff} (s)	β_{eff}	C_{eff}	k_{eff} (kN)	c_{eff}
NL20	San Fernando	0.43	14827.58	1.85	0.09	782.68	593.10	31.31
	Superstition Hills-02	0.73	13929.26	1.90	0.06	486.51	557.17	19.46
	Cape Mendocino	0.3	15775.87	1.79	0.12	1063.73	631.03	42.55
	Landers	0.31	15650.38	1.80	0.11	1028.27	626.02	41.13
	Northridge-01	0.52	14432.53	1.87	0.08	656.23	577.30	26.25
	Kobe, Japan	0.29	15887.60	1.78	0.12	1094.88	635.50	43.80
NL25	San Fernando	0.35	10760.95	2.17	0.15	1108.23	430.44	44.33
	Superstition Hills-02	0.76	9317.19	2.33	0.08	566.20	372.69	22.65
	Cape Mendocino	0.34	10874.96	2.16	0.15	1146.43	435.00	45.86
	Landers	0.4	10437.45	2.20	0.14	996.43	417.50	39.86
	Northridge-01	0.48	10034.03	2.24	0.12	849.57	401.36	33.98
	Kobe, Japan	0.25	11802.63	2.07	0.18	1435.67	472.11	57.43
NL30	San Fernando	0.38	8119.92	2.49	0.19	1199.06	324.80	47.96
	Superstition Hills-02	0.76	6860.42	2.71	0.11	666.98	274.42	26.68
	Cape Mendocino	0.36	8220.88	2.48	0.19	1236.89	328.84	49.48
	Landers	0.47	7637.61	2.57	0.16	1009.12	305.50	40.36
	Northridge-01	0.43	7784.73	2.55	0.17	1068.73	311.39	42.75
	Kobe, Japan	0.23	9762.22	2.28	0.25	1743.76	390.49	69.75
NL35	San Fernando	0.40	6503.54	2.79	0.22	1275.63	260.14	51.03
	Superstition Hills-02	0.69	5484.58	3.04	0.15	812.08	219.38	32.48
	Cape Mendocino	0.38	6619.23	2.76	0.23	1322.50	264.77	52.90
	Landers	0.51	5969.36	2.91	0.19	1044.78	238.77	41.79
	Northridge-01	0.39	6551.15	2.78	0.22	1295.05	262.05	51.80
	Kobe, Japan	0.23	8134.97	2.49	0.29	1852.74	325.40	74.11

Table 3.4: properties of the equivalent linear isolation system models in y direction

Equivalent linear Isolation System	Earthquake Name	Dx (m)	K_{eff} (m)	T_{eff} (s)	β_{eff}	C_{eff}	k_{eff} (kN)	c_{eff}
NL20	San Fernando	0.24	16561.66	1.75	0.14	1274.57	662.47	50.98
	Superstition Hills-02	0.21	17095.76	1.72	0.15	1407.42	683.83	56.30
	Cape Mendocino	0.11	21521.56	1.53	0.21	2238.99	860.86	89.56
	Landers	0.04	38966.45	1.14	0.19	2678.43	1558.66	107.14
	Northridge-01	0.31	15632.18	1.80	0.11	1023.09	625.29	40.92
	Kobe, Japan	0.13	19710.11	1.60	0.19	1951.15	788.40	78.05
NL25	San Fernando	0.20	12884.67	1.98	0.21	1729.76	515.39	69.19
	Superstition Hills-02	0.22	12288.43	2.03	0.20	1573.06	491.54	62.92
	Cape Mendocino	0.11	17004.97	1.72	0.27	2525.65	680.20	101.03
	Landers	0.04	29942.35	1.30	0.25	3083.10	1197.69	123.32
	Northridge-01	0.36	10710.12	2.17	0.15	1091.00	428.40	43.64
	Kobe, Japan	0.14	14693.14	1.85	0.25	2134.79	587.73	85.39
NL30	San Fernando	0.18	10744.9	2.17	0.27	2008.86	429.80	80.35
	Superstition Hills-02	0.23	9638.756	2.29	0.24	1707.54	385.55	68.30
	Cape Mendocino	0.11	14406.67	1.87	0.32	2713.71	576.27	108.55
	Landers	0.06	22683.31	1.49	0.31	3291.18	907.33	131.65
	Northridge-01	0.32	8526.498	2.43	0.20	1347.62	341.06	53.90
	Kobe, Japan	0.17	11242.33	2.12	0.28	2128.80	449.69	85.15
NL35	San Fernando	0.18	9267.247	2.34	0.31	2167.52	370.69	86.70
	Superstition Hills-02	0.22	8453.152	2.44	0.30	1947.27	338.13	77.89
	Cape Mendocino	0.11	12768.66	1.99	0.35	2844.85	510.75	113.79
	Landers	0.06	19819.26	1.60	0.34	3385.66	792.77	135.43
	Northridge-01	0.31	7115.119	2.66	0.25	1512.19	284.60	60.49
	Kobe, Japan	0.18	9305.119	2.33	0.32	2177.07	372.20	87.08

3.3. EARTHQUAKE RECORDS

The Earthquake records used in this study was obtained from the database named “Peer Strong Motion Databases” and belong to Berkeley University. Six earthquake records were obtained from the data base and applied bidirectionally (both in X and Y directions) on the seismically isolated building in case of nonlinear isolation systems. The earthquake records selected are all near-fault earthquakes with distances from the fault being less than 10 km. These types of earthquakes are characterized with ground motions having high-amplitude, long-duration acceleration or velocity pulses occurring primarily in the fault-normal direction also referred to as “pulse-like” ground motions (Cao *et al.*, 2016). The PGAs of near fault earthquakes are generally high and exceed the 0.4g PGA adopted by many Building Earthquake Codes around the world for first earthquake zone.

Each of the earthquake records obtained from PEER Data Base contained time histories in two directions namely H1 and H2 representing ground motion time histories in the two horizontal directions. Both directions do not necessarily contain pulses. Therefore, first, ground velocity time histories in both directions were plotted and the direction containing a pulse was observed. The earthquake direction with the larger Peak Ground Velocity was the one that contained pulse like motion. The direction with the pulse was applied on the X direction and the other Earthquake in the Y direction. In Table 3.5, the earthquake recording names, occurrence year, Rupture distance (Rrup), moment magnitudes (Mw), peak ground acceleration (PGA), peak ground velocity (PGV), and peak ground displacement (PGD) values are given. The peak ground velocity of the direction with the pulse-like motion is higher than and is shown in bold in the table. Also, the spectral acceleration and spectral displacement graphs (with 5% damping) for each earthquake in both in H1 and H2 directions are given in Figure 3.4 - Figure 3.17.

Table 3.5: Characteristics of earthquake records

Earthquake Name	Year	Rrup (km)	Mw	H1			H2		
				PGA (g)	PGV (cm/s)	PGD (cm)	PGA (g)	PGV (cm/s)	PGD (cm)
San Fernando	1971	1.81	6.61	1.22	**114.47**	39.02	1.24	57.28	12.8
Superstition Hills-02	1987	0.95	6.54	0.43	**134.29**	46.18	0.38	53.06	17.82
Cape Mendocino	1992	8.18	7.01	0.59	49.33	16.61	0.66	**88.51**	33.23
Landers	1992	2.19	7.28	0.73	**133.4**	113.93	0.79	28.11	25.54
Northridge-01	1994	6.5	6.69	0.87	**148**	41.88	0.47	74.77	23.1
Kobe, Japan	1995	0.96	6.9	0.83	**91.11**	21.11	0.63	38.06	4.58

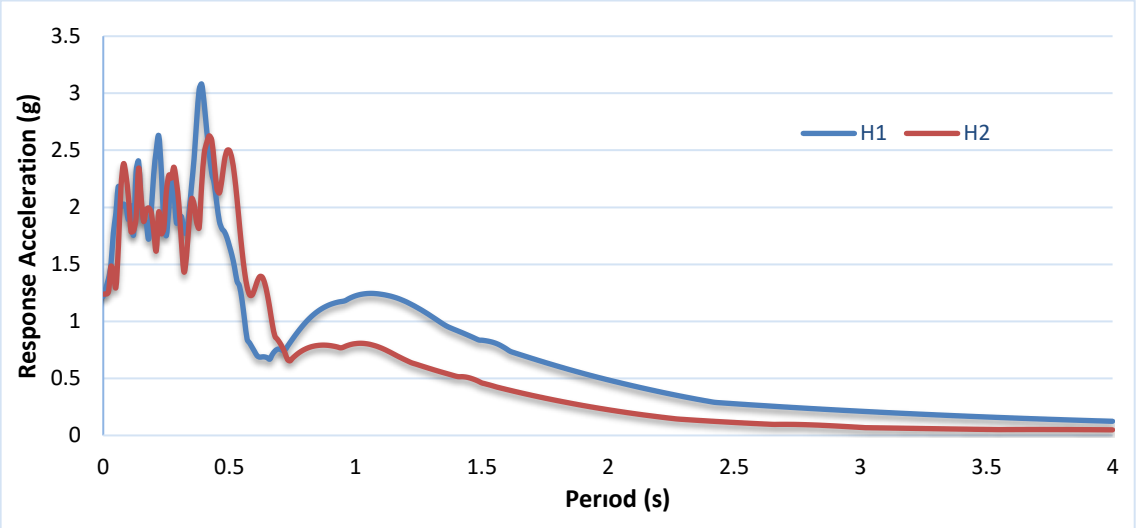

Figure 3.4: San Fernando earthquake spectral acceleration with 5% damping

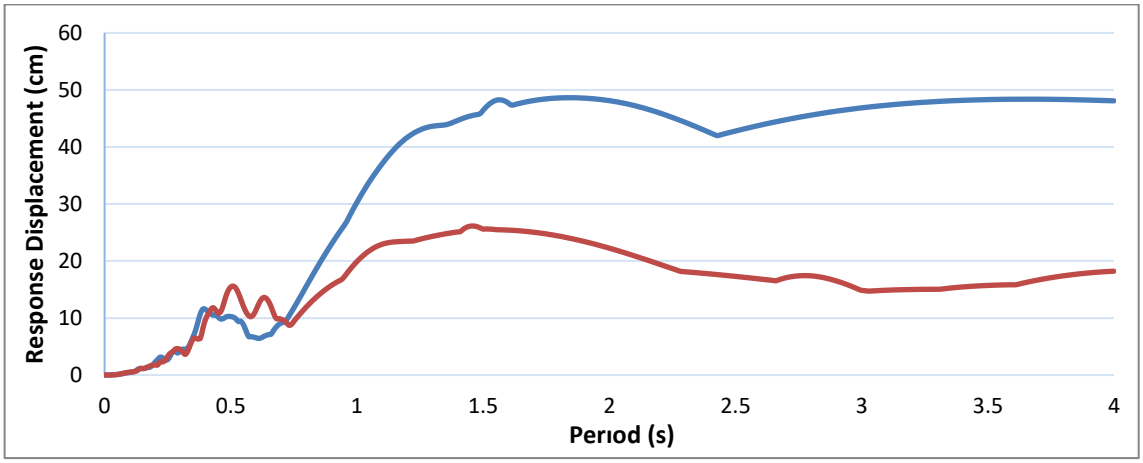

Figure 3.5: San Fernando earthquake spectral displacement with 5% damping

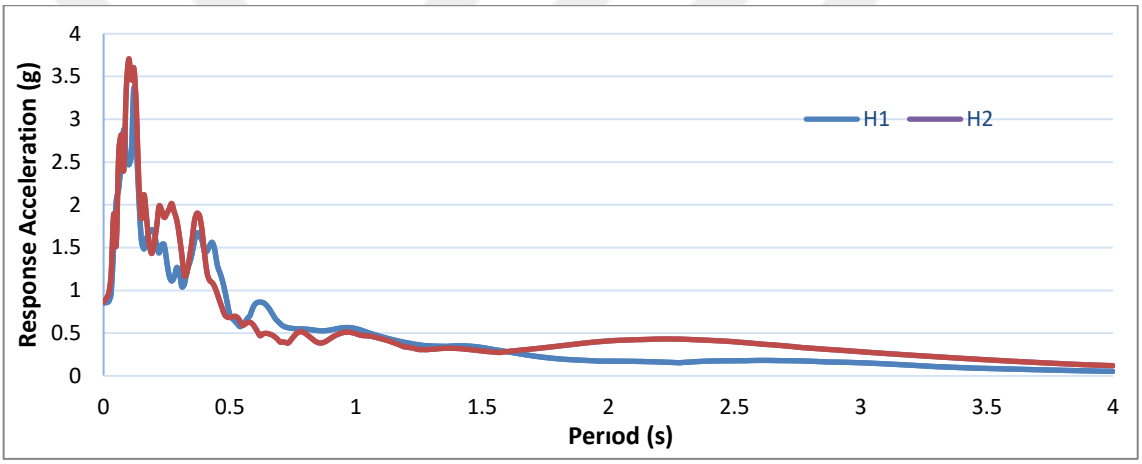

Figure 3.6: Tabas earthquake spectral acceleration with 5% damping

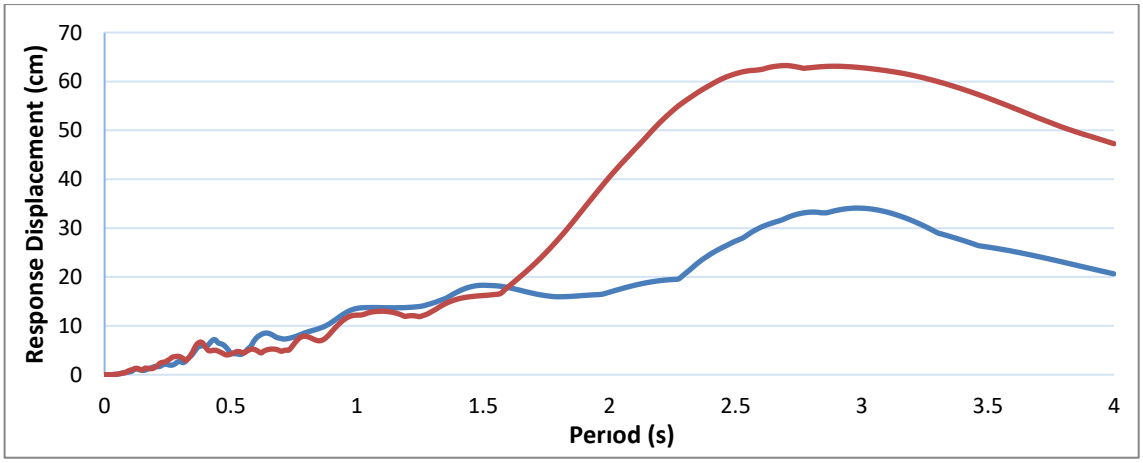

Figure 3.7: Tabas earthquake spectral displacement with 5% damping

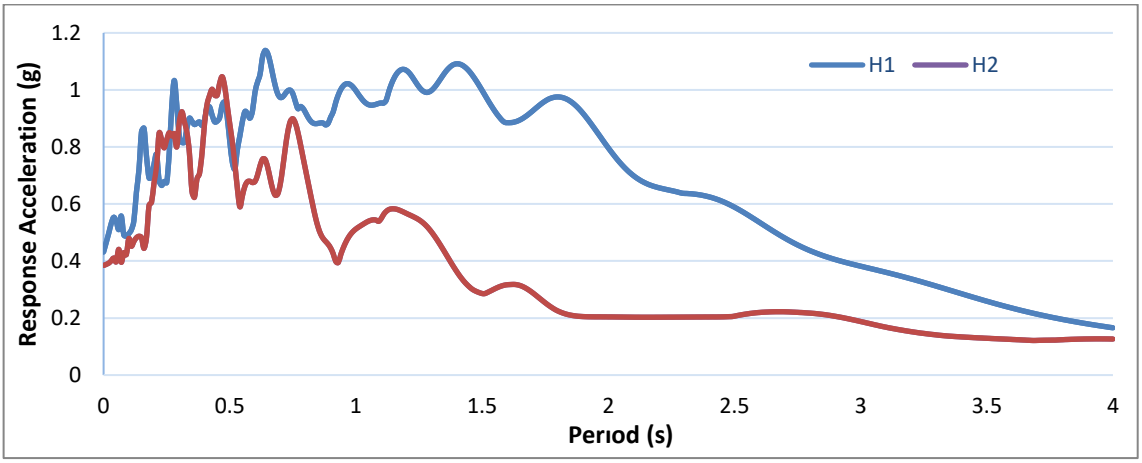

Figure 3.8: Superstition Hills-02 earthquake spectral acceleration with 5% damping

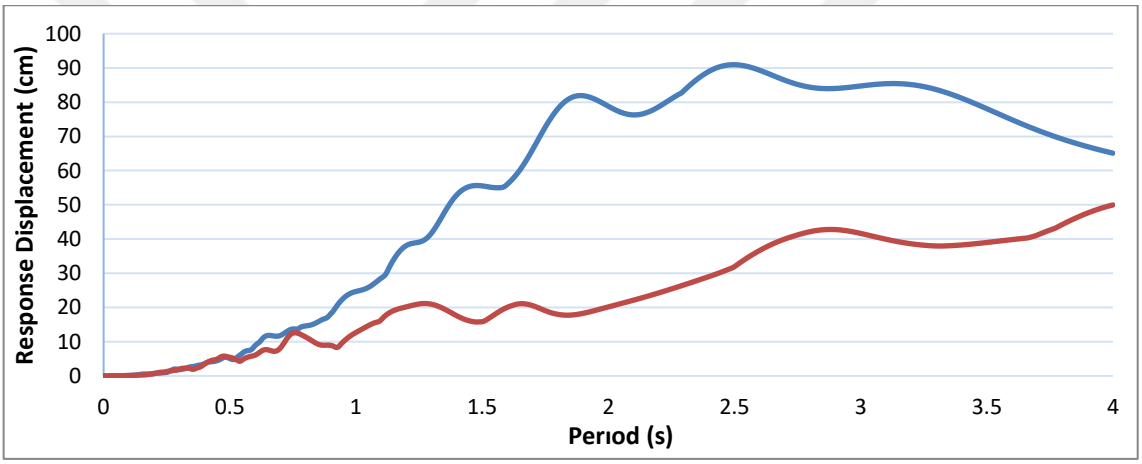

Figure 3.9: Superstition Hills-02 earthquake spectral displacement with 5% damping

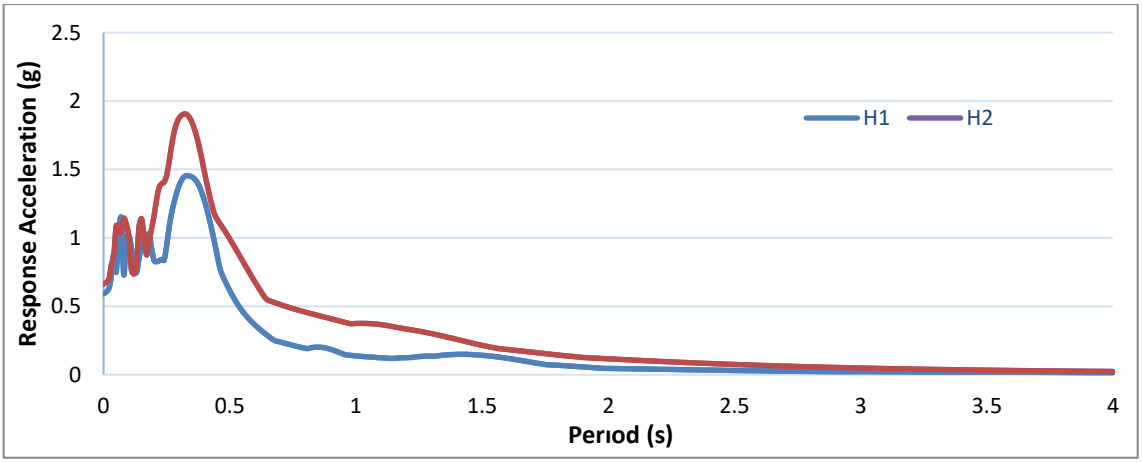

Figure 3.10: Cape Mendocino earthquake spectral acceleration with 5% damping

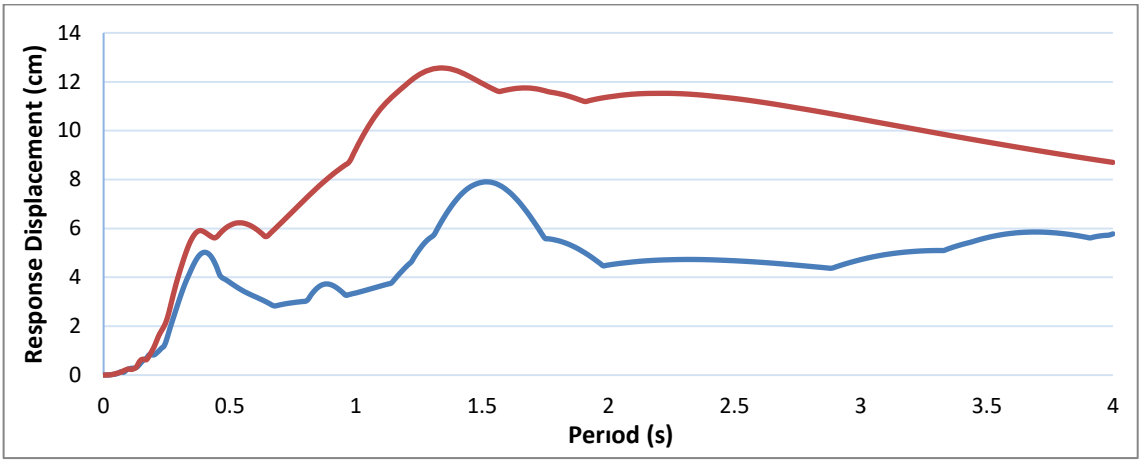

Figure 3.11: Cape Mendocino earthquake spectral displacement with 5% damping

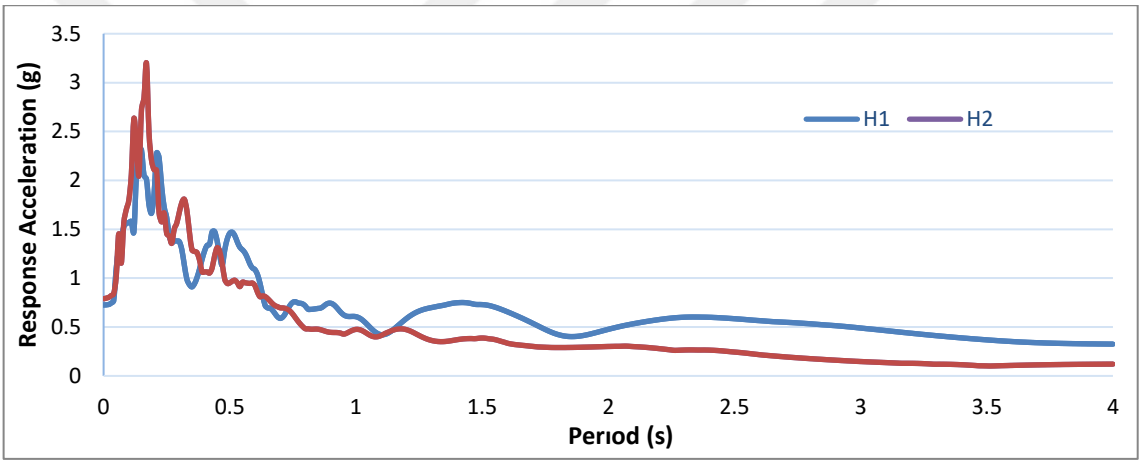

Figure 3.12: Lander earthquake spectral acceleration with 5% damping

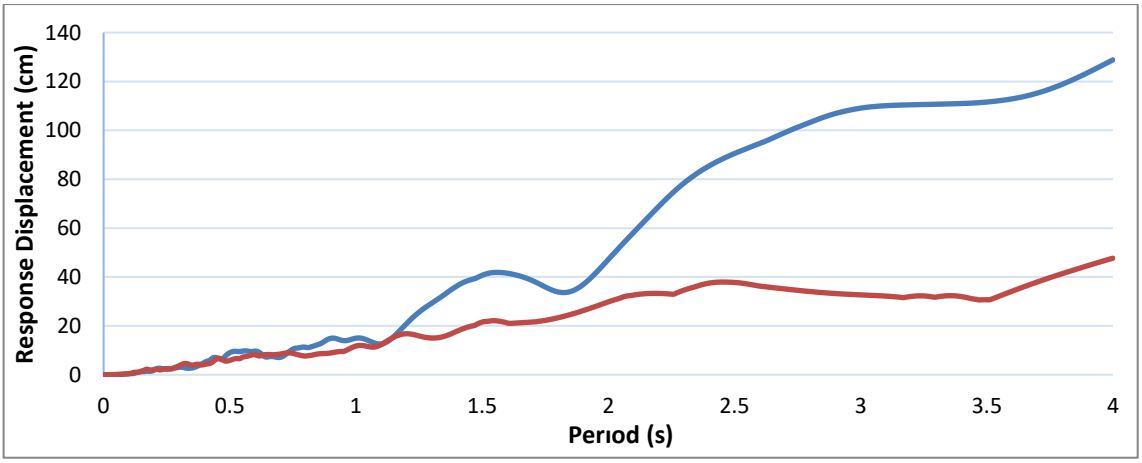

Figure 3.13: Lander earthquake spectral displacement with 5% damping

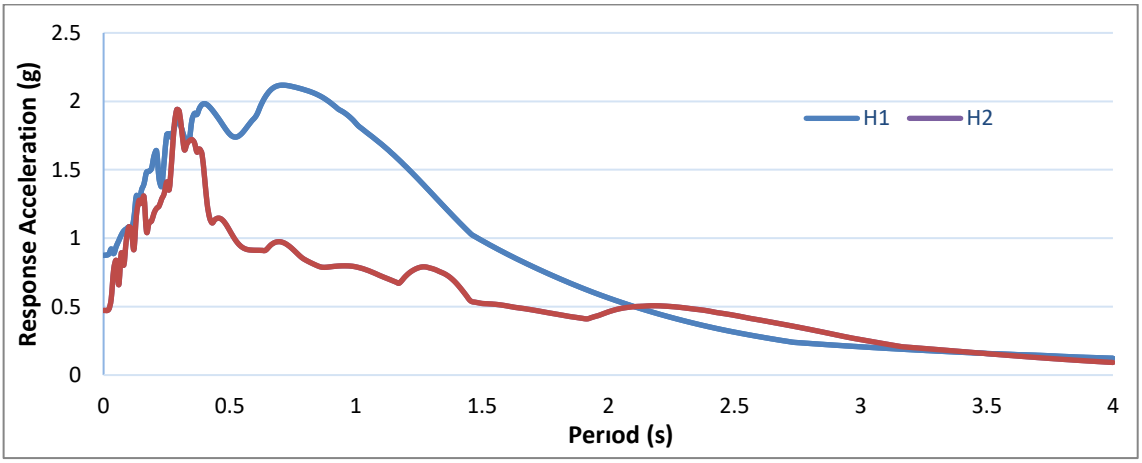

Figure 3.14: Northridge-01 earthquake spectral acceleration with 5% damping

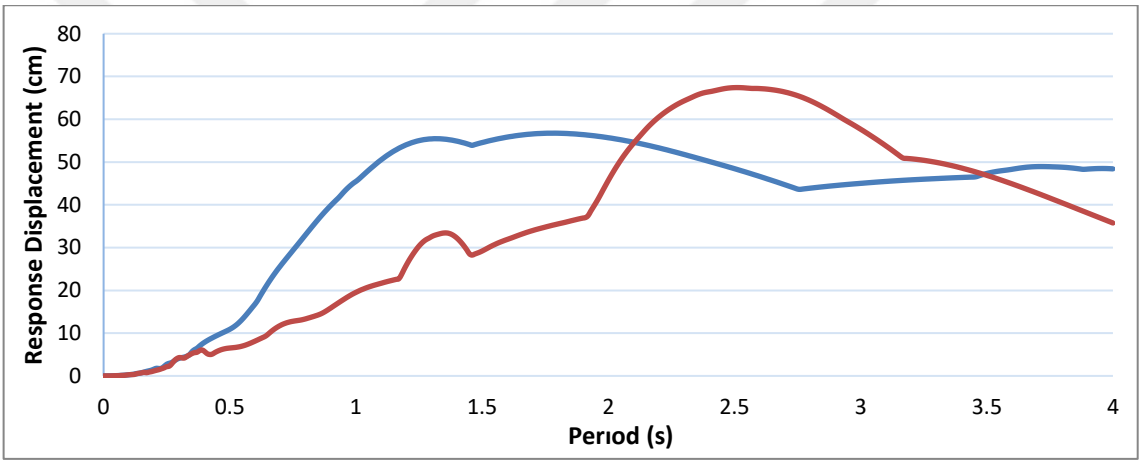

Figure 3.15: Northridge-01 earthquake spectral displacement with 5% damping

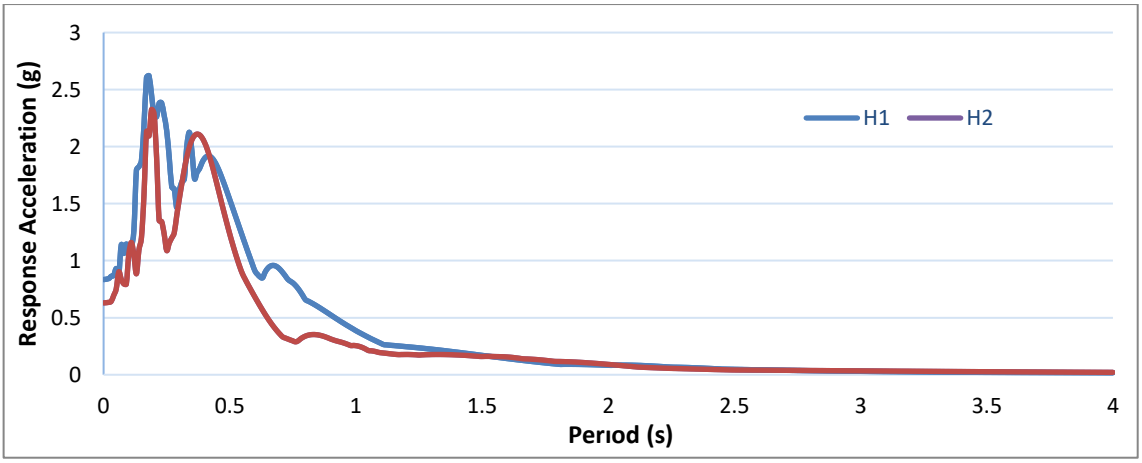

Figure 3.16: Kobe earthquake spectral acceleration with 5% damping

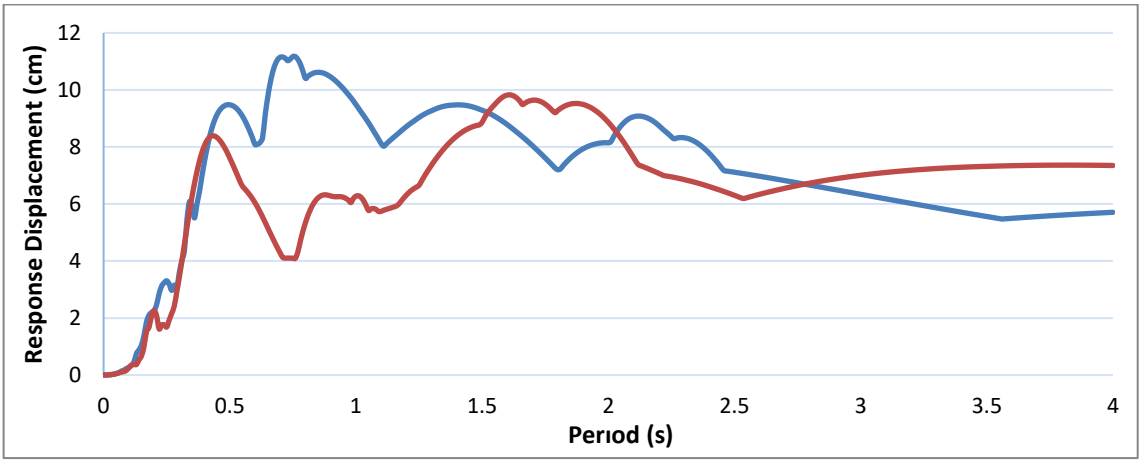

Figure 3.17: Kobe earthquake spectral displacement with 5% damping

3.4. SEISMIC ISOLATION SYSTEM MODELING AND ANALYSIS IN 3DBASIS

3DBASIS is a software that is used to conduct 3D modelling and analysis of seismically isolated buildings. The program does not have a user interface and data is entered by creating a separate input file.

This input file contains information such as superstructure parameters, number of floors of the building, floor height, floor masses, stiffness value of the superstructure or eigenvectors and the eigenvalues of the structure. The eigenvector and the eigenvalues of the building is obtained by modelling the superstructure as fixed base and carrying a modal analysis of the structure in a separate software. It also accepts data on isolation system parameters including the coordinates of the isolation system elements, record length, time step and the loading type (unidirectional or bidirectional) of the earthquake. All this data is entered in separate blocks.

For nonlinear analysis of the isolation system, in the input file, information such as the yield force (F_y), the yield displacement (D_y) and the ratio of post-yield stiffness to pre-yield stiffness (α) are entered for each isolator. To indicate the positions of the İsolator, the plan coordinates of the isolators are also entered into the file. Acceleration records for the performed analysis are created in a separate .dat format files. These files contain the earthquake records and are named WAVEX.dat and WAVEY.dat for X and Y directions, respectively.

Figure 3.18 and Figure 3.19 shows the 3DBASIS input for the case of nonlinear and equivalent linear analysis respectively. As shown in the figures, the isolator property input for each case

is different. For the case of equivalent linear modelling, the effective stiffness for each isolator and the effective viscous damping coefficient of each isolator is input.

As output, floor accelerations, relative floor displacements, floor shear forces, isolation system displacements and peak values of the isolation system elements can be obtained. While 3DBASIS software can analyse in the time domain, it cannot perform spectral analysis. The software gives results on a floor basis rather than on an element basis. Analysis results are given in degrees of freedom. The degrees of freedom are given in the order from the top floor to the bottom. For a 3-storey seismic isolated building: isolation Base + 3 floors = 4 x 3 DOF = 12 DOF. For example, for the 3-story building examined in this study, the 10th degree of freedom indicates the ground floor x direction values.

When the 3DBASIS program is run, it also creates an output file that contains detailed time history analysis results. This information in the output file includes time history outputs at floor degrees of freedom for displacement and acceleration, structure shear at top of base, force and displacement time history of specifically selected bearings. For the purpose of this study, the acceleration time history for the top floor of the structure was obtained and applied at the base of the rack system modelled separately on Sap2000 program as will be explained in the proceeding sections.

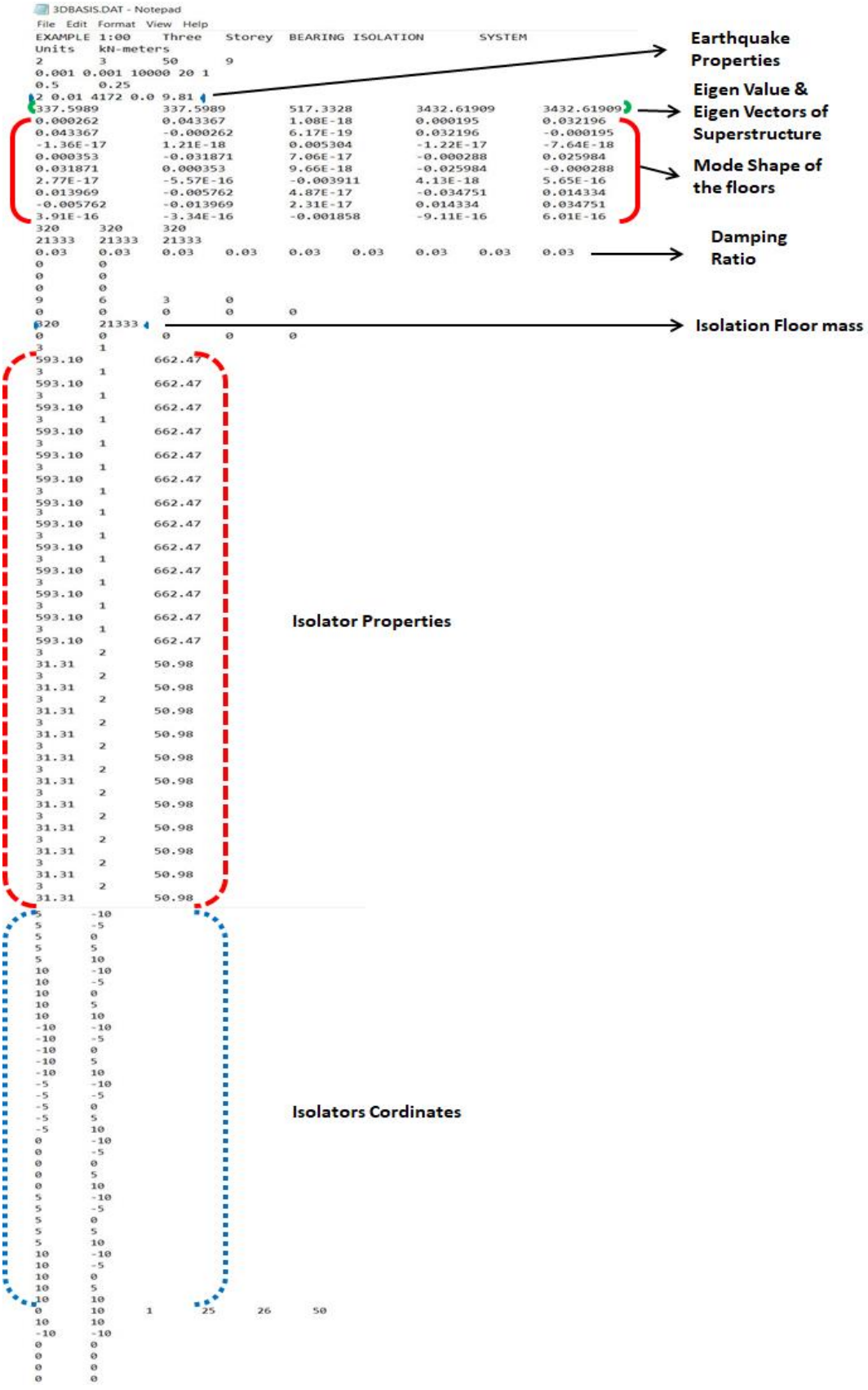

Figure 3.18: 3DBASIS input for equivalent linear analysis

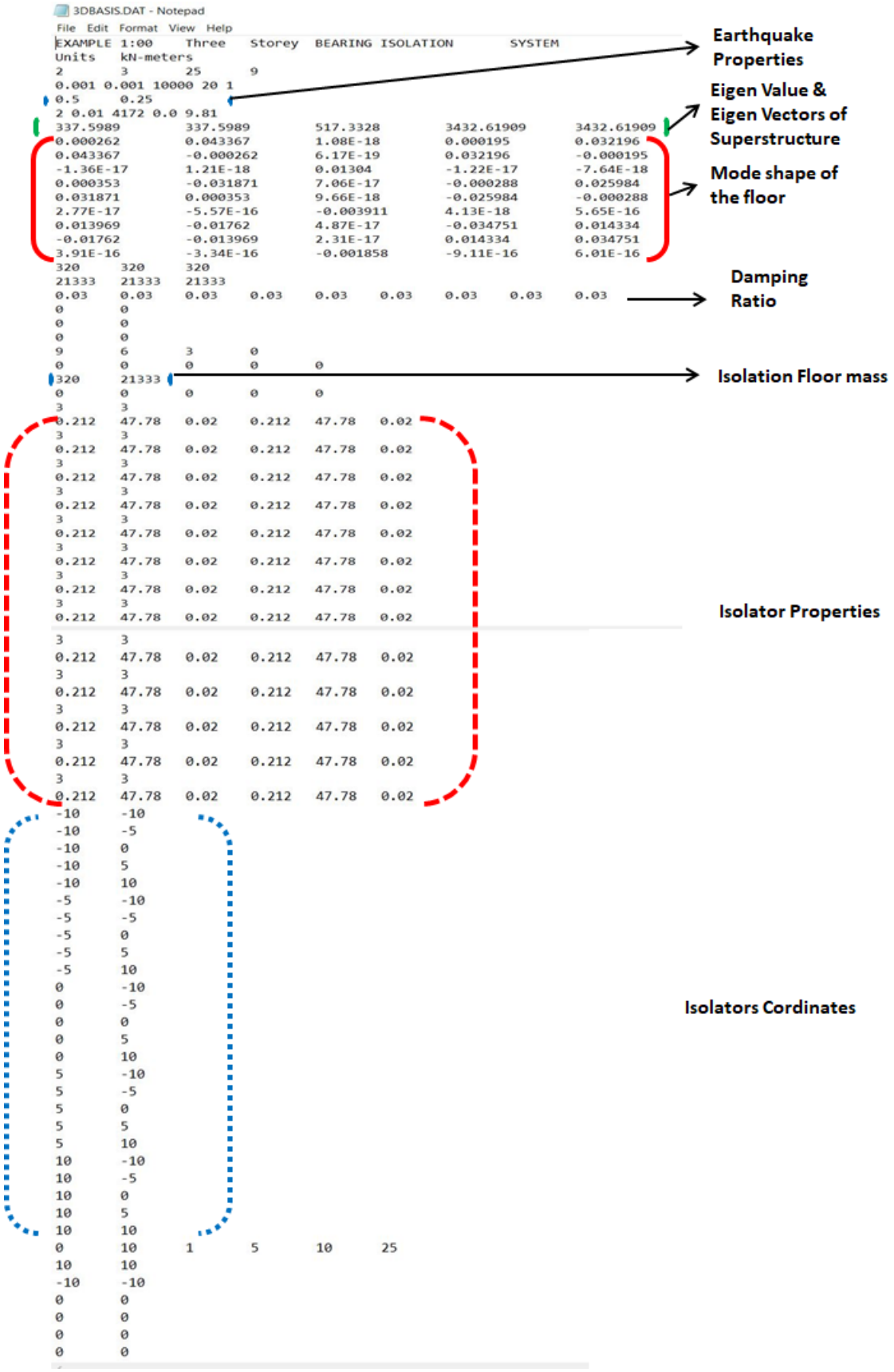

Figure 3.19: 3DBASIS input for nonlinear analysis

3.5. MODELLING OF THE RACK SYSTEM

The rack models used in the study all have 3 floors with natural periods of vibration of 0.1 s, 0.2 s, and 0.3 s. Each of the rack is given a distinct label and is given in Table 3.6. The first 3 modes of the rack with 0.1 s is shown Figure 3.21. The racks are assumed to be placed at the top floor of the isolated structure and their responses are observed under six different earthquakes. They are modelled in finite element analysis program Sap2000 as a fixed base frame. These frames were modelled as single bay along both the x-axis and the y-axis. (see Figure 3.20). The building is initially analysed in 3DBASIS. The time history obtained at the top floor of the isolated building for both equivalent linear and nonlinear analysis is applied to the rack model at the base of the rack. This is done in the Sap 2000 program which is used to model the racks. The time histories obtained from the 3DBASIS is input into Sap2000 for both equivalent linear and nonlinear cases as shown in Figure 3.22.

Table 3.6: Rack name and period

Rack Label	Rack Period (s)
RT01	0.1
RT02	0.2
RT03	0.3

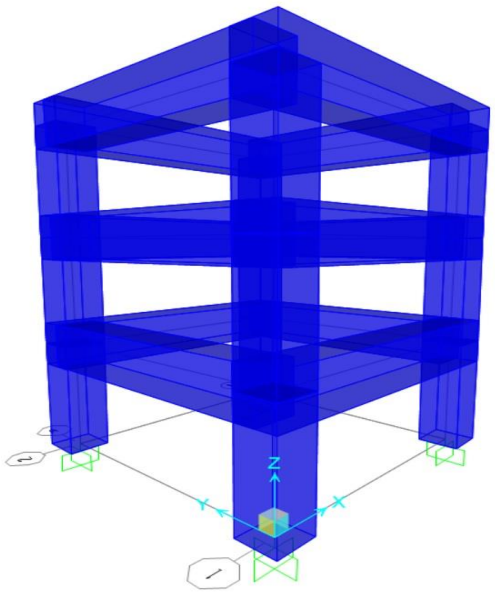

Figure 3.20: 3D Rack Model

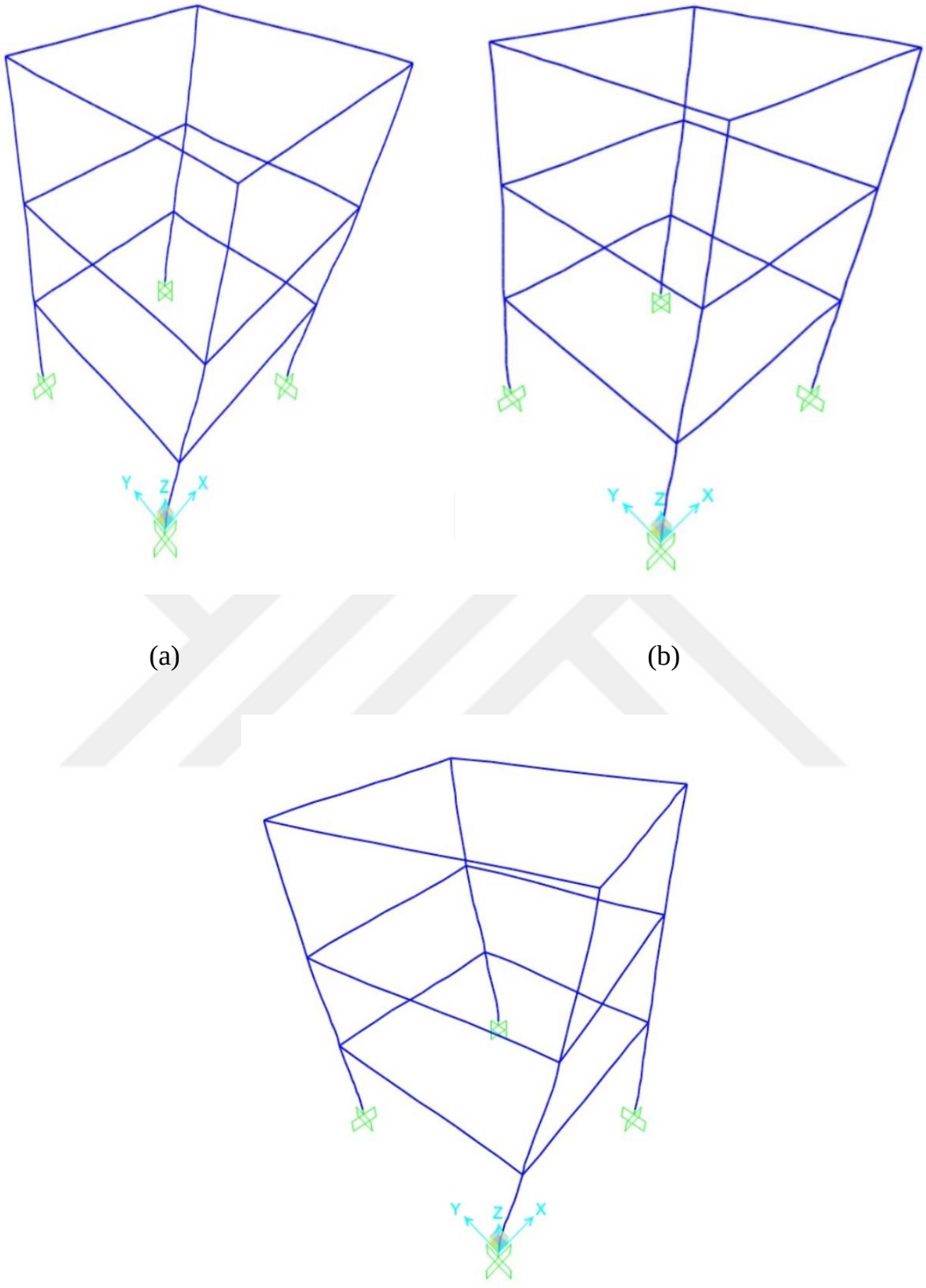

(a) (b)

(c)

Figure 3.21: Mode forms of 3-storey Rack (a) first mode (b) second mode (c) third mode torsion.

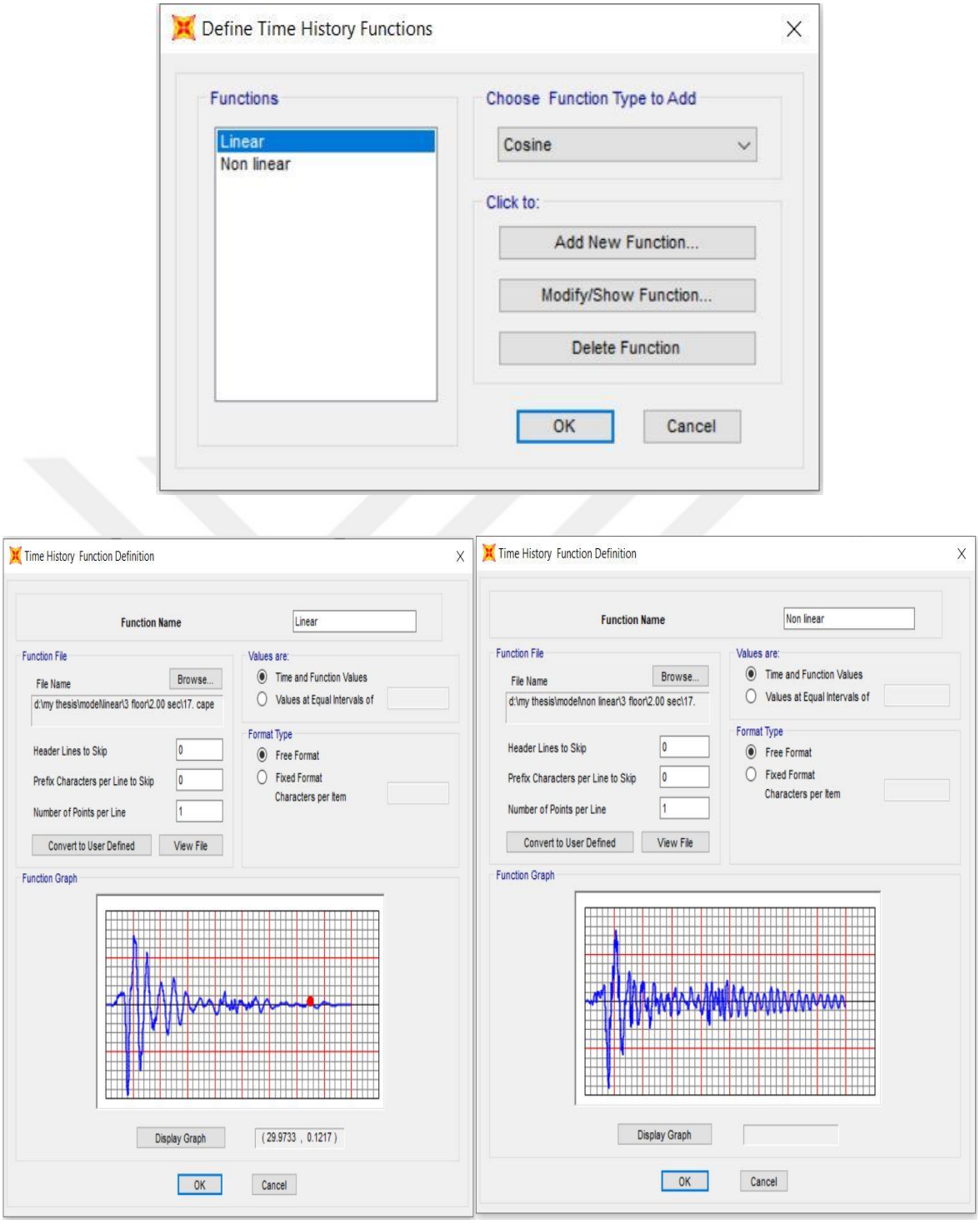

Figure 3.22: Definition of acceleration time history on Sap 2000 program for both equivalent linear and nonlinear cases

4. RESULTS

In this section, the response of the rack models will be investigated. The results obtained from the analyses of the rack models both for equivalent linear and nonlinear analysis are presented below.

We will investigate how the response of the racks on an isolated structure discussed in section 3 is affected by different modelling and analysis methods (i.e. nonlinear and equivalent linear). The structural responses obtained from the rack analyses presented in this section are floor accelerations and floor displacements. In order to interpret these results comprehensively, the following comparisons shall be done.

1. Rack floor acceleration time history
2. Peak Rack floor acceleration
3. Root Mean Square (RMS) rack floor acceleration
4. Rack floor displacement time history
5. Peak Rack floor displacement
6. Root Mean Square (RMS) rack floor displacement

There are 6 near fault earthquakes used in this study. For the rack floor acceleration and displacement time histories, plots of two earthquakes as representatives are presented. Similarly, graphs of two of the four isolation systems used in this study are presented in the analysis of the acceleration and displacement time histories.

The comparison of the time history results may give us an idea on how close the results of the two analysis methods are but it is not enough to make a judgement. That is why along with the time history plots, peak floor accelerations and displacements are also compared. The peak value is the maximum absolute of the time history results. The peak rack floor accelerations and the peak rack floor displacements obtained from nonlinear analyses are divided by those obtained from equivalent linear analyses to obtain “ratios”. The plots of these ratios for all racks and all isolation systems under each earthquake are presented.

In addition, the Root Mean Square (RMS) values from the time history results are also calculated. This is because in some cases, time history analysis results may have close peak values for equivalent linear and nonlinear cases but that may not necessarily mean that the time

history results would overlap at all time points. RMS is a good tool to study this. RMS is obtained by squaring all the values of the acceleration (or displacement) values in the time set and then finding the arithmetic mean of the squares. Then the square root of the result taken. The RMS rack floor acceleration (or displacement) obtained from nonlinear analysis is divided by the RMS rack floor acceleration (or displacement) obtained from equivalent linear analysis to obtain a ratio. The plots of these ratios for all racks and all isolation systems under each earthquake are presented.

Finally, the average of the ratios in terms of peak floor accelerations, peak floor displacements, RMS floor accelerations, and RMS floor displacements are studied for each earthquake and for each isolation system to observe how the type of the isolator and the earthquake type influence the outcome.

4.1. RACK FLOOR ACCELERATION

The floor acceleration results of the analyses made for the rack models placed on seismically isolated buildings are shown in Figure 4.1 to Figure 4.20.

4.1.1. Rack Floor Acceleration Time History

The comparison of the floor acceleration time histories of racks that are located on nonlinear and equivalent linear isolation systems are presented.

4.1.1.1 RT01 Rack Model

The acceleration time history response of the rack with period of 0.1s located on buildings with nonlinear and equivalent linear isolation systems are presented for two representative isolation systems (NL20 and NL30) and under two representative historical earthquakes namely Cape Mendocino and Northridge. The response at each floors of the rack is presented in Figure 4.1 - Figure 4.4.

As it can be seen from Figure 4.1 - Figure 4.2, the result obtained for Cape Mendocino earthquake follows the general trend and the two plots overlap for both NL20 and NL30 at all floors of the rack. In other words, the result response obtained is almost same for both equivalent linear and nonlinear analysis methods. However, for the case of Northridge earthquake as shown in Figure 4.3- Figure 4.4 the plots for both equivalent linear and nonlinear

tend to follow the general trend except that the equivalent linear plot is seen to be smoother than the nonlinear plot. This is expected as the nonlinear plot tend to capture more detailed behaviour of the earthquake motion. In addition to that, there is slight variation of the peak values of the two plots at all floor of the rack model. This is more visible specially at higher floors (2^{nd} and 3^{rd} rack Floor). It is seen that the success of equivalent linear modelling for predicting rack response depends on the earthquake type characteristic and isolation system type.

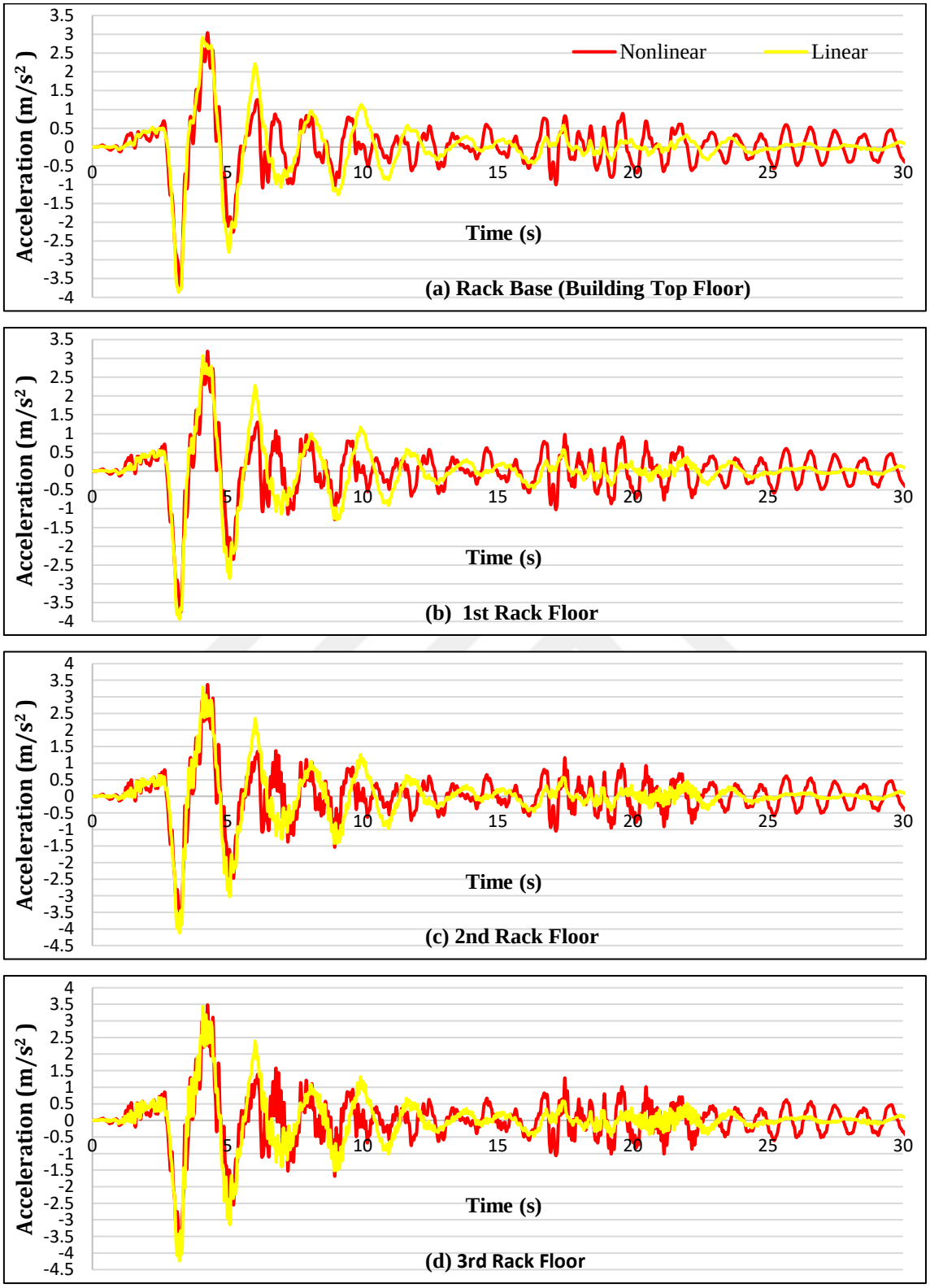

Figure 4.1: Acceleration at each floor for RT01 rack model under NL20 isolation system (Cape Mendocino EQ)

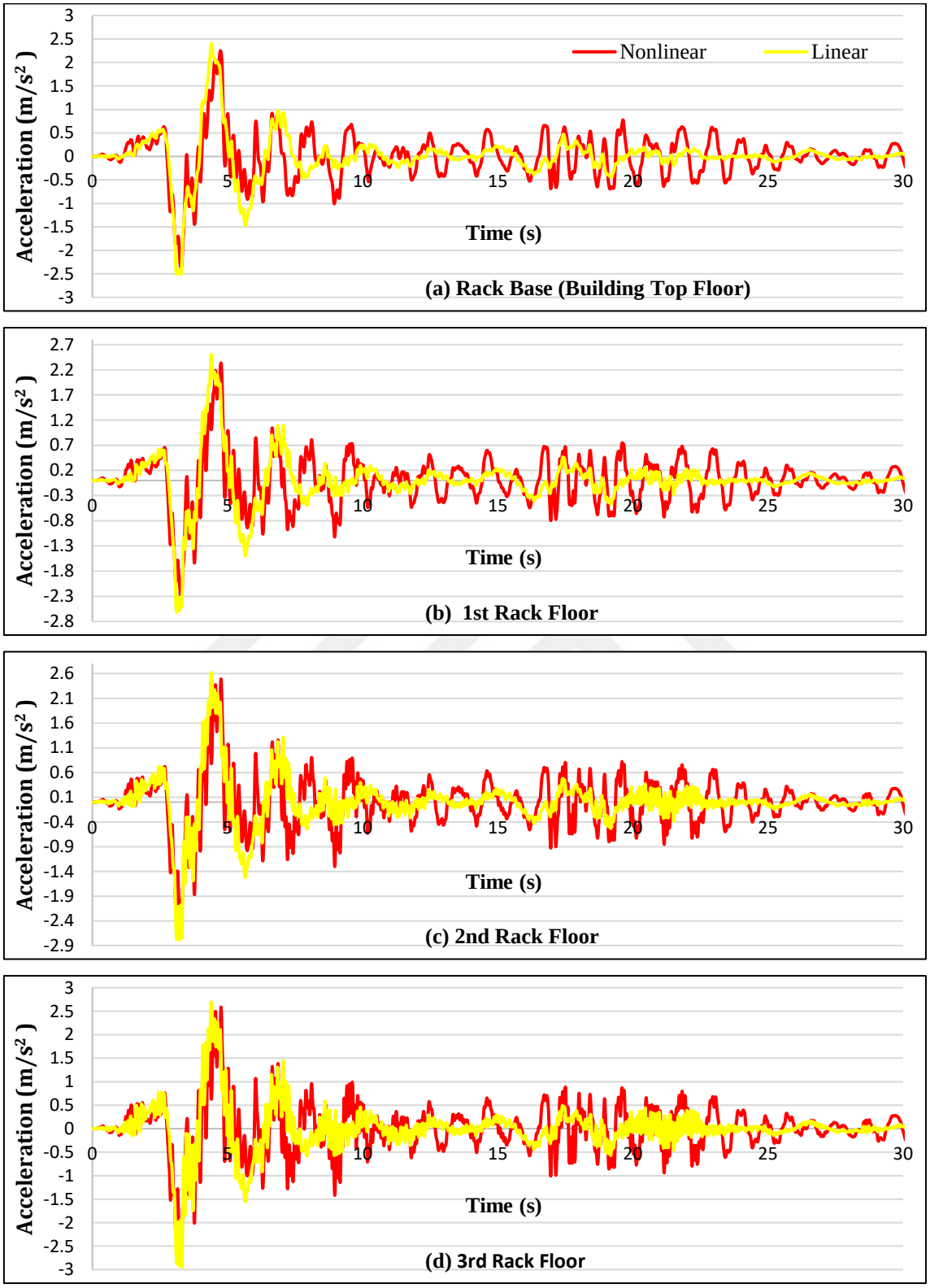

Figure 4.2: Acceleration at each floor for RT01 rack model under NL30 isolation system (Cape Mendocino EQ)

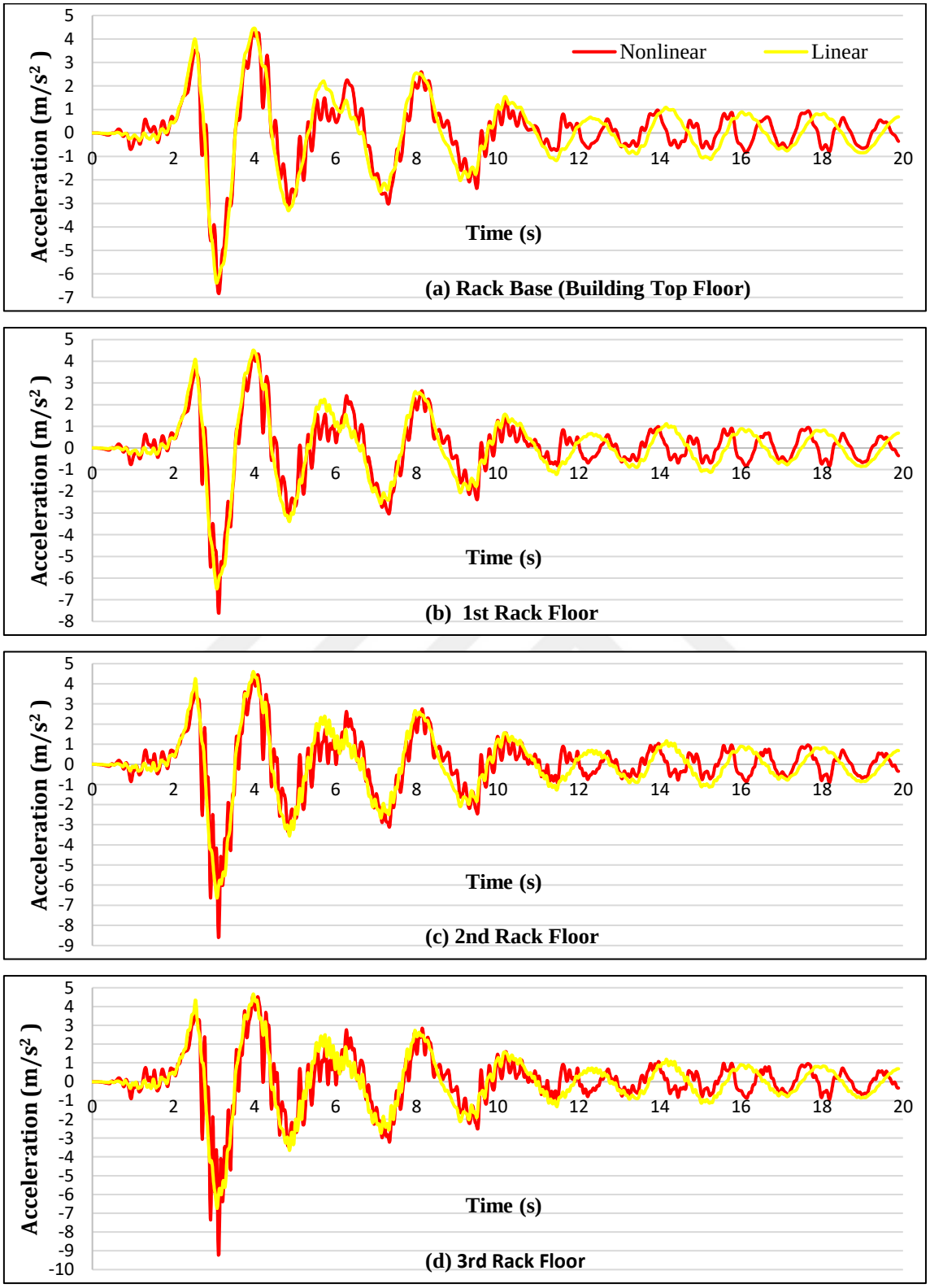

Figure 4.3: Acceleration at each floor for RT01 rack model under NL20 isolation system (Northridge EQ)

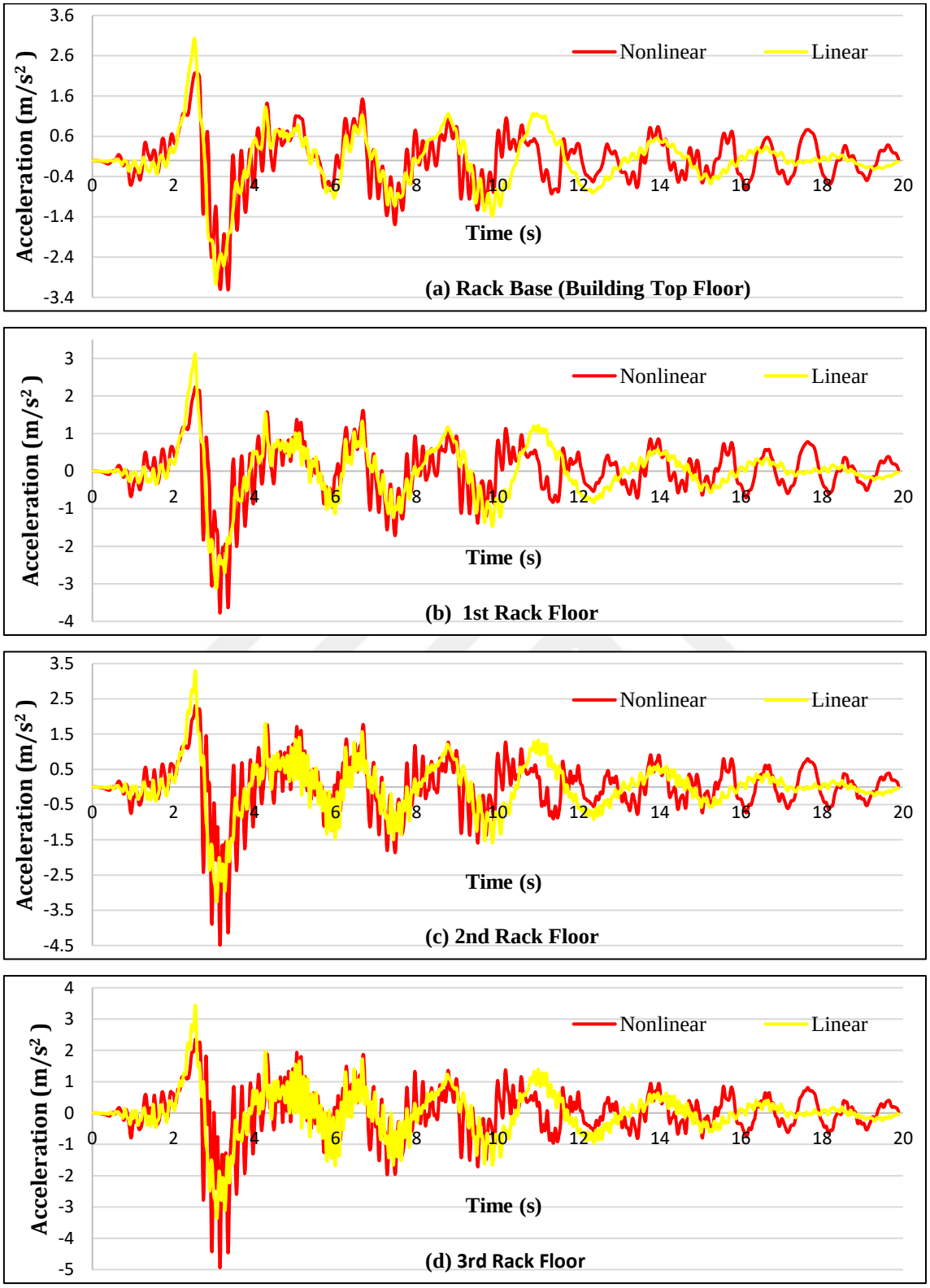

Figure 4.4: Acceleration at each floor for RT01 rack model under NL30 isolation system (Northridge EQ)

3.1.1.2. RT02 Rack Model

The acceleration time history response of the rack with period of 0.2s located on building with nonlinear and equivalent linear isolation systems are presented for two representative isolation systems (NL20 and NL30) and under two representative historical earthquakes namely Cape Mendocino and Northridge. The response at each floors of the rack is presented in Figure 4.5 - Figure 4.8.

The results obtained for both Cape Mendocino earthquake and Northridge earthquake for the case of RT02 indicate higher discrepancy between the equivalent linear and nonlinear compared to RT01, which shows that the success of equivalent linear modelling also depends on the dynamic characteristics of the rack. While the difference in the plots are only visible at the peak points for the case of RT01, for the case of RT02 the difference in the plot is clearly visible and spread along the entire plot. Also as was the case with RT01 the difference in the plots is more at the higher floors of the rack.

The peak accelerations for equivalent linear and nonlinear cases are highly different. For example, as can be seen in Figure 4.5, while peak acceleration for equivalent linear case is around 3 m/s^2 for the 3^{rd} floor of the rack, the Nonlinear analysis plot indicate a peak acceleration of higher than 6 m/s^2. The same can be observed for Figure 4.6, Figure 4.7 and Figure 4.8. The results in terms of peak accelerations will be discussed in more depth in the following subsections but it can be said that equivalent linear models underestimate the rack's response acceleration compared to their real values obtained using nonlinear models. In study conducted by (Alhan and Özgür, 2015) it was observed that the equivalent linear models underestimated the response of the isolation system. However, in that study the focus was on the isolated building and not on the content of the building.

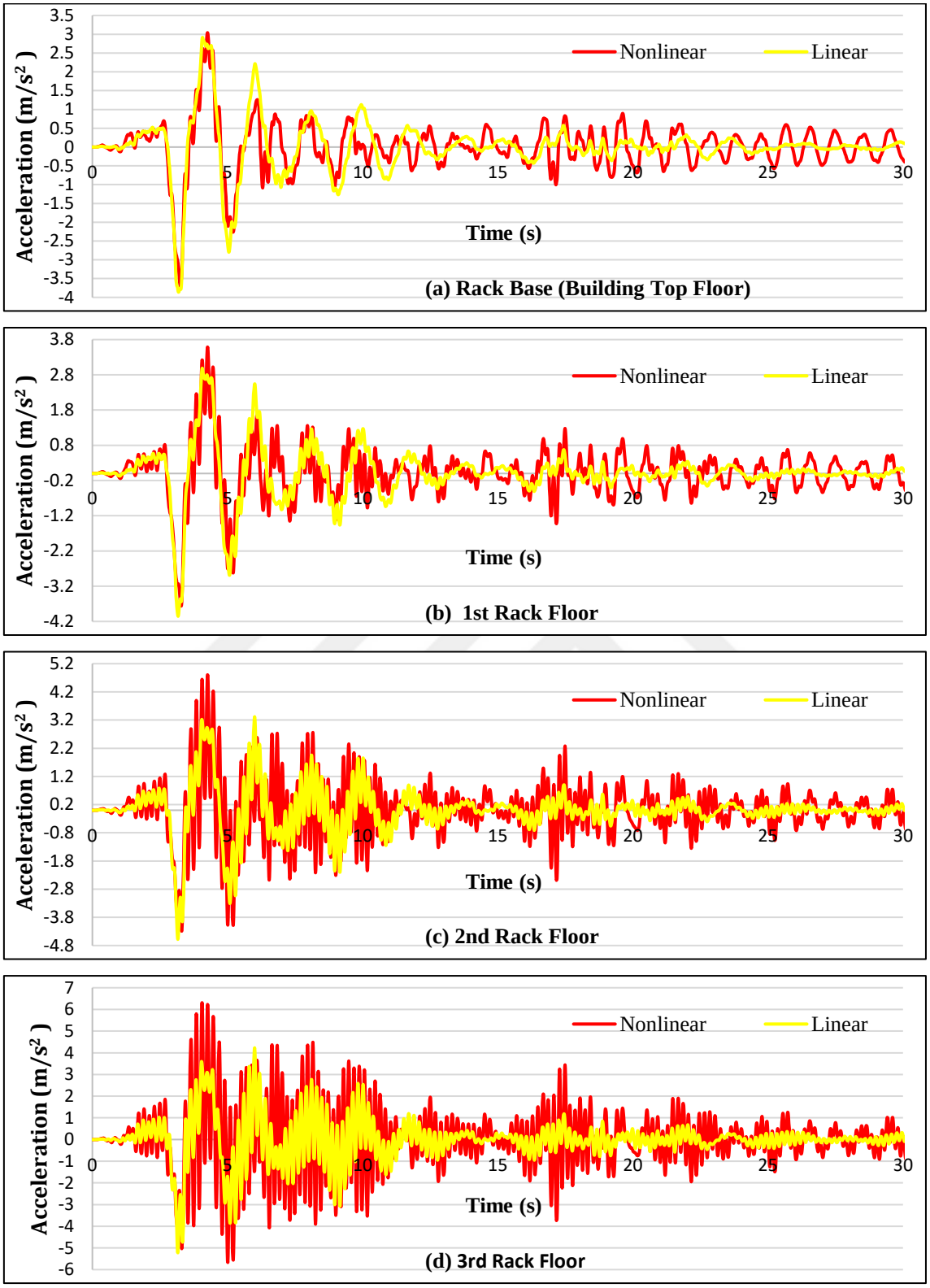

Figure 4.5: Acceleration at each floor for RT02 rack model under NL20 isolation system (Cape Mendocino EQ)

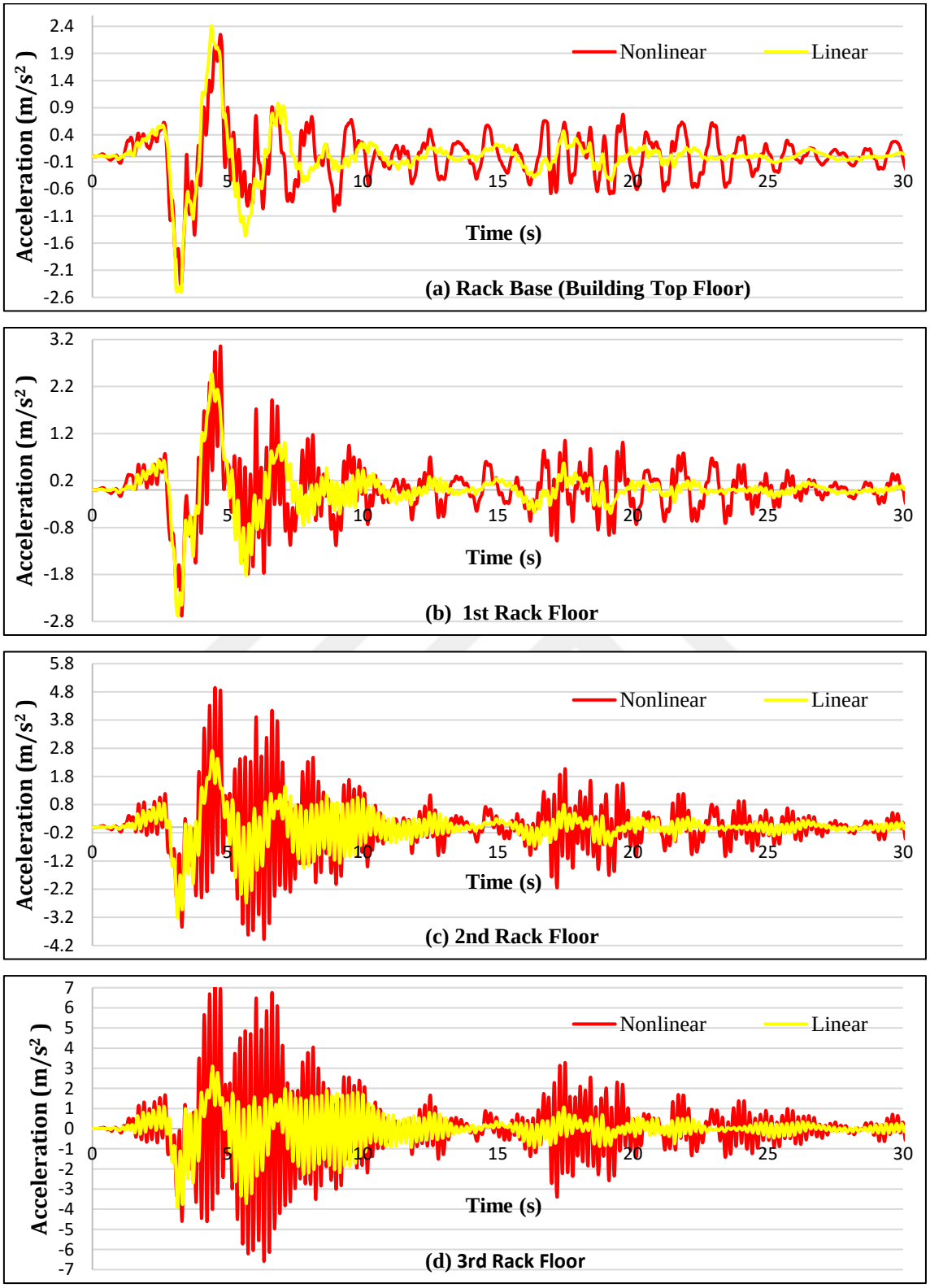

Figure 4.6: Acceleration at each floor for RT02 rack model under NL30 isolation system (Cape Mendocino EQ)

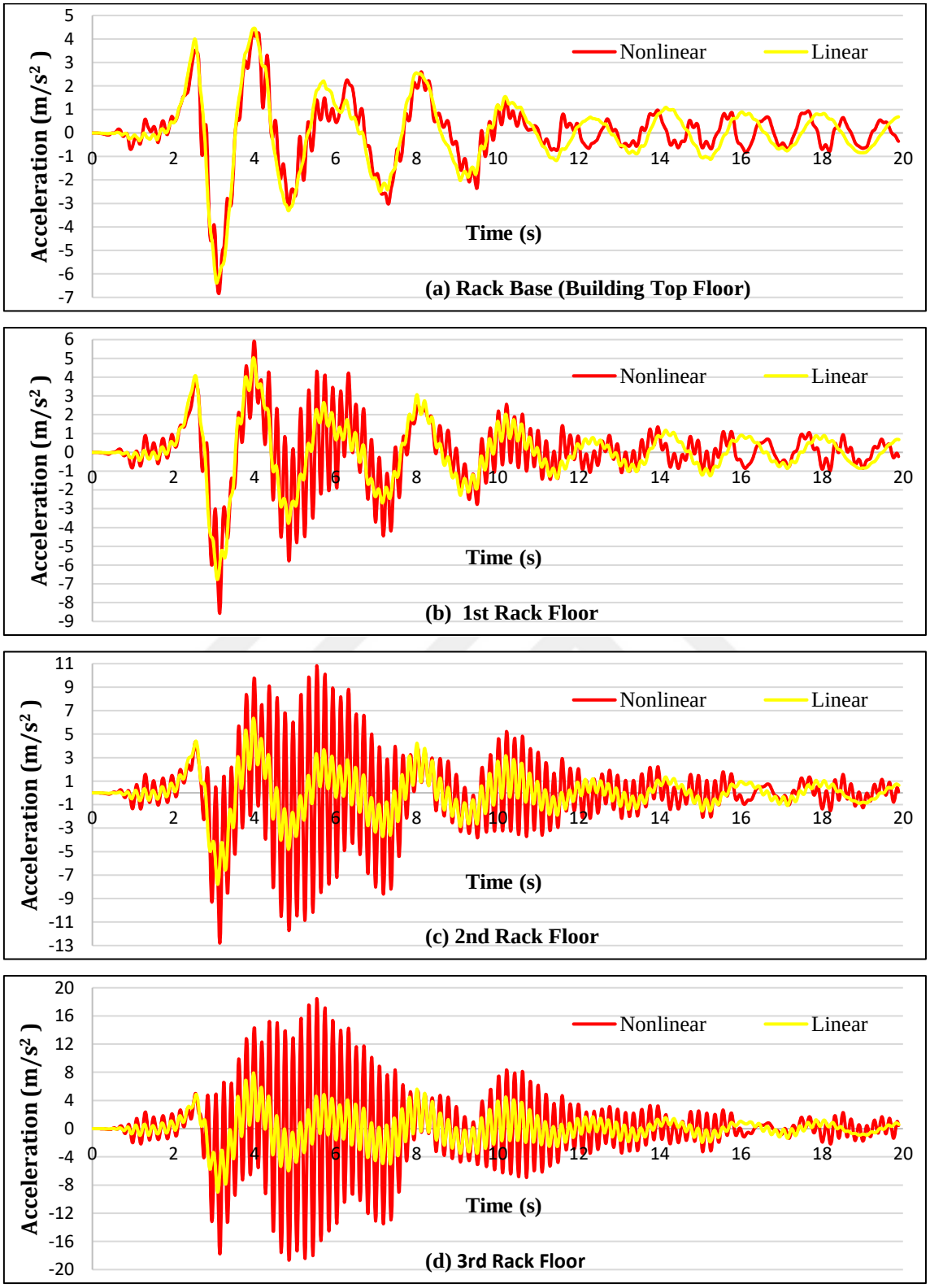

Figure 4.7: Acceleration at each floor for RT02 rack model under NL20 isolation system (Northridge EQ)

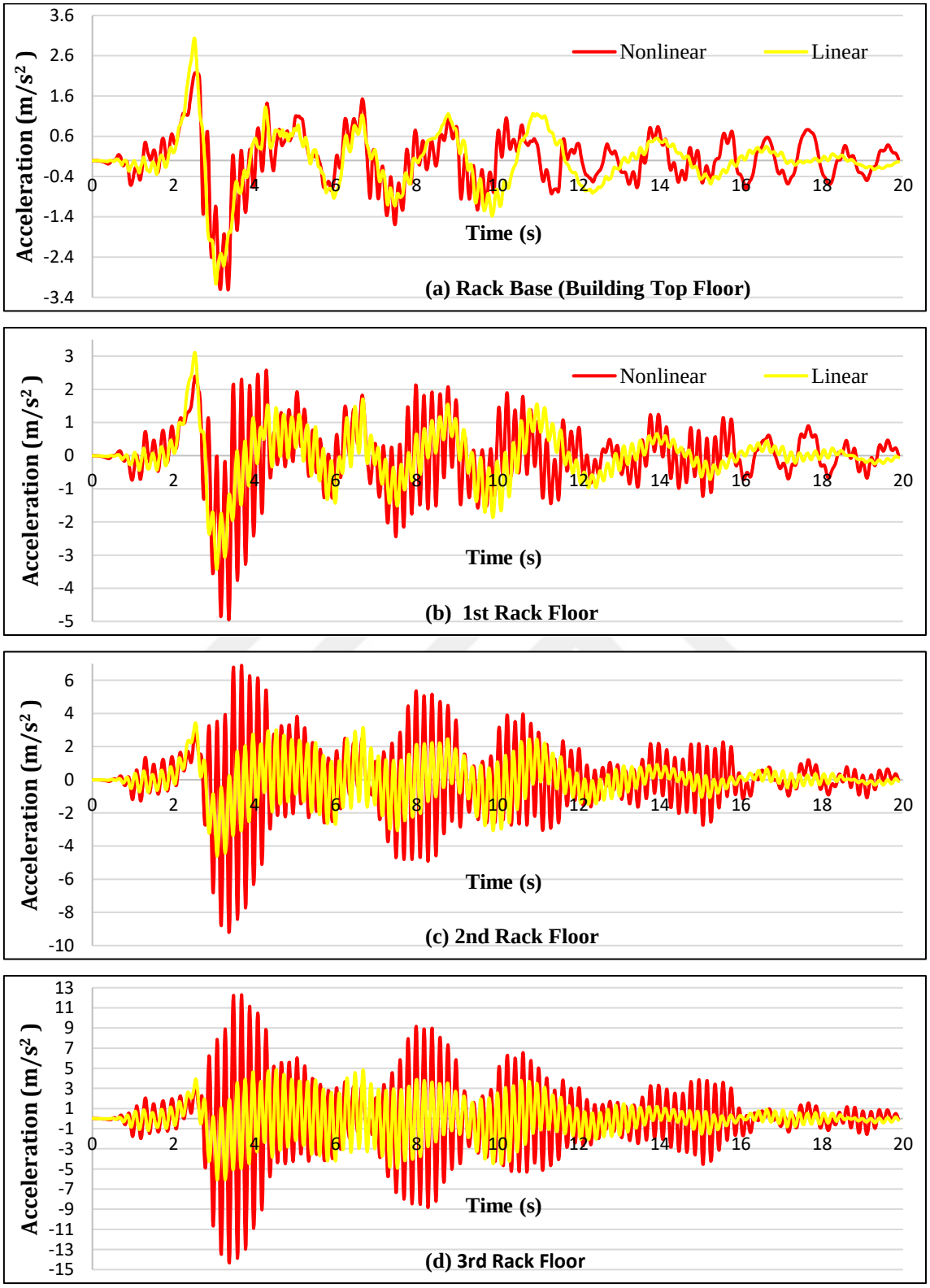

Figure 4.8: Acceleration at each floor for RT02 rack model under NL30 isolation system (Northridge EQ)

3.1.1.3. RT03 Rack Model

The acceleration time history response of the rack with period of 0.3s located on buildings with nonlinear and equivalent linear isolation systems are presented for two isolation systems (NL20 and NL30) and under two historical earthquakes namely Cape Mendocino and Northridge. The responses at each floor of the rack are presented in Figure 4.9 - Figure 4.12.

As it can be seen from Figure 4.9 - Figure 4.12, the result obtained depends on the earthquake and the isolation system. In general, the plots for RT03 exhibit less differences compared with RT02 discussed before. While there is little to none difference between the plots in case of Northridge earthquake for NL20 isolation system as shown in Figure 4.11, the plot of the same earthquake for NL30 isolation system shows visible difference.

For the case of Cape Mendocino earthquake there is visible difference between the plots for the case of both NL20 and NL30. However, this difference in the plots are less compared to plots observed for RT02 discussed before.

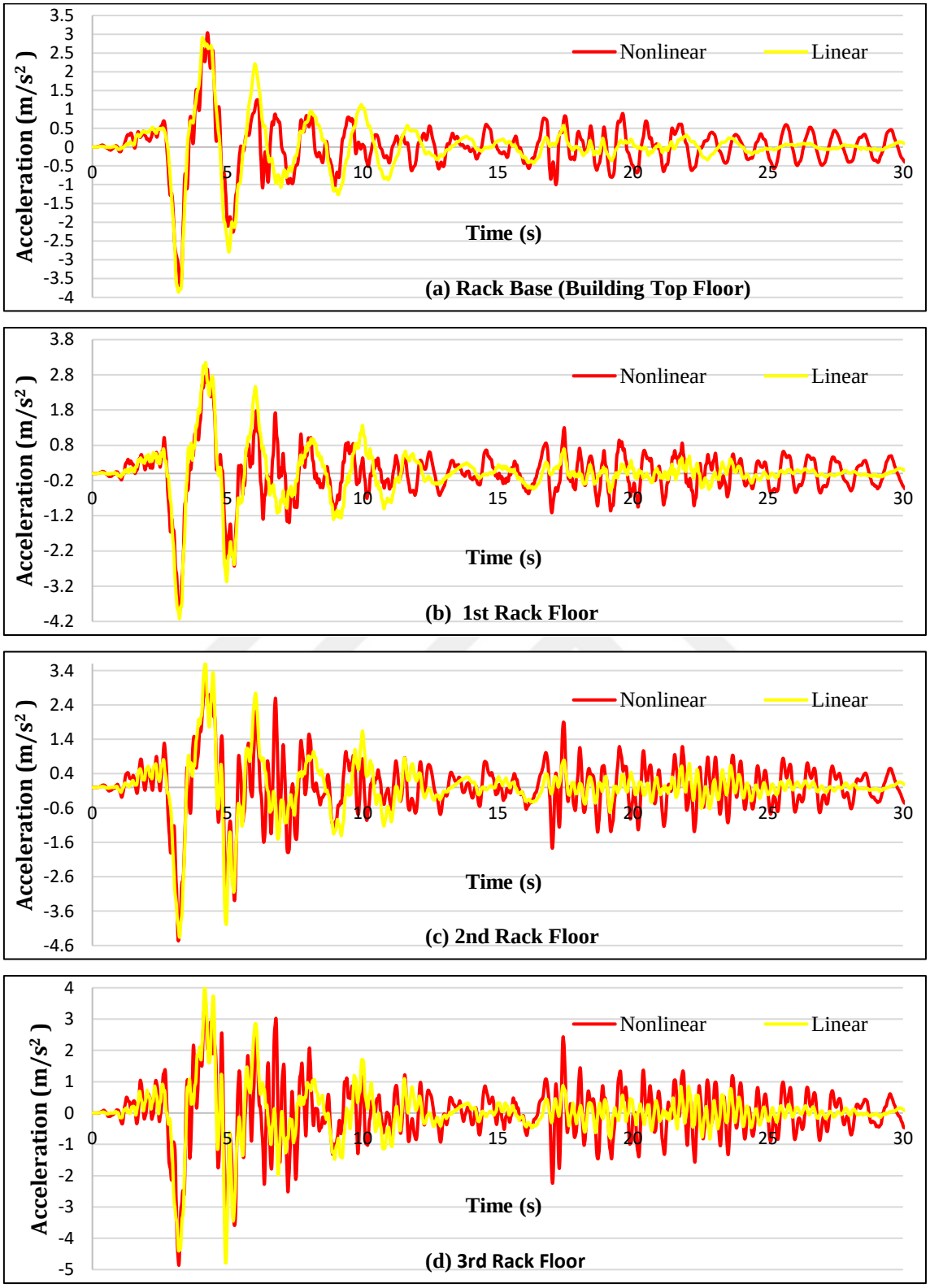

Figure 4.9: Acceleration at each floor for RT03 rack model under NL20 isolation system (Cape Mendocino EQ)

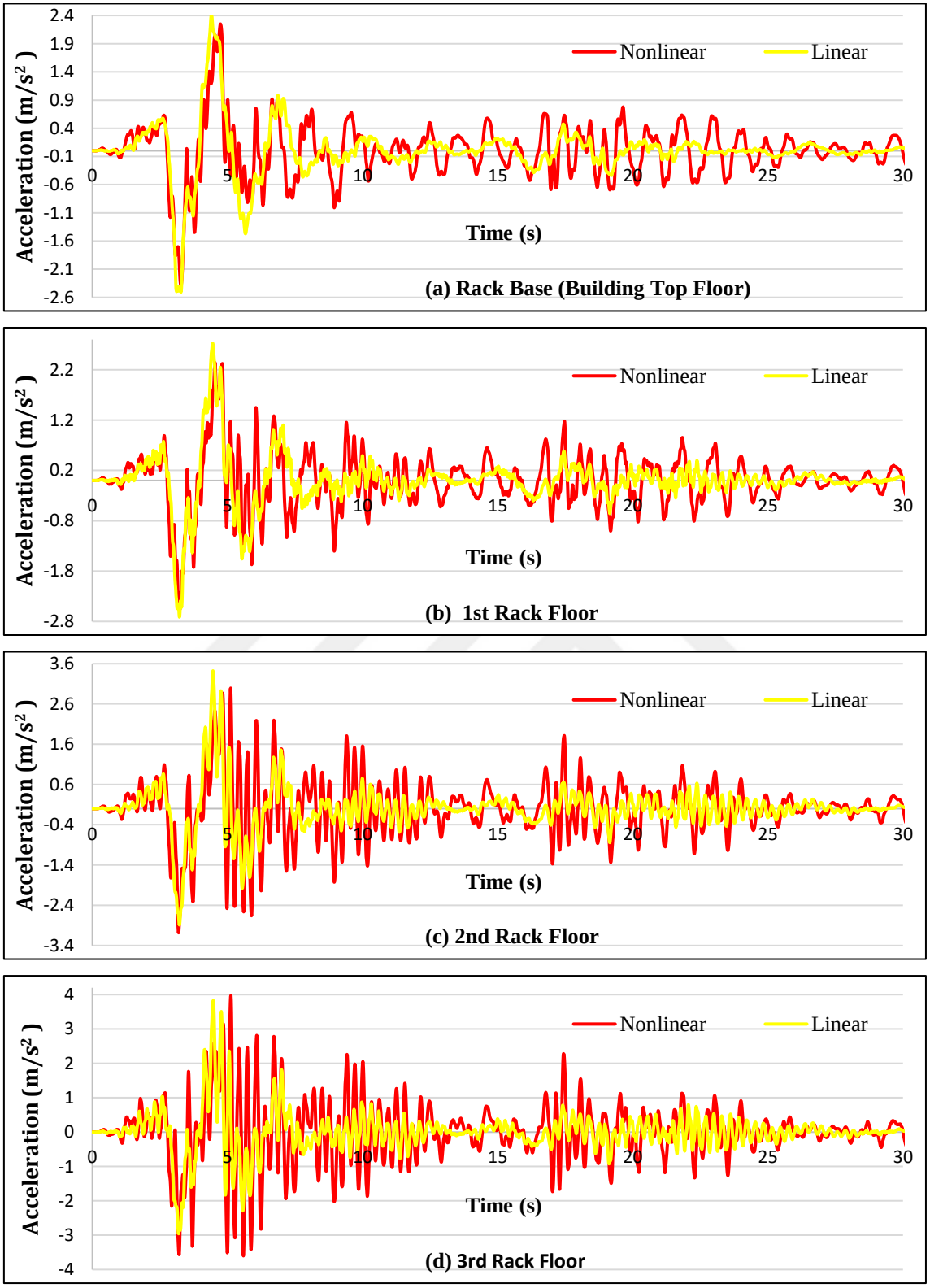

Figure 4.10: Acceleration at each floor for RT03 rack model under NL30 isolation system (Cape Mendocino EQ)

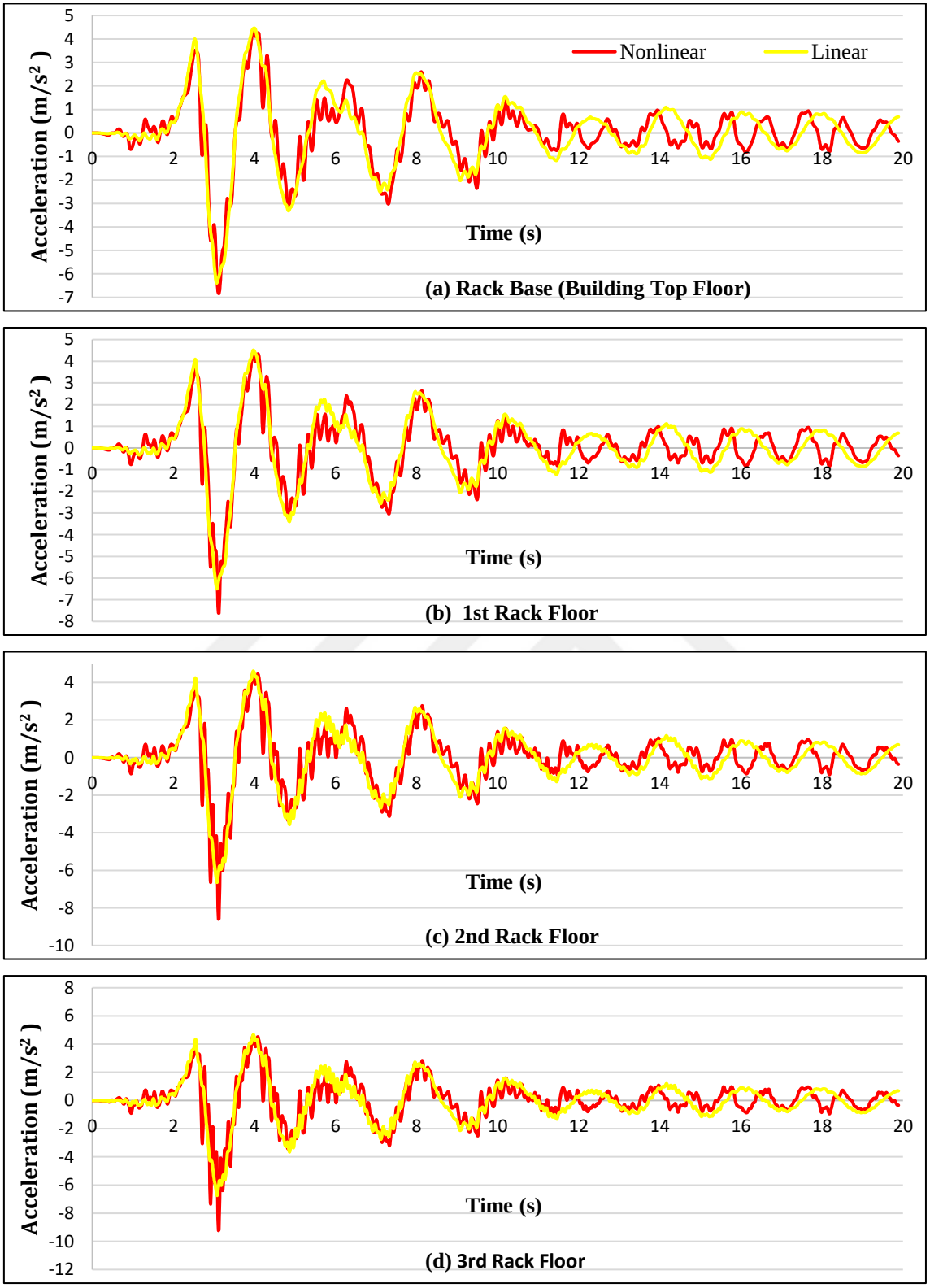

Figure 4.11: Acceleration at each floor for RT03 rack model under NL20 isolation system (Northridge EQ)

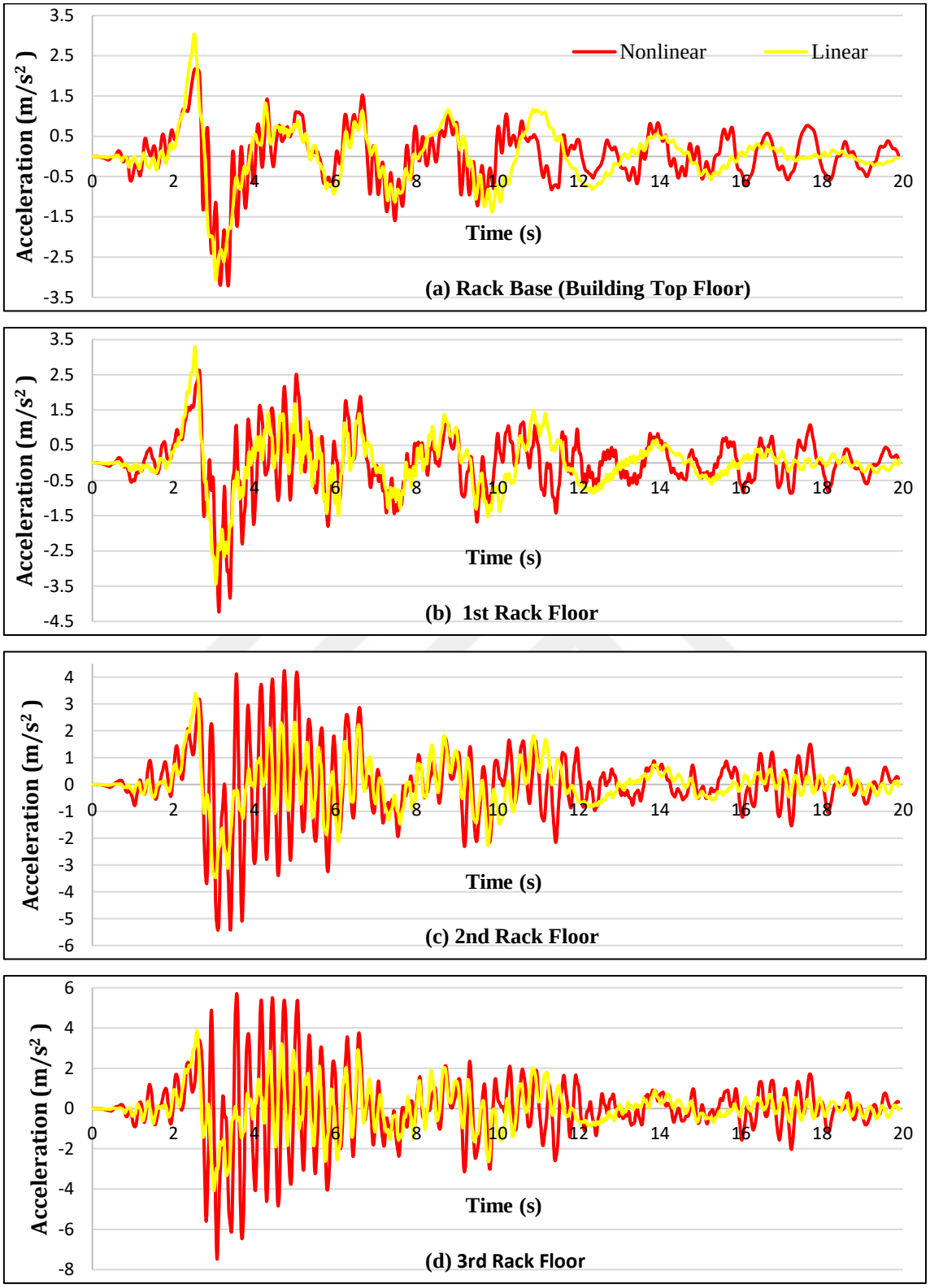

Figure 4.12: Acceleration at each floor for RT03 rack model under NL30 isolation system (Northridge EQ)

4.1.2. Peak Rack Floor Acceleration

In order to further understand the behaviour of floor acceleration of the racks for both equivalent linear and nonlinear case, the nonlinear to equivalent linear ratio of peak acceleration for all the racks for all isolation systems and for each earthquake are presented. To better visualize, a solid dashed line is drawn at 1.0 in each graph, to indicate a perfect estimate of equivalent linear modelling. Results below and above this line corresponds to conservative and unconservative estimates of the equivalent linear modelling, respectively.

To illustrate the earthquake-based change, nonlinear to equivalent linear peak rack floor acceleration plots for the all floors of the rack models are presented for all isolation systems. As can be observed from Figure 4.13 and Figure 4.14, the ratio of peak acceleration is dependent on the type of earthquake loaded. For example, in the case of isolation system NL20, at the top floor of the rack RT02, the smallest ratio is 1.79 (Landers Earthquake) and the highest rate can go up to 3.01 (Kobe Earthquake). Similarly, for the case of NL30 and RT03 the smallest ratio is observed for the Cape Mendocino Earthquake (1.04) and the highest ratio for San Fernando Earthquake (2.01).

The efficacy of the equivalent linear modelling also varies depending on the isolation system. For example, as can be seen in Figure 4.13 (a) in the case of San Fernando Earthquake at the top floor of the rack RT02, the smallest peak acceleration ratio is observed for isolation system NL30 (1.72) while the highest ratio for NL20 (2.55). Similarly, as shown in Figure 4.14 (d), for the case of Lander Earthquake, for RT03, the smallest peak acceleration ratio is observed for isolation system NL35 (1.0) and the highest peak acceleration ratio observed for isolation system NL20 (1.37).

In Figure 4.15 the average peak acceleration ratio of the isolation system per earthquake is presented. The dependence of the response ratio on the rack period can be observed. While the highest ratio for RT01 is 1.38 (Northridge Earthquake), for RT02 it is 3.20 (Kobe Earthquake) and for RT03 it is 1.82 (San Fernando Earthquake). Additionally, in Figure 4.16, the average peak acceleration ratio of the earthquakes per isolation system is presented. It can be observed that the response depends on the rack type (rack period) with RT02 exhibiting the highest ratio followed by RT03 and finally RT01.

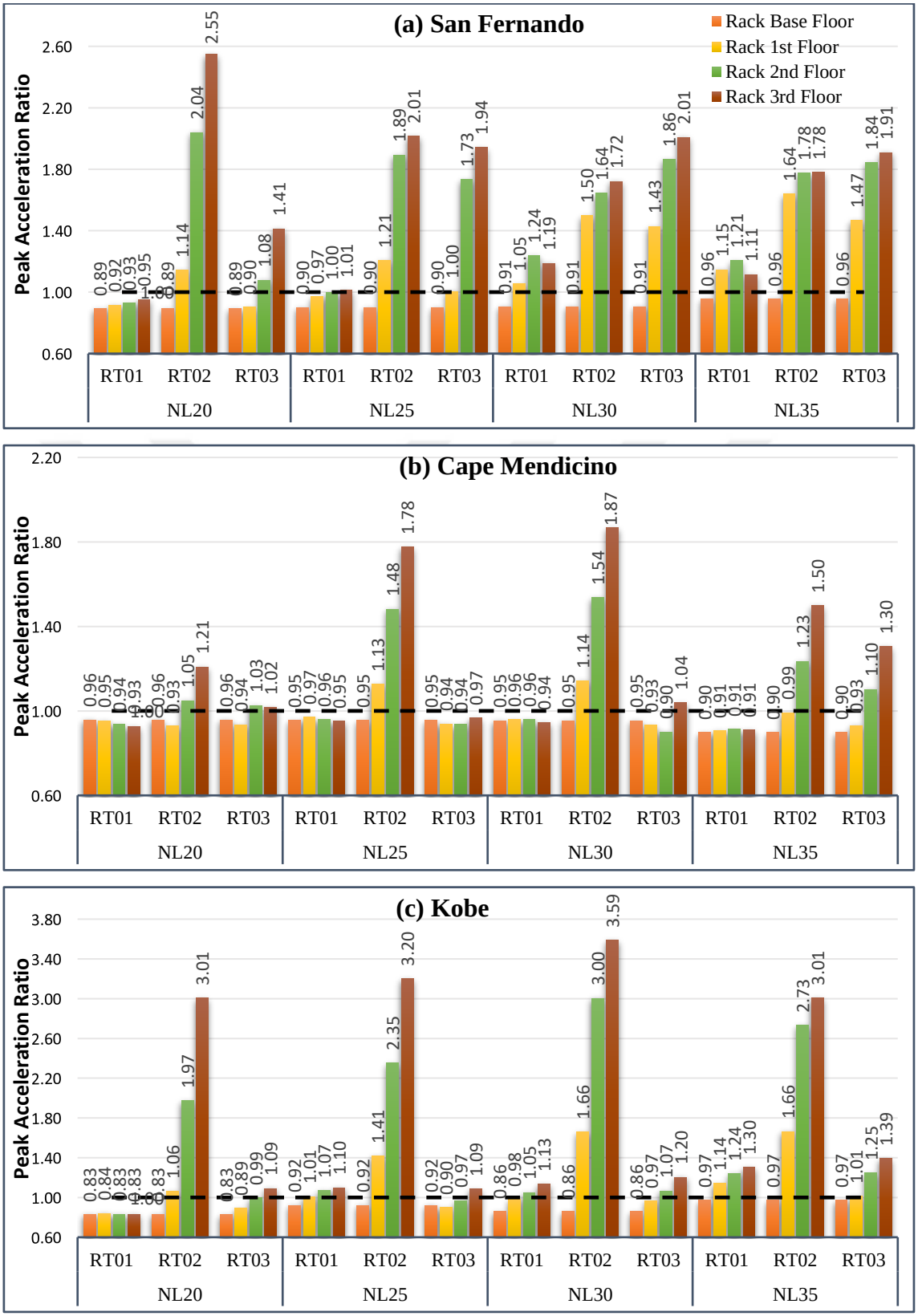

Figure 4.13: Peak acceleration ratio for each earthquake per isolation system and per rack period

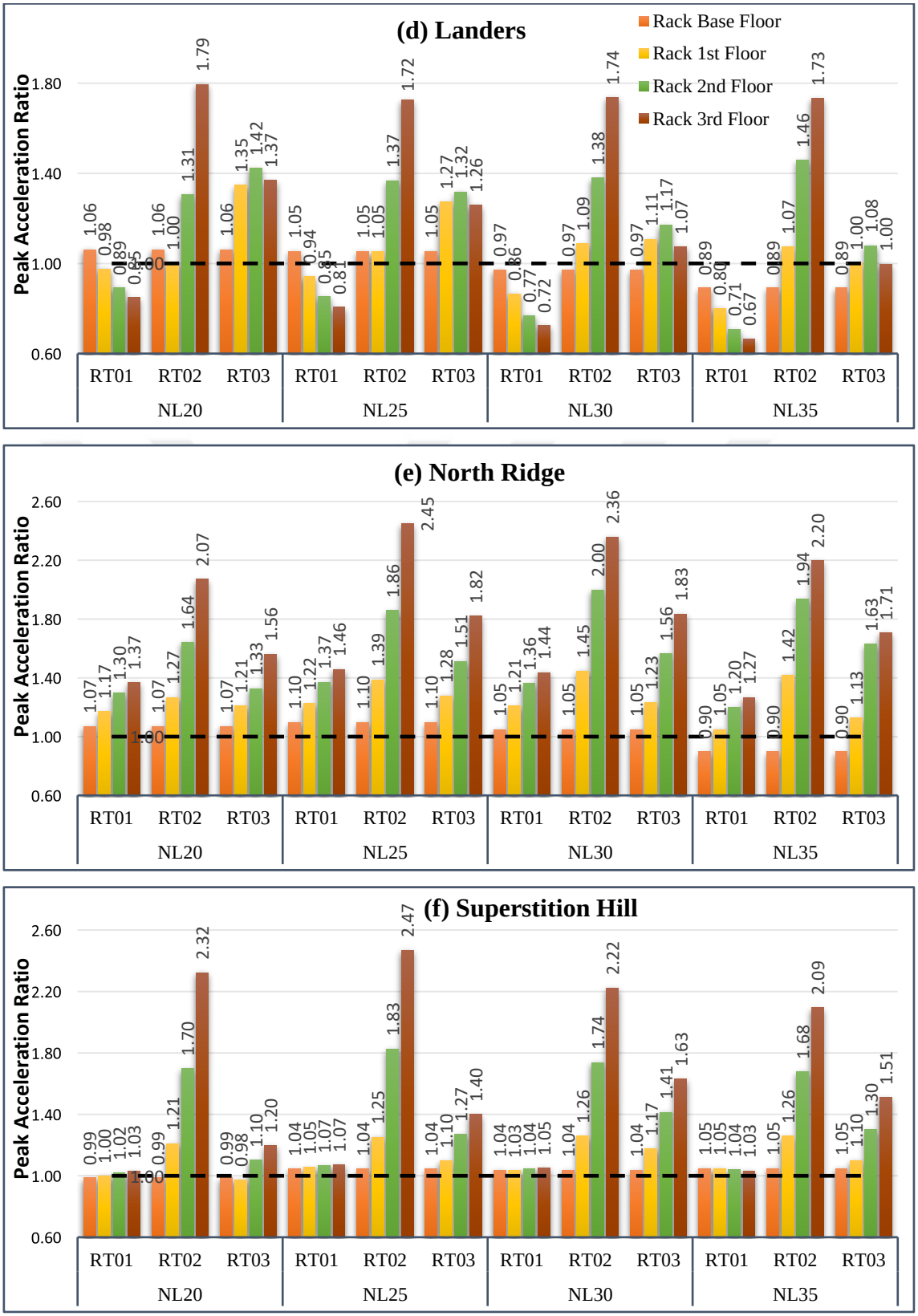

Figure 4.14: Peak acceleration ratio for each earthquake per isolation system and per rack period

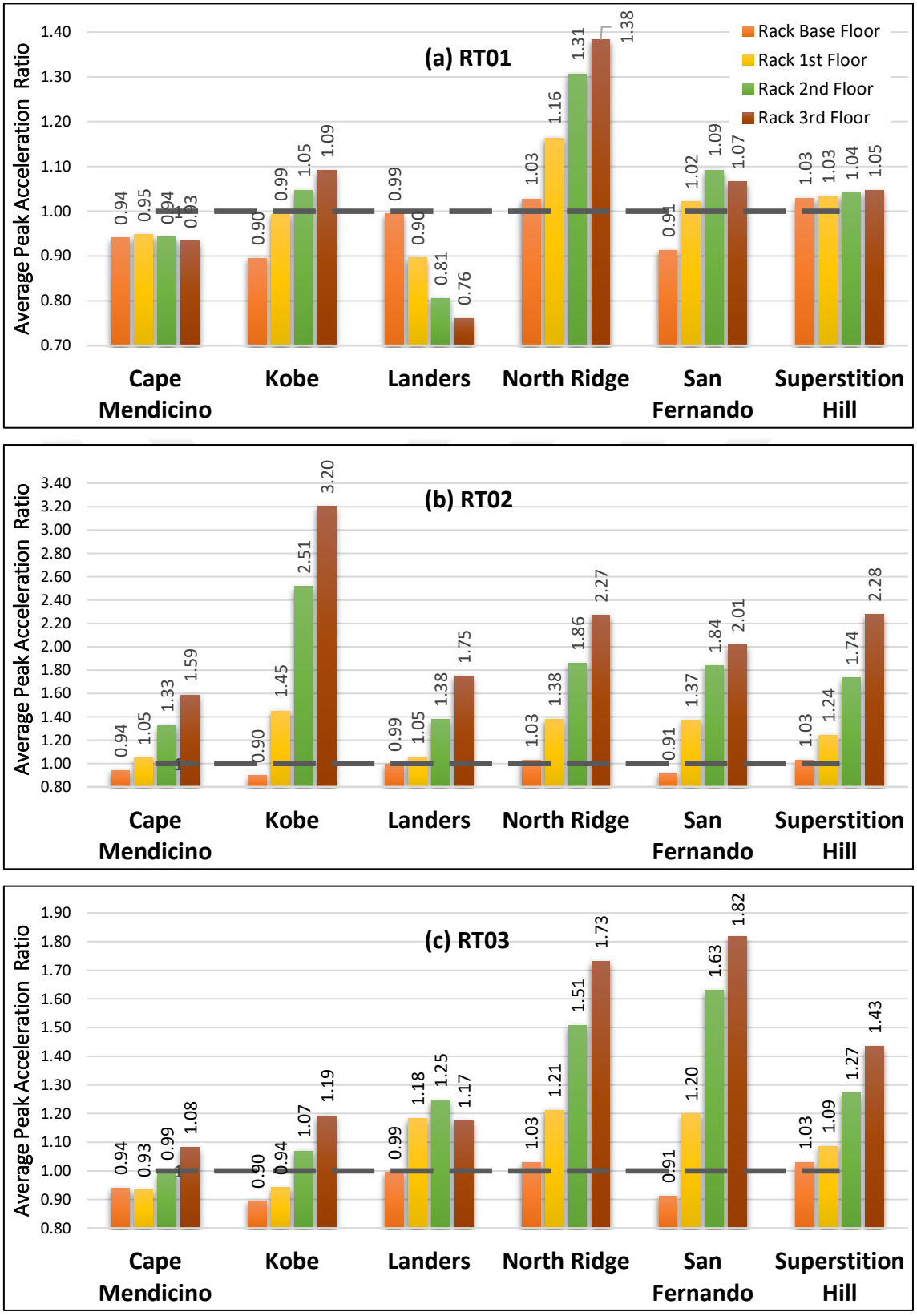

Figure 4.15: Average of Peak Acceleration Ratio for Each Earthquakes per Rack Period

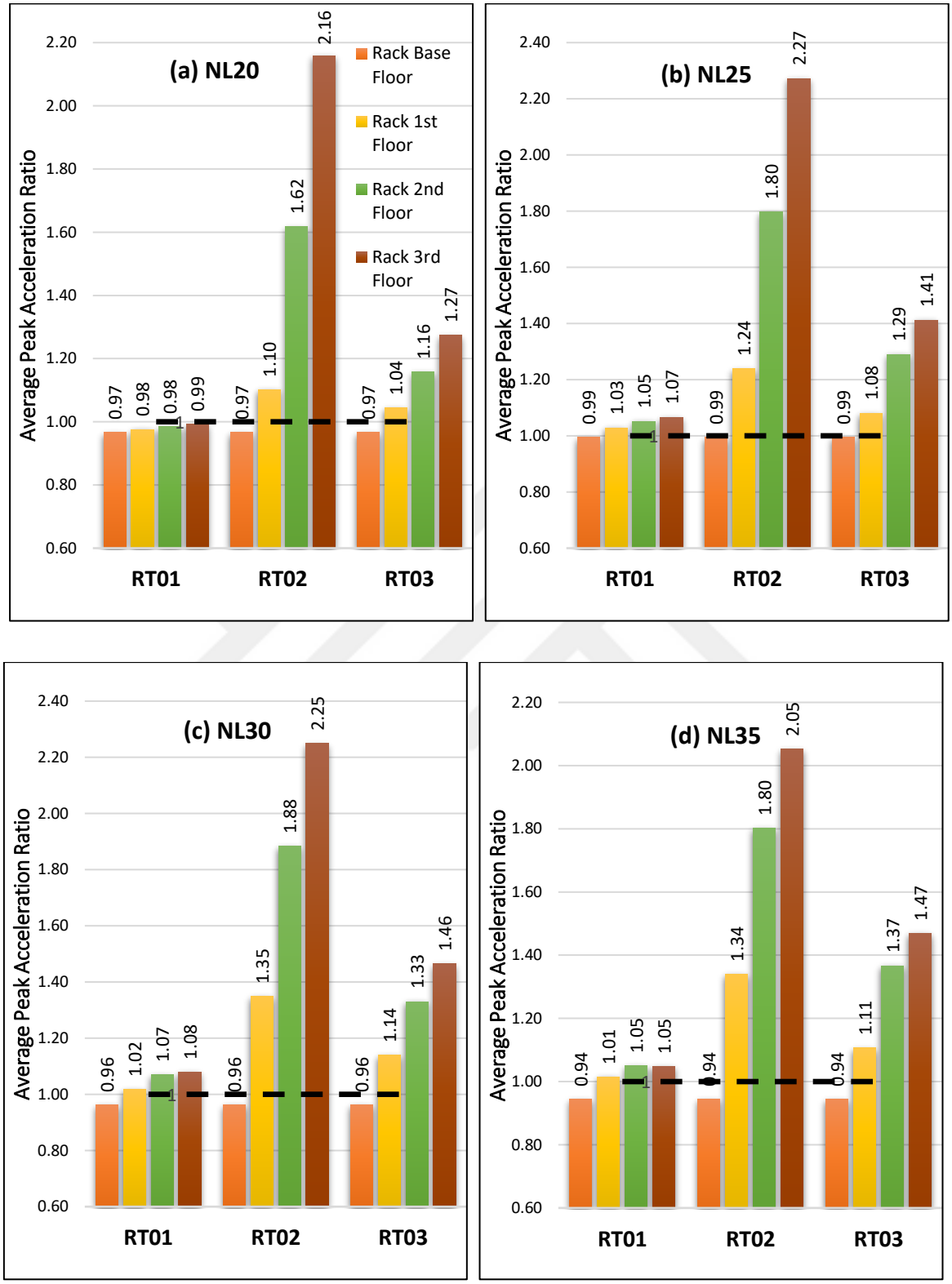

Figure 4.16: Peak acceleration ratio for each earthquake per isolation system and per rack period

4.1.3. RMS Rack Floor Acceleration

While the study of the peak acceleration ratio is a good method to observe how close the equivalent linear model to the nonlinear model is at the peak point, RMS is a good tool to study how well the equivalent linear model results match the nonlinear model results. RMS is obtained by squaring all the values of the acceleration in the set and then finding the arithmetic mean of the squares. Then the square root of the result taken.

In order to further understand the behaviour of rack floor acceleration for both equivalent linear and nonlinear cases, the nonlinear to equivalent linear ratio of RMS accelerations for all the racks, for all isolation systems and for each earthquake are presented. To better visualize, a solid dashed line is drawn at 1.0 in each graph, to indicate a perfect estimate of equivalent linear modelling. Results below and above this line corresponds to conservative and unconservative estimates of the equivalent linear modelling, respectively.

To illustrate the earthquake-based change, nonlinear/equivalent linear RMS floor acceleration graphs for all floors of the rack models are presented for all isolation systems. As can be observed from Figure 4.17 and Figure 4.18, the RMS acceleration ratio is dependent on the type of earthquake loaded. The obtained RMS acceleration ratios vary quantitatively for each earthquake. For example, in the case of isolation system NL25, at the top floor of the rack RT02, the smallest ratio is 1.51 (Cape Mendocino Earthquake) and the highest rate can go up to 3.66 (Kobe Earthquake). Similarly, for the case of NL35 and RT03, the smallest ratio is observed for the Lander Earthquake (1.23) and the highest ratio for San Fernando Earthquake (1.88).

The RMS acceleration ratio also depends on the isolation system. For example, as can be seen in Figure 4.17 (b) in the case of Cape Mendocino earthquake at the top floor of the rack RT02, the smallest RMS acceleration ratio is observed for isolation system NL25 (1.51) while the highest ratio for NL30 (1.98). Similarly, as shown in Figure 4.18 (e) for the case of Northridge Earthquake for RT03 the smallest RMS acceleration ratio is observed for isolation system NL20 (1.15) and the highest peak acceleration ratio observed for isolation system NL30 (1.67).

In Figure 4.19 the average RMS acceleration ratio of the isolation system per earthquake is presented. The dependence of the response ratio on the rack period can be observed. While the highest ratio for RT01 is 1.19 (Kobe Earthquake), for RT02 it is 3.59 (Kobe Earthquake) and for RT03 it is 1.60 (San Fernando Earthquake). Additionally, in Figure 4.20, the average RMS

acceleration ratio of the earthquakes per isolation system is presented. It can be observed that the response depends on the rack type (rack period) with RT02 exhibiting the highest ratio followed by RT03 and finally RT01.

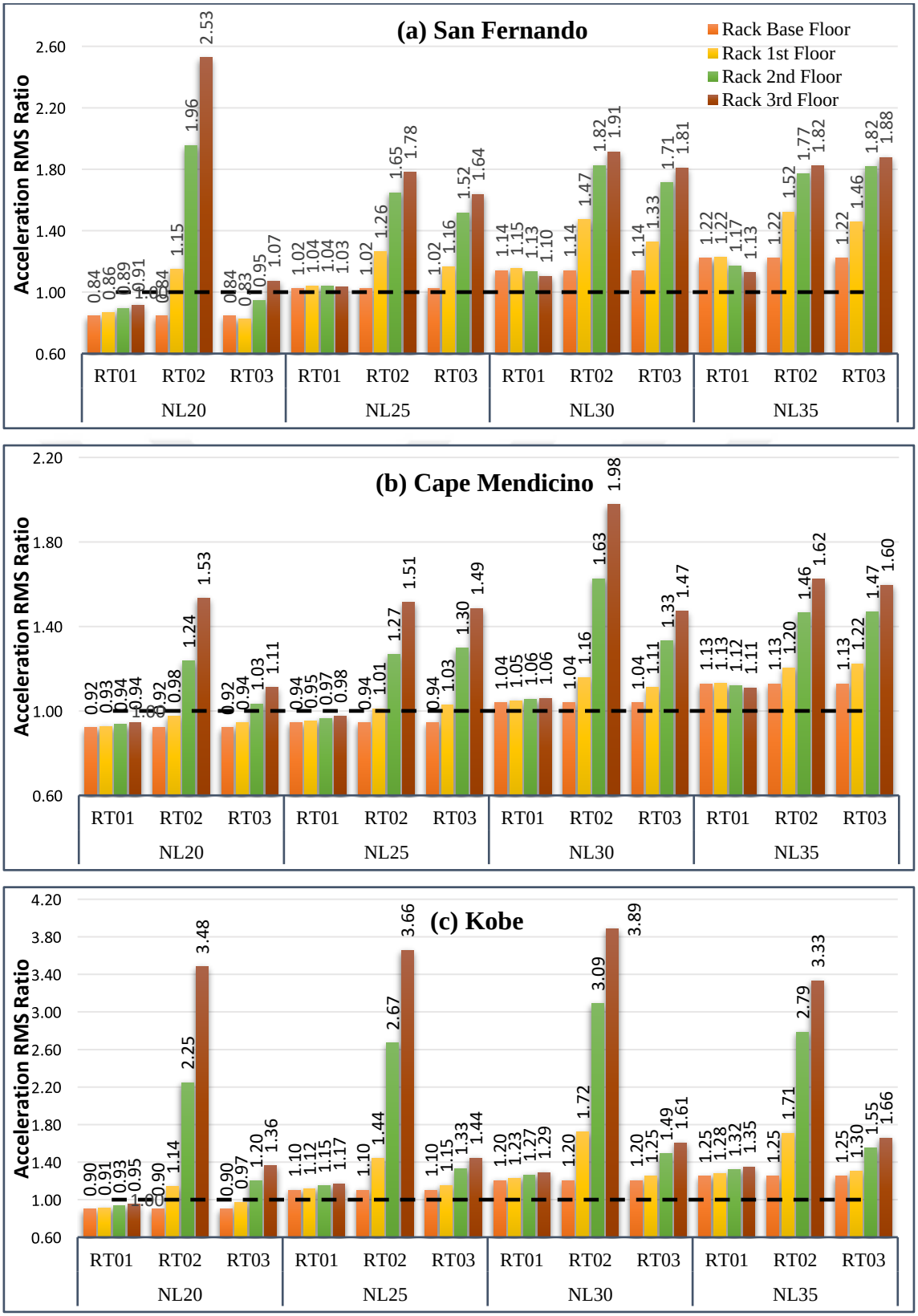

Figure 4.17: Acceleration RMS ratio for each earthquake per isolation system and per rack period

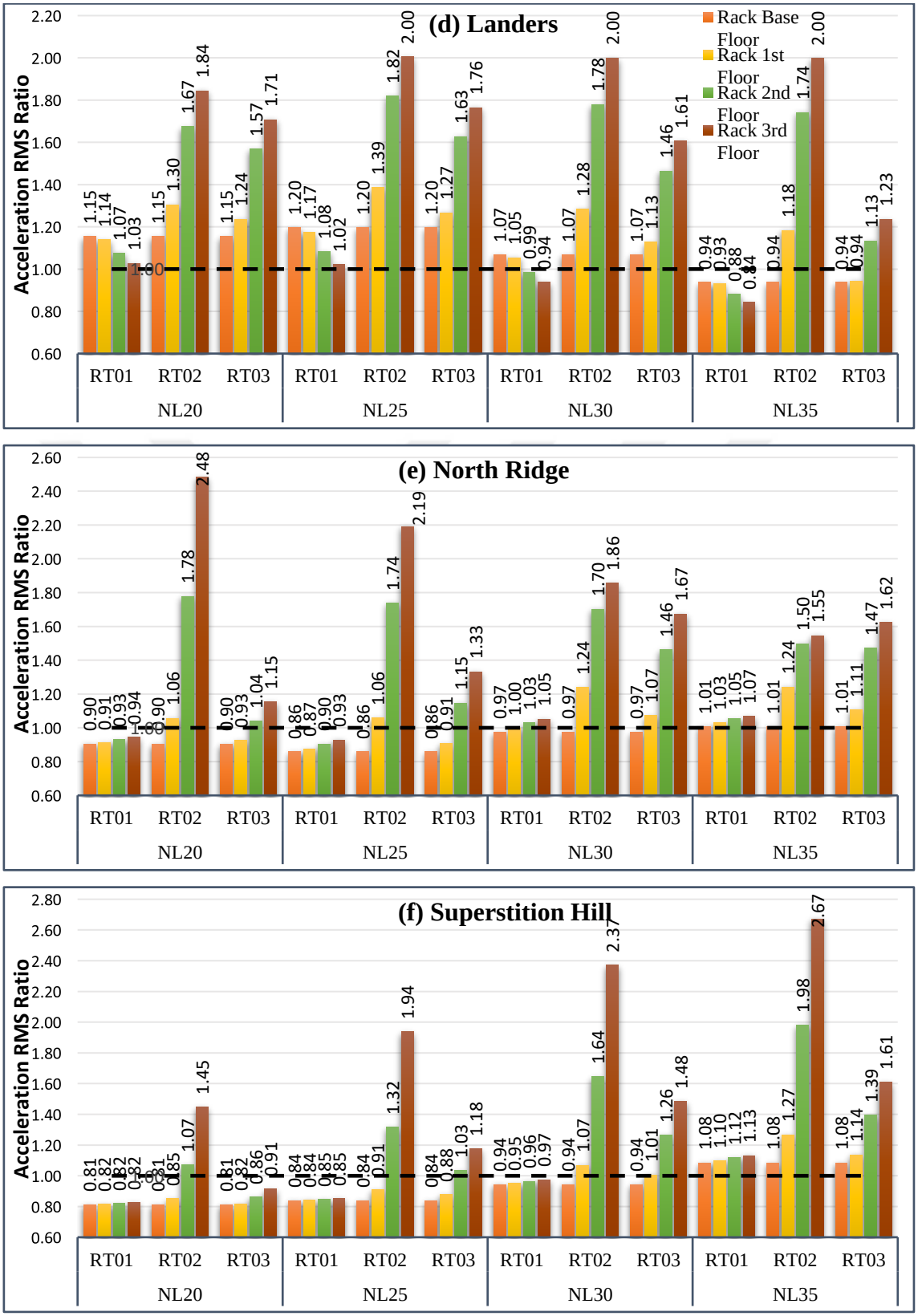

Figure 4.18: Acceleration RMS ratio for each earthquake per isolation system and per rack period

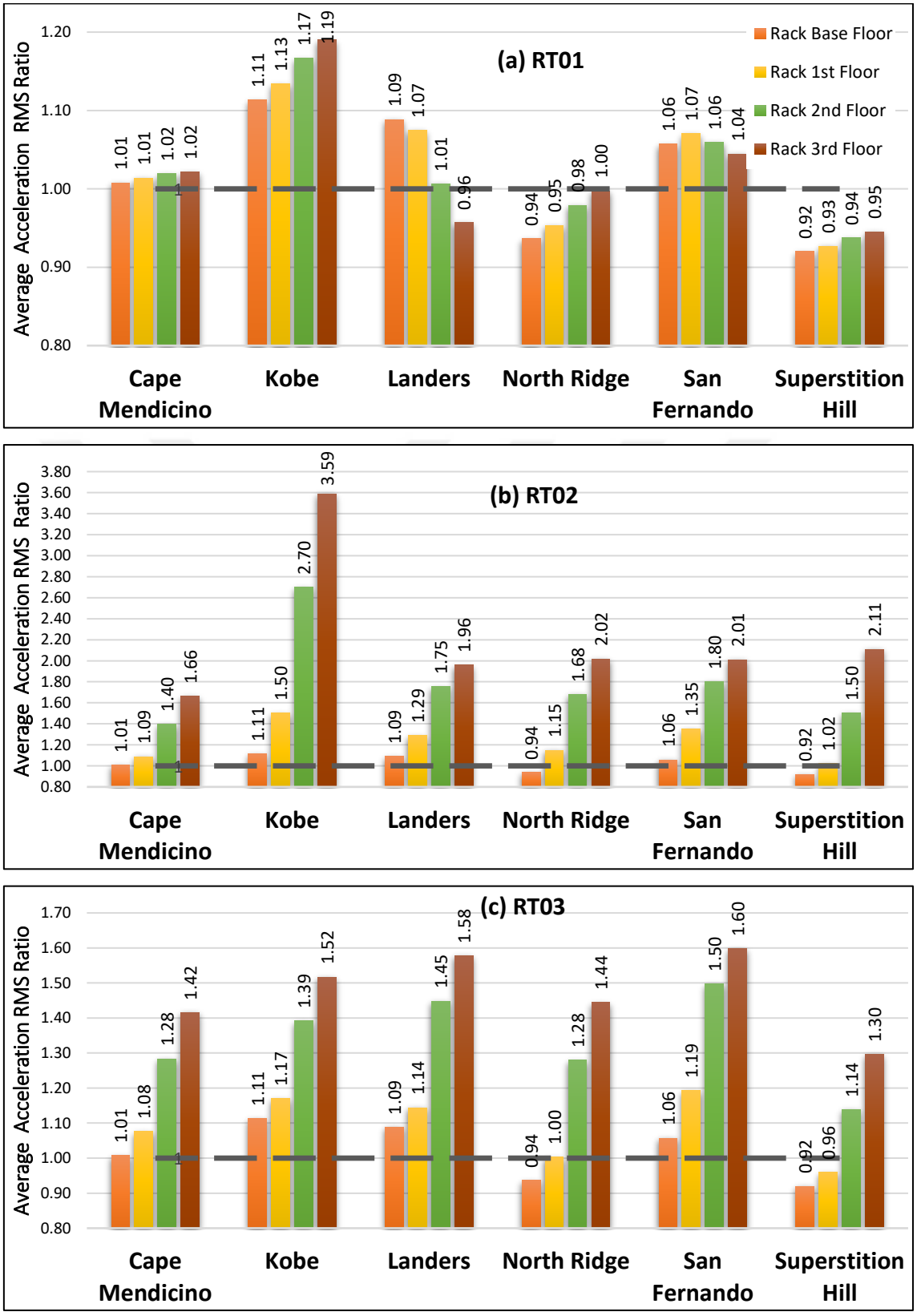

Figure 4.19: Average of acceleration RMS ratio for each earthquake per rack period

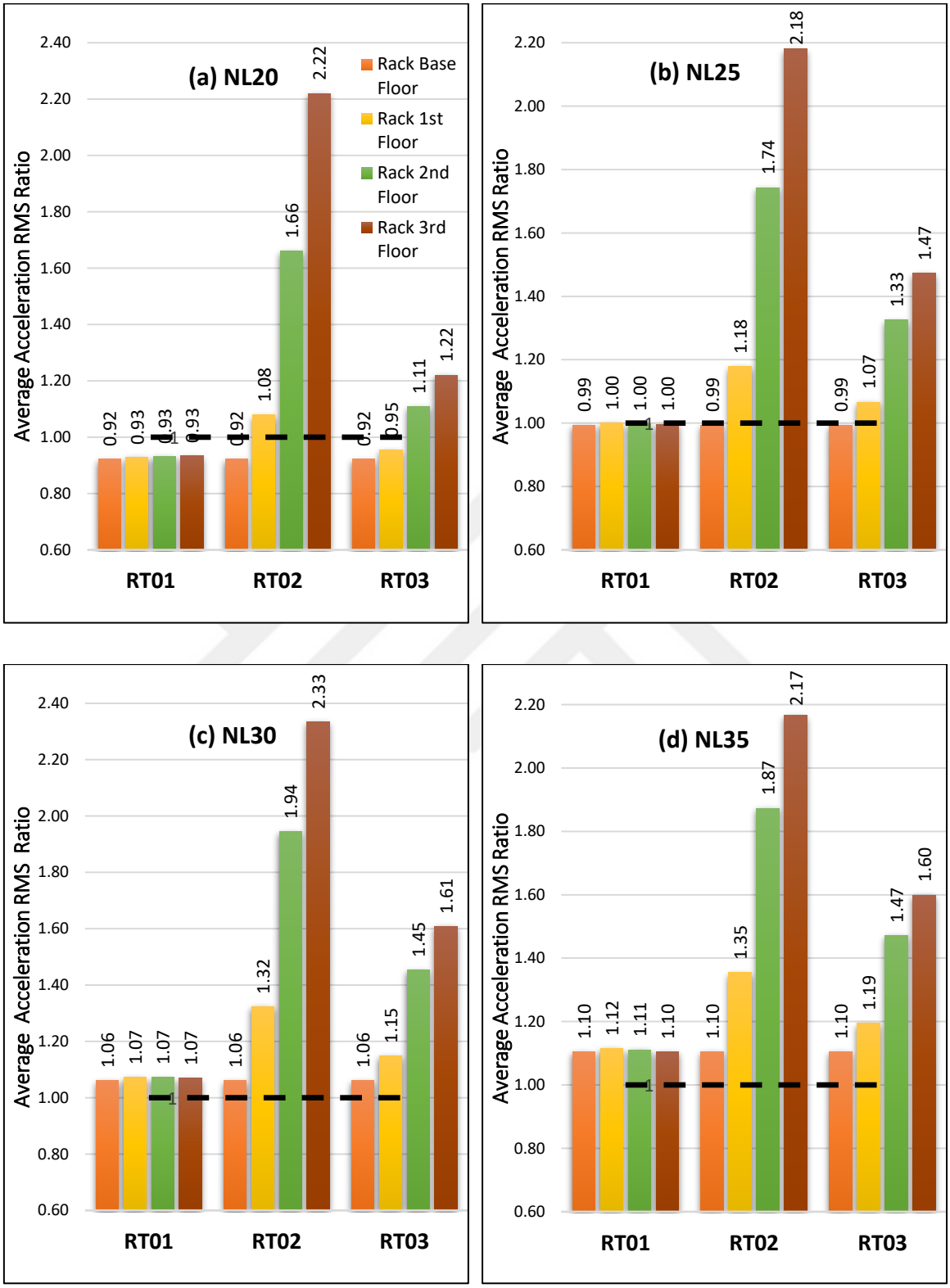

Figure 4.20: Average of acceleration RMS ratio for each isolation system per rack period

4.2. RACK FLOOR DISPLACEMENT

The floor displacement results of the analyses made for the rack models placed on seismically isolated buildings are shown in Figure 4.21 - Figure 4.32.

4.2.1. Rack Floor Displacement Time History

The comparison of the floor displacement time histories of racks that are located on nonlinear and equivalent linear isolation systems are presented.

4.2.1.1 RT01 Rack Model

The displacement time history response of the rack with period of 0.1s located on buildings with nonlinear and equivalent linear isolation systems are presented for representative isolation systems (NL20 and NL30) and under two representative historical earthquakes namely Cape Mendocino and Northridge. The response at each floors of the rack is presented in Figure 4.21 - Figure 4.24.

As it can be seen from Figure 4.21 - Figure 4.22, the result obtained for Cape Mendocino earthquake follows the general trend and the two plots overlap for both NL20 and NL30 at all floors of the rack. However, for the case of Northridge earthquake as shown in Figure 4.23 - Figure 4.24, the plot for both equivalent linear and nonlinear tend to follow the general trend except that the equivalent linear plot is seen to be smoother than the nonlinear plot. This is expected as the nonlinear plot tend to capture more detailed behaviour of the earthquake motion as we already saw in the acceleration plots. In addition to that, there is slight variation of the peak values of the two plots at each floor of the rack model. This is more visible specially at higher floors (2^{nd} and 3^{rd} rack Floor). Similar behaviour was observed during the analysis of the floor acceleration time history. This show us once again why it is necessary to study the peak values of the time history plots.

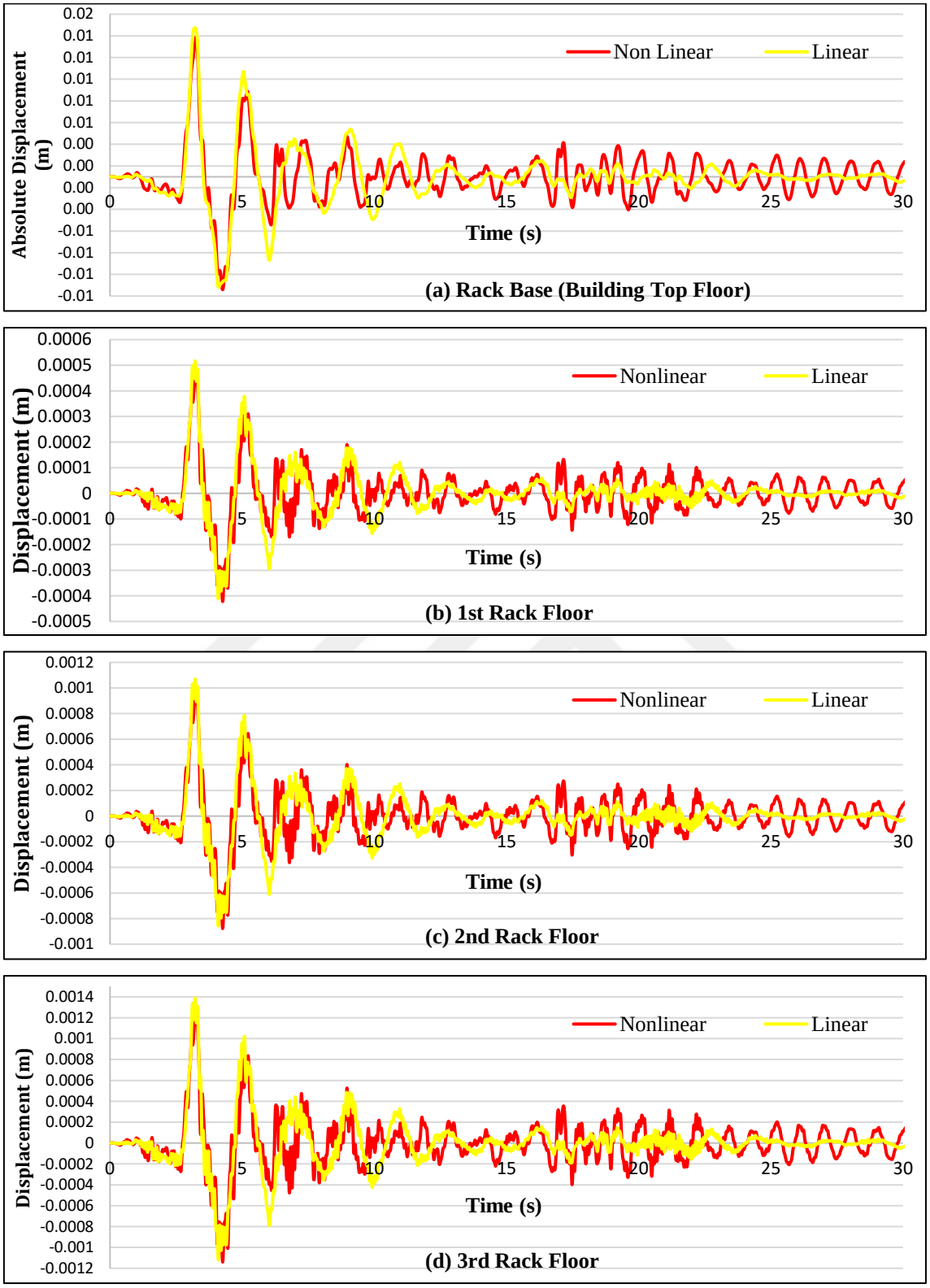

Figure 4.21: Displacement at each floor for RT01 rack model under NL20 isolation system (Cape Mendocino EQ)

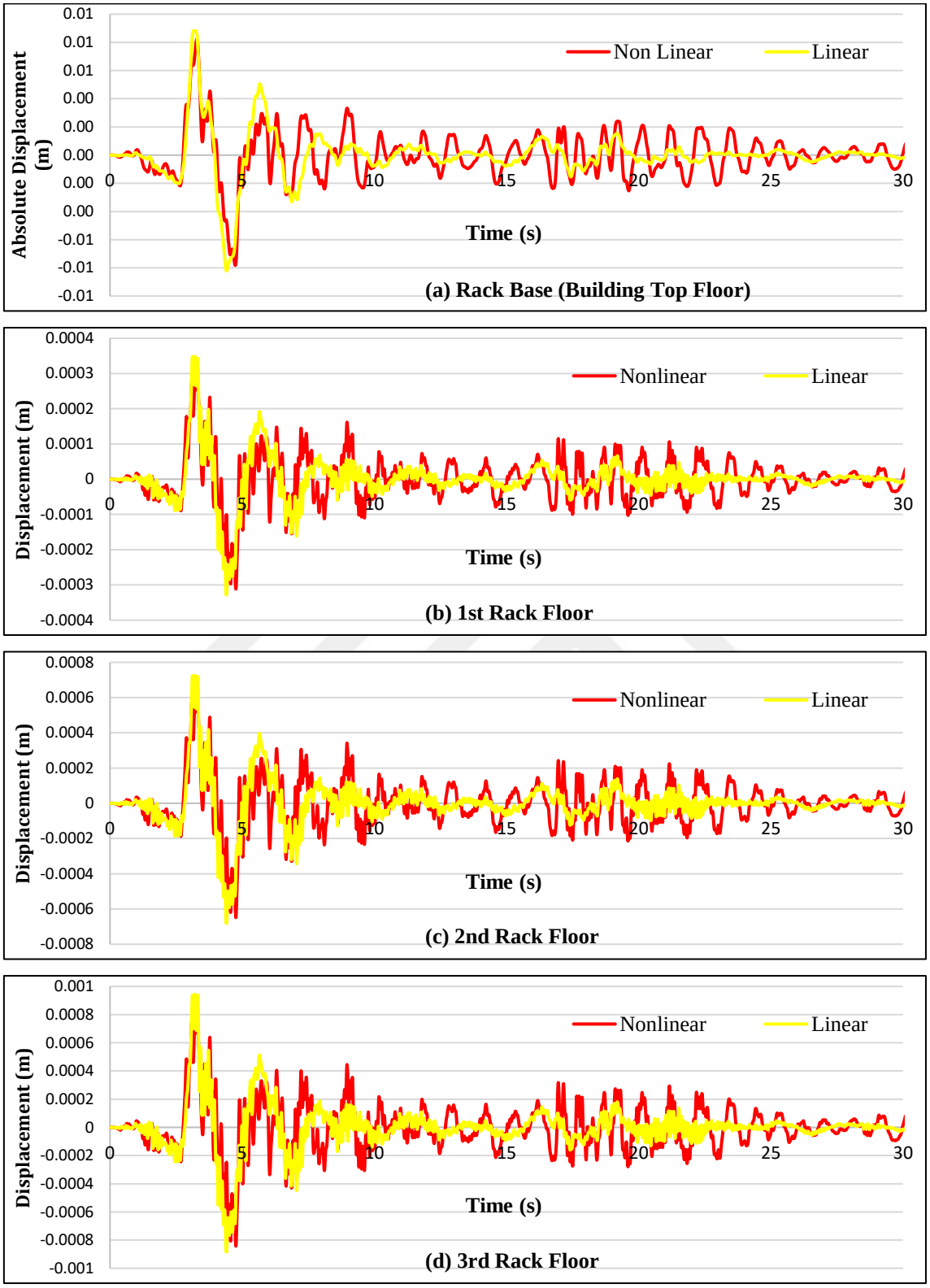

Figure 4.22: Displacement at each floor for RT01 rack model under NL30 isolation system (Cape Mendocino EQ)

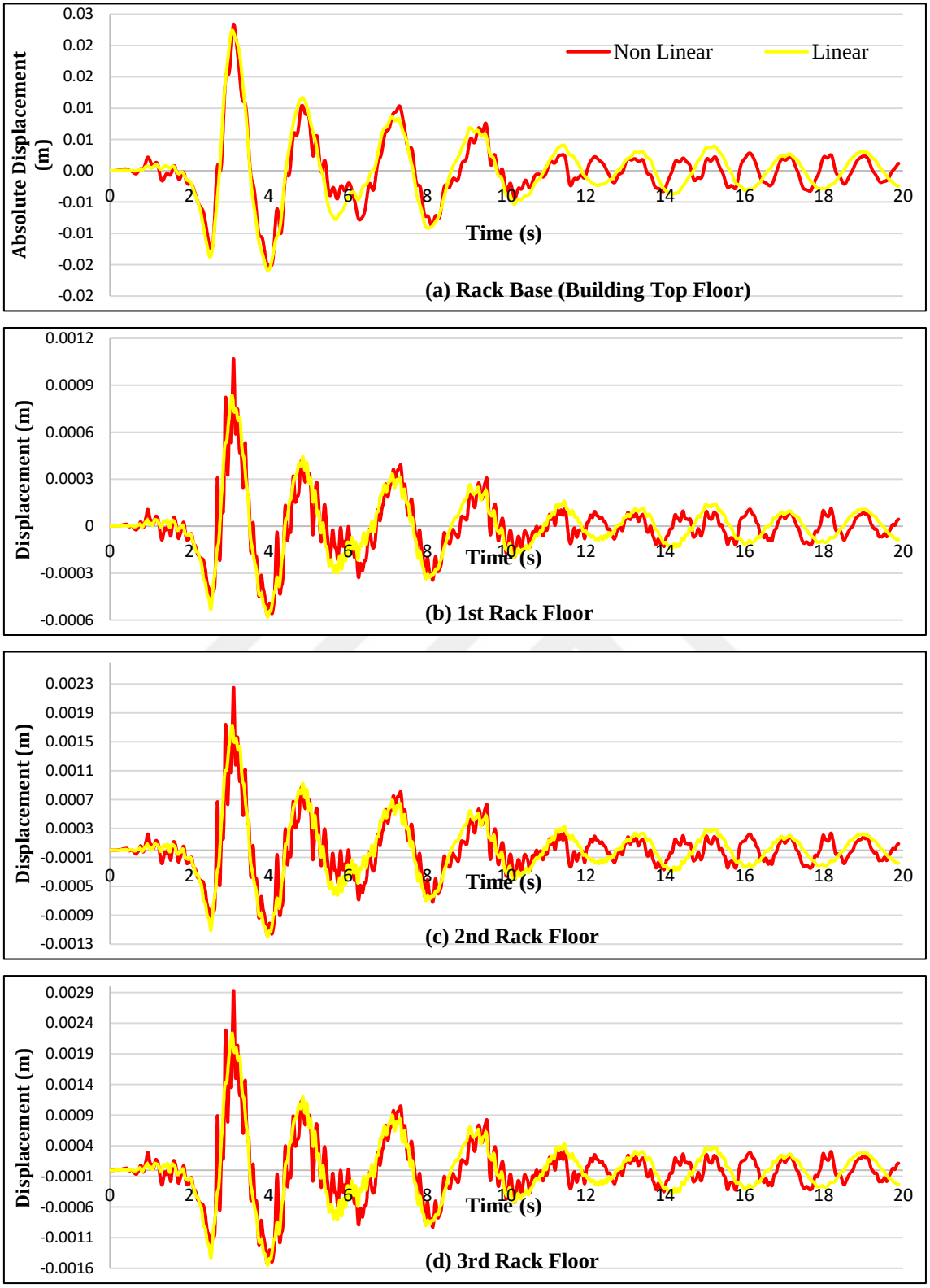

Figure 4.23: Displacement at each floor for RT01 rack model under NL20 isolation system (Northridge EQ)

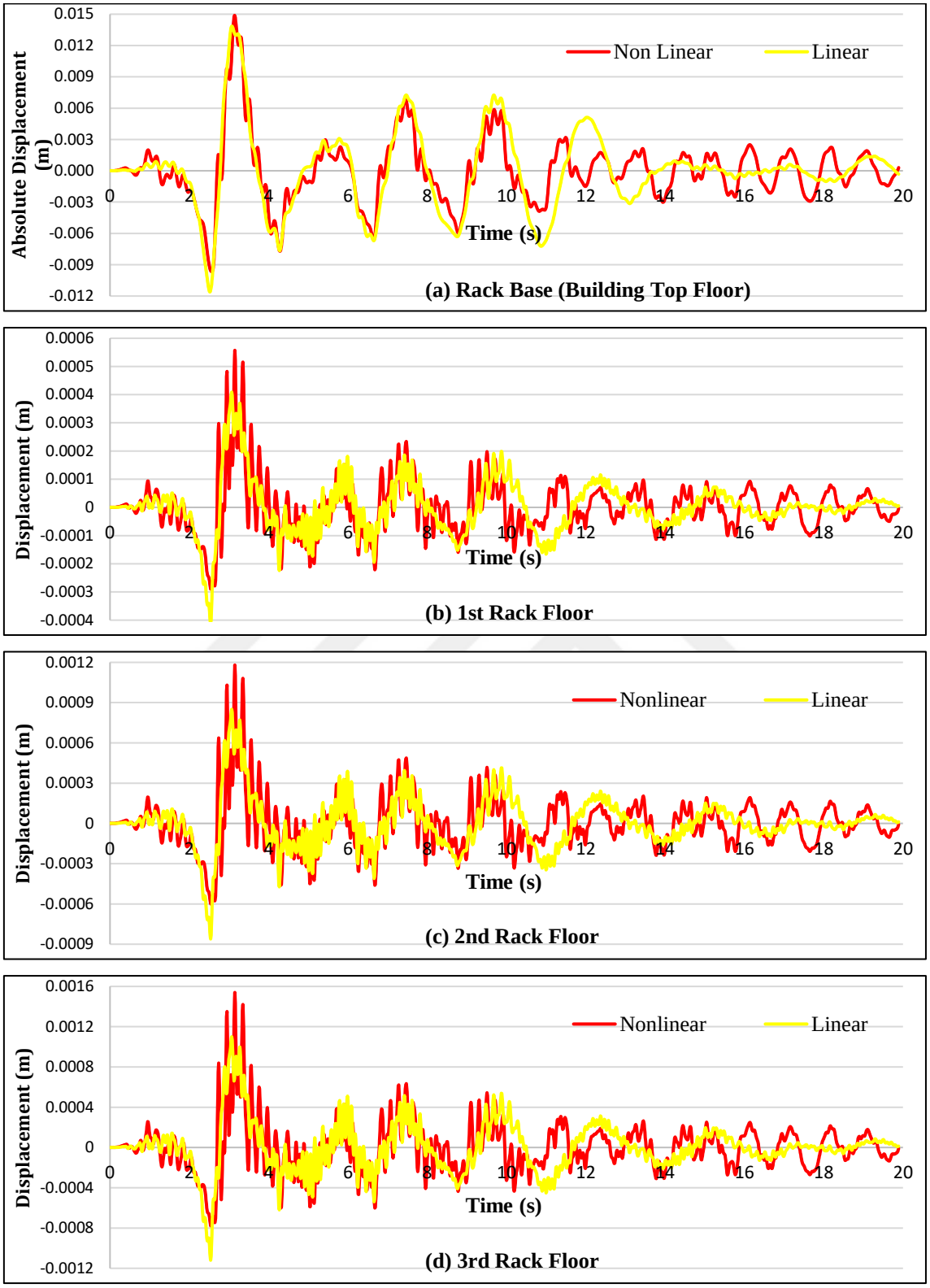

Figure 4.24: Displacement at each floor for RT01 rack model under NL30 isolation system (Northridge EQ)

4.2.1.2. RT02 Rack Model

The displacement time history response of the rack with period of 0.2s located on building with nonlinear and equivalent linear isolation systems are presented for two isolation systems (NL20 and NL30) and under two historical earthquakes namely Cape Mendocino and Northridge. The response at each floors of the rack is presented in Figure 4.25 - Figure 4.28.

The results obtained for both Cape Mendocino Earthquake and Northridge Earthquake for the case of RT02 indicate high discrepancy between the equivalent linear and nonlinear compared to RT01. While the difference in the plots were only visible at the peak points for the case of RT01, for the case of RT02, the difference in the plot is clearly visible and spread along the entire plot. Also as was the case with RT01 the difference in the plots is more at the higher floors of the rack. Once again same observation was also made for the study of the floor acceleration time history.

The peak displacement for equivalent linear and nonlinear cases show high difference. For example, as can be seen in Figure 4.26 while peak displacement for equivalent linear plot is around 0.004 m, for the 3rd floor of the rack, the nonlinear analysis plot indicate a peak displacement of higher than 0.006 m. The same can be observed for Figure 4.25, Figure 4.27 and Figure 4.28. This shows that equivalent linear models underestimate the rack's response displacement from their real values.

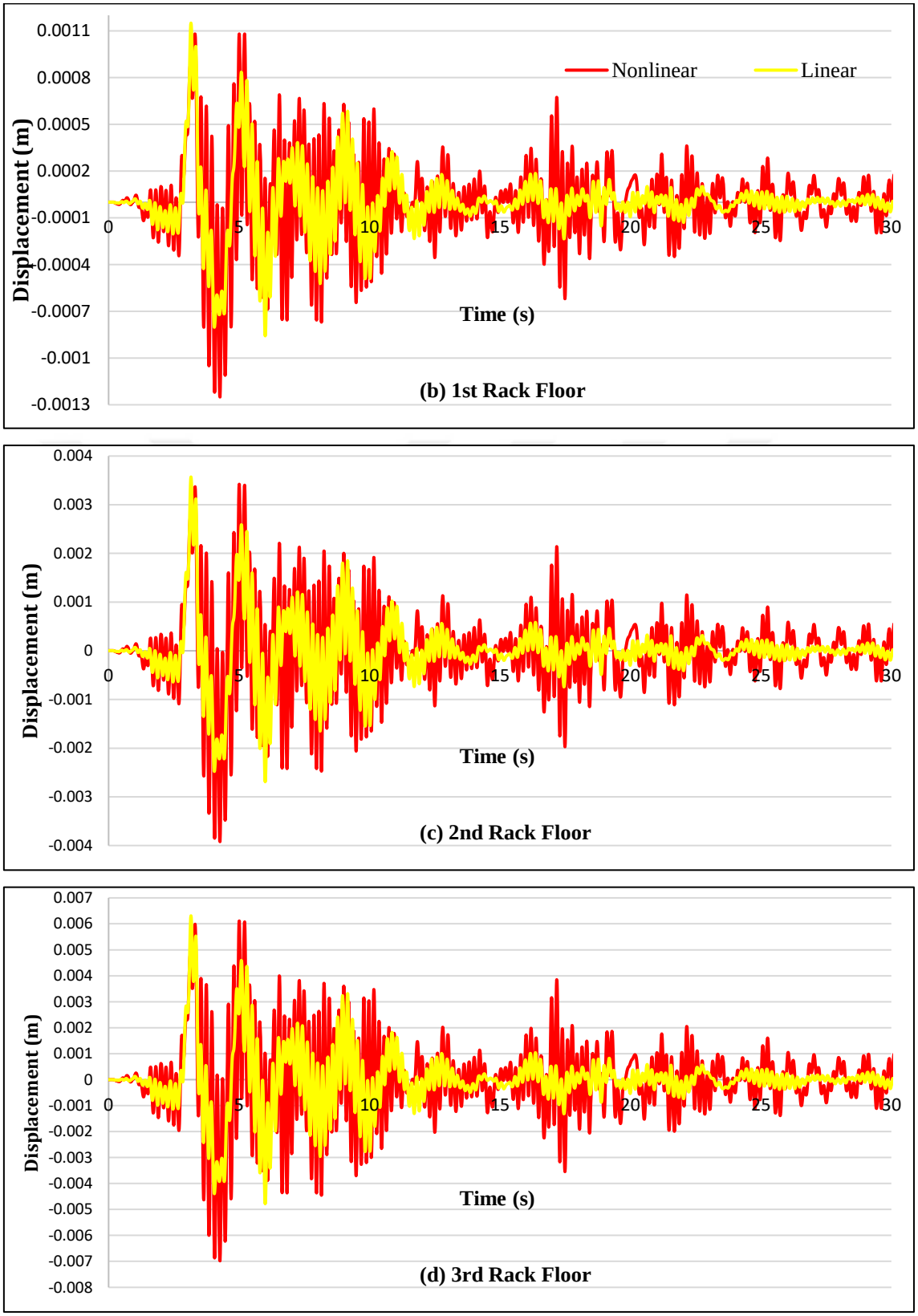

Figure 4.25: Displacement at each floor for RT02 rack model under NL20 isolation system (Cape Mendocino EQ)

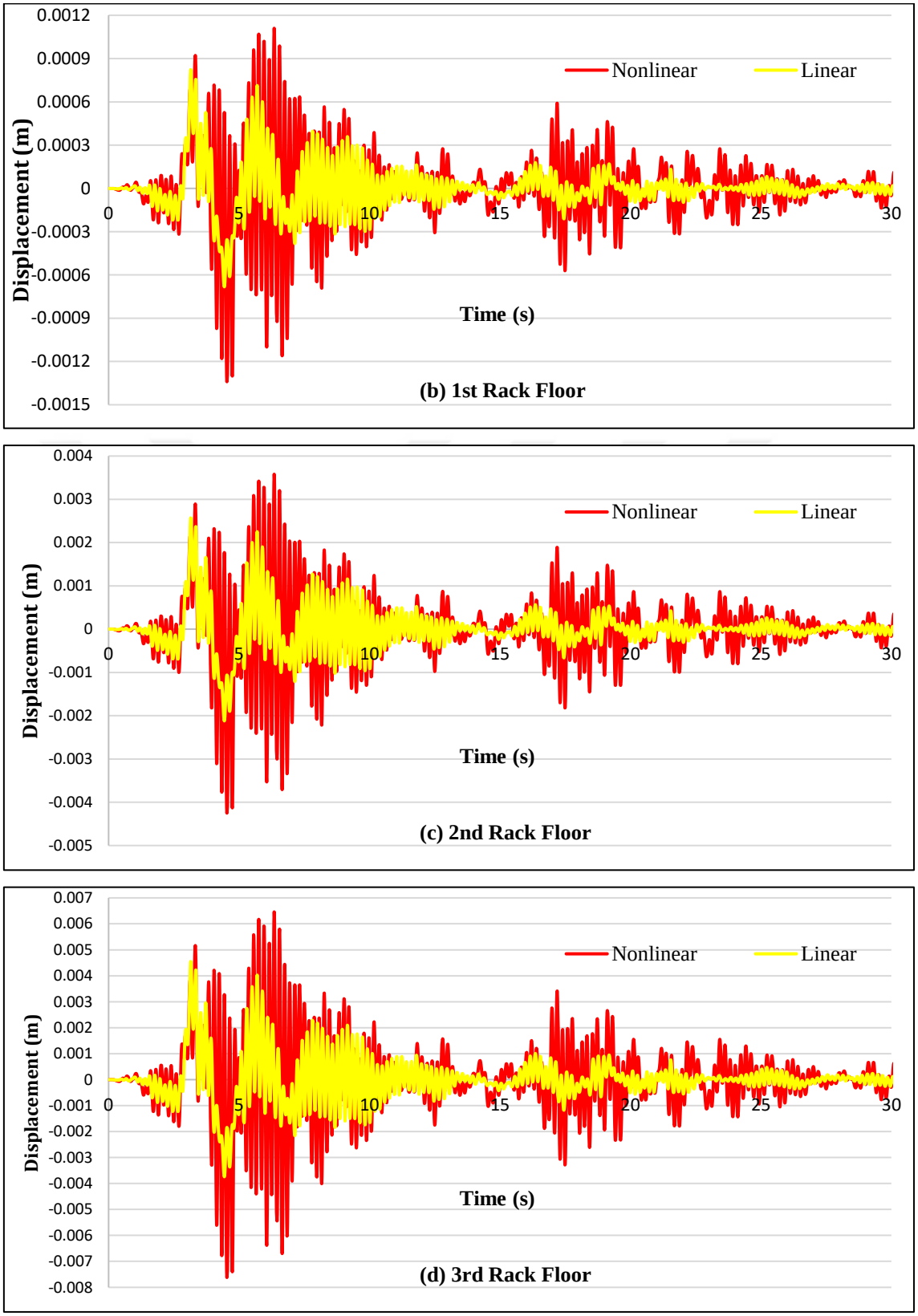

Figure 4.26: Displacement at each floor for RT02 rack model under NL30 isolation system (Cape Mendocino EQ)

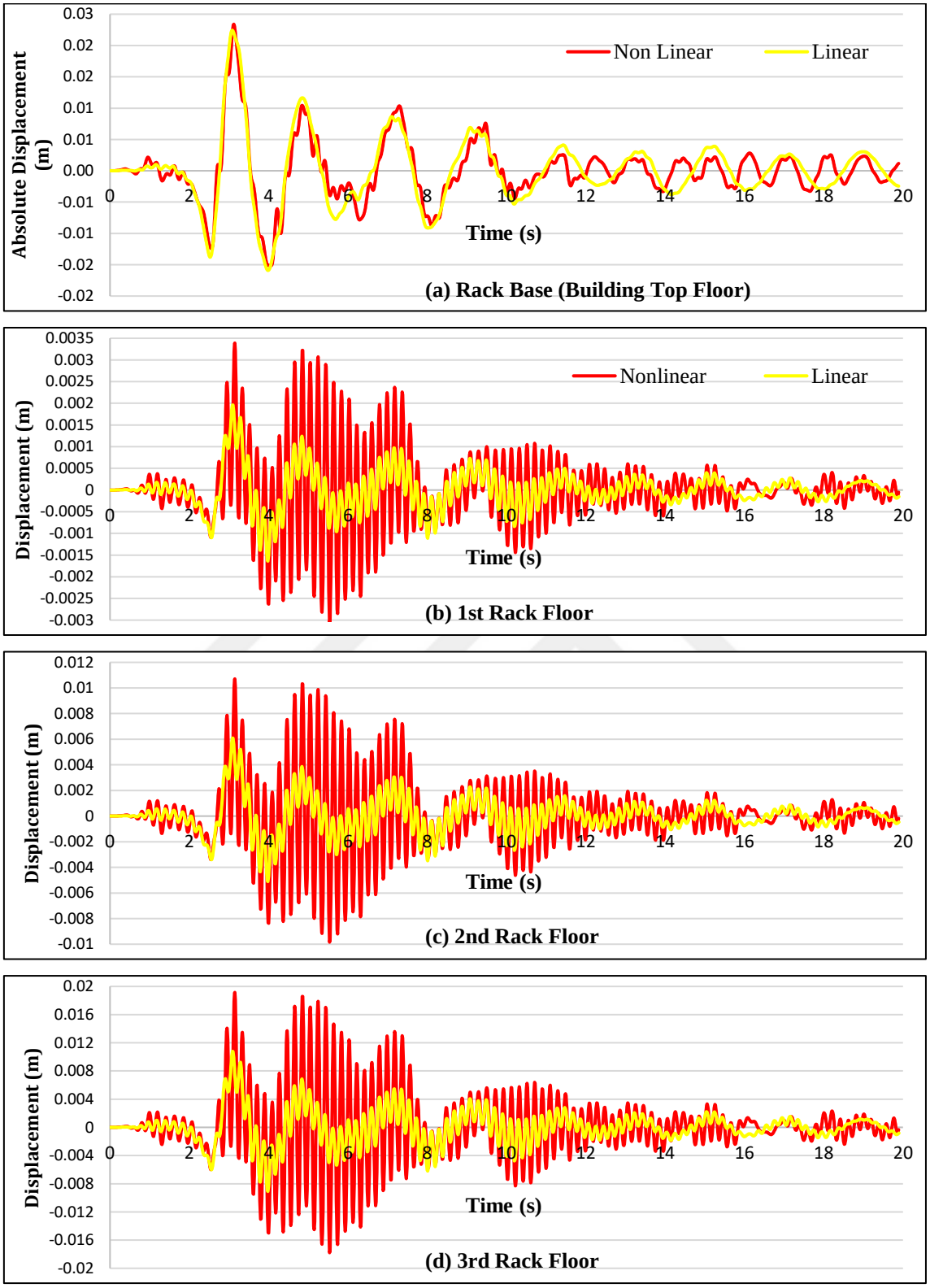

Figure 4.27: Displacement at each floor for RT02 rack model under NL20 isolation system (North Ridge EQ)

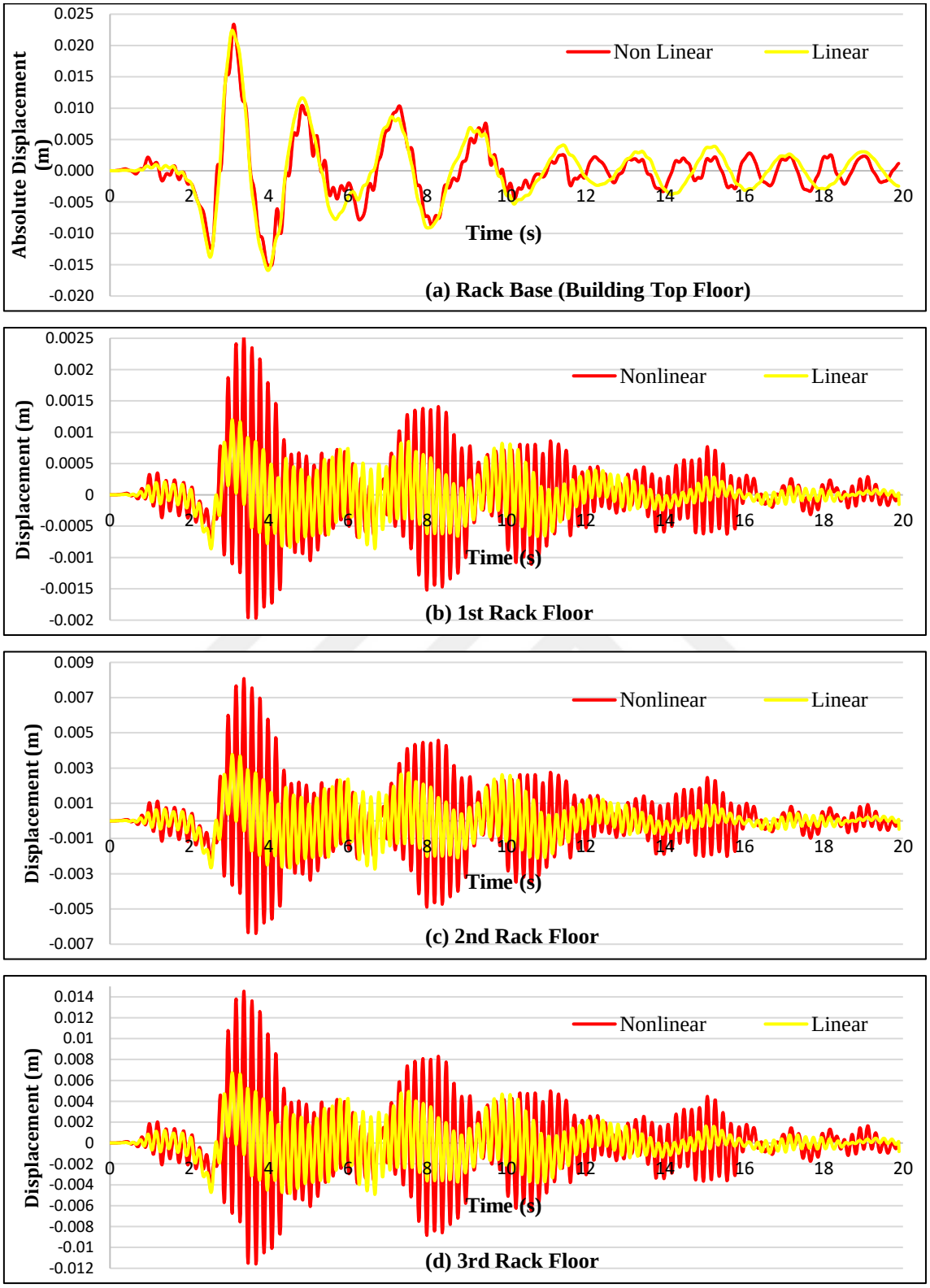

Figure 4.28: Displacement at each floor for RT02 rack model under NL30 isolation system (Northridge EQ)

4.2.1.3. RT03 Rack Model

The displacement time history response of the rack with period of 0.3s under nonlinear and equivalent linear isolation system are presented for two isolation systems (NL20 and NL30) and under two historical earthquakes namely Cape Mendocino and Northridge. The response at each floors of the rack is presented in Figure 4.29 - Figure 4.32.

As it can be seen from the plots the result obtained depends on the earthquake and the isolation system. In general, the plots for RT03 exhibit less differences compared with RT02 discussed before. While there is little to none difference between the plots for the case of Northridge earthquake under isolation system NL20 as shown in Figure 4.31 the plot of the same earthquake under isolation system NL30 shows visible difference as shown in Figure 4.32.

For the case of Cape Mendocino Earthquake there is visible difference between the plots for the case of both NL20 and NL30 isolation systems. However, these differences in the plots are less compared to plots observed for RT02 discussed before.

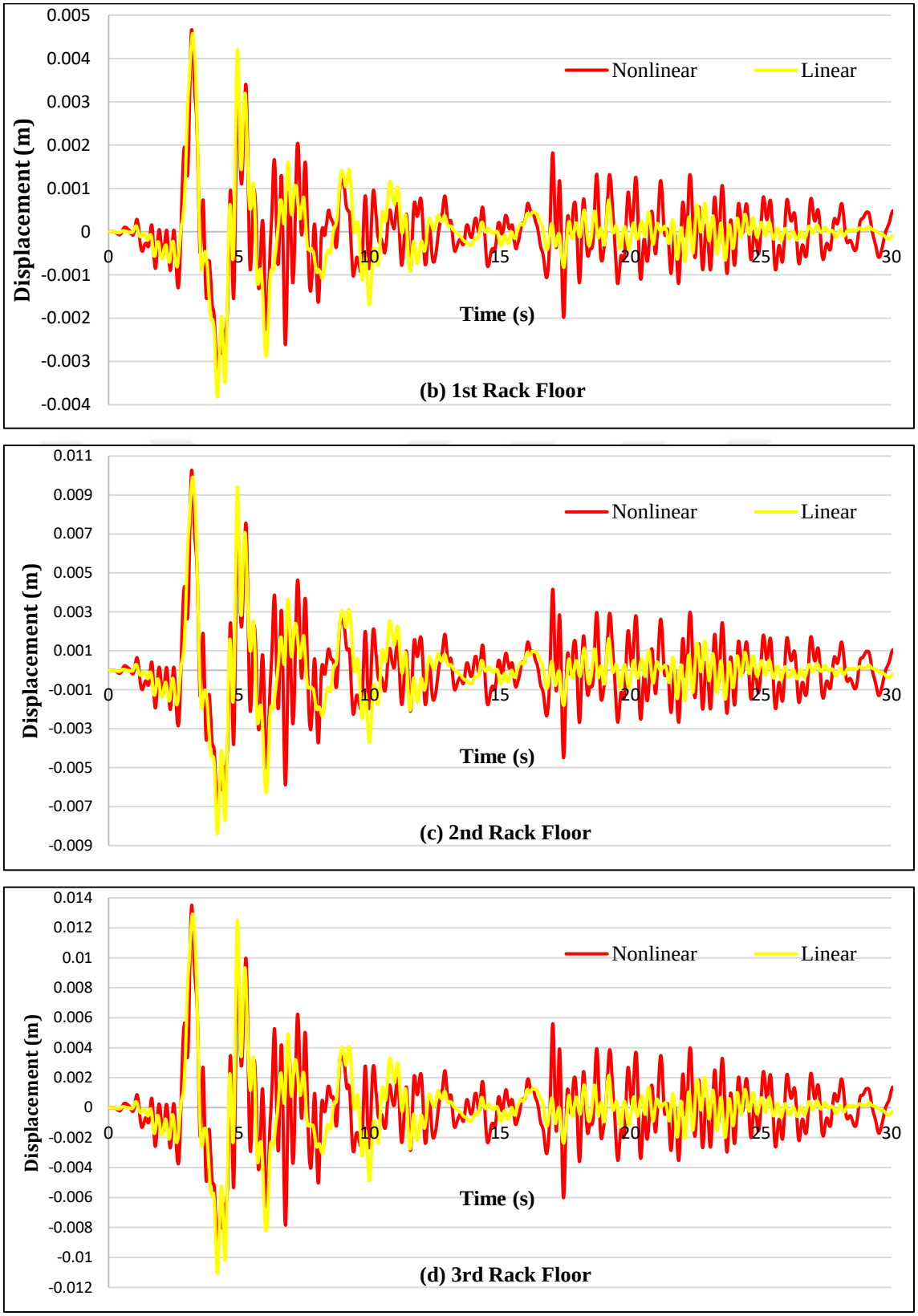

Figure 4.29: Displacement at each floor for RT03 rack model under NL20 isolation system (Cape Mendocino EQ)

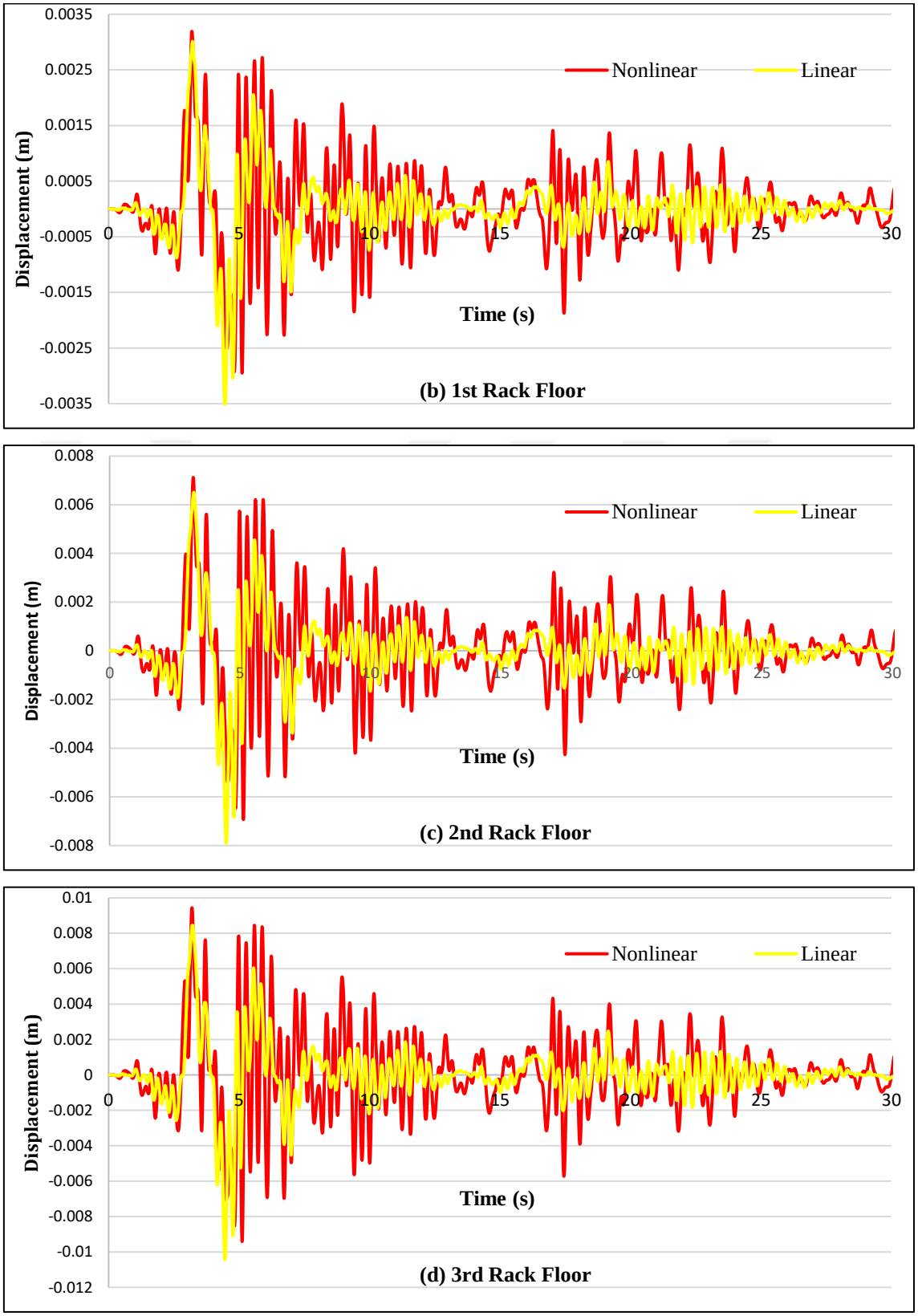

Figure 4.30: Displacement at each floor for RT03 rack model under NL30 isolation system (Cape Mendocino EQ)

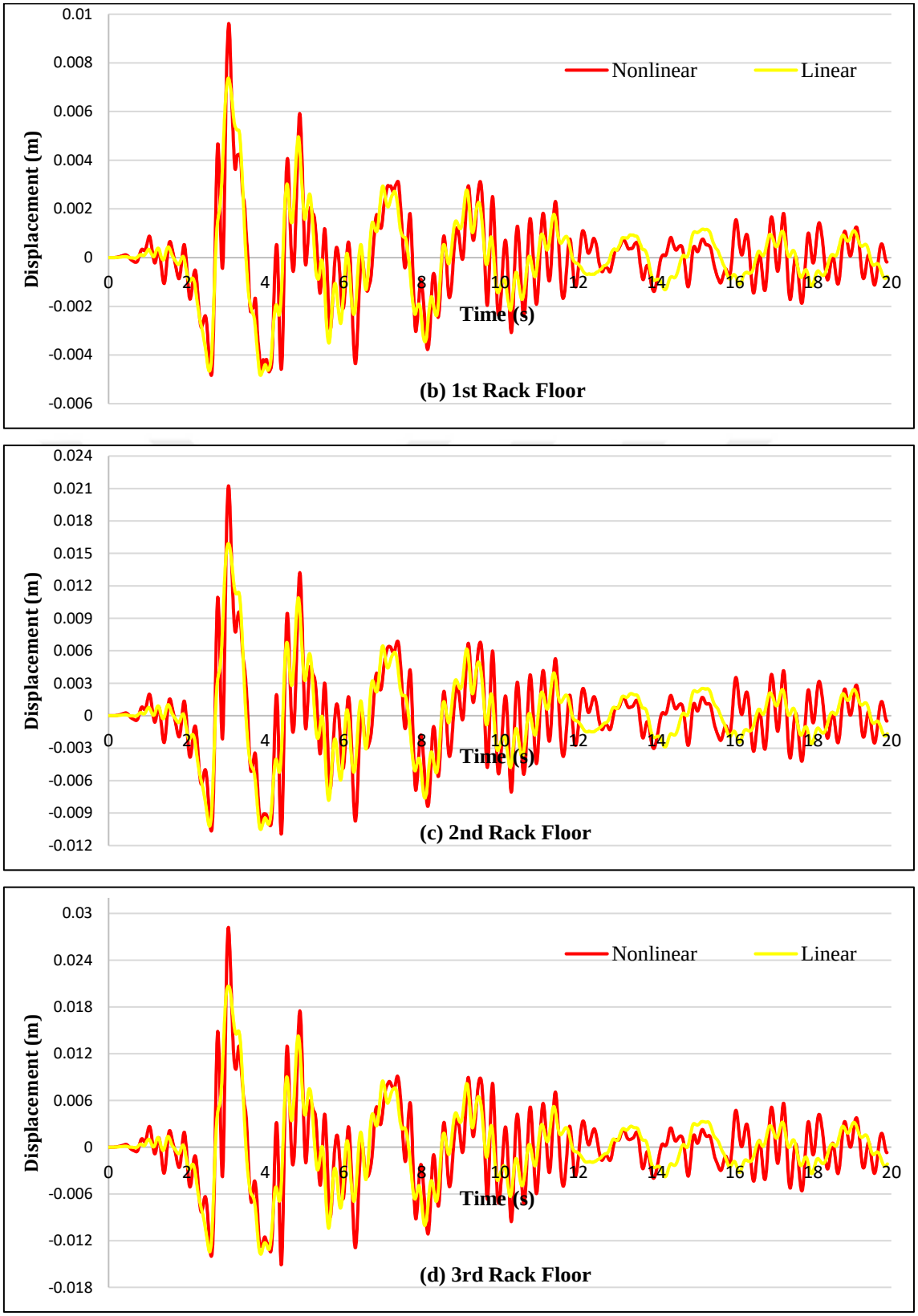

Figure 4.31: Displacement at each floor for RT03 rack model under NL20 isolation system (Northridge EQ)

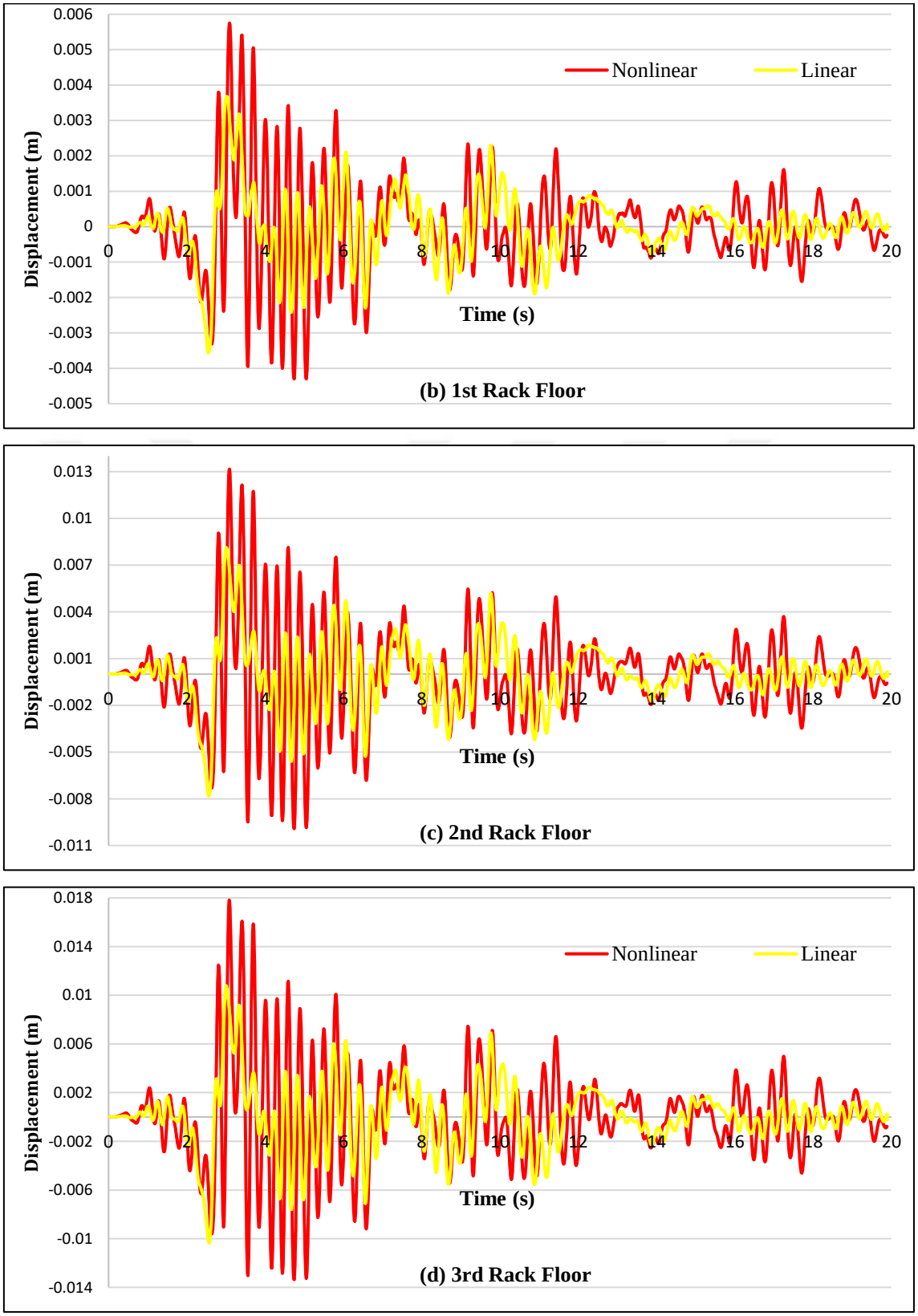

Figure 4.32: Displacement at each floor for RT03 rack model under NL30 isolation system (Northridge EQ)

4.2.2. Peak Floor Displacement

In order to further understand the behaviour of floor displacement of the racks for both equivalent linear and nonlinear case, the nonlinear to equivalent linear peak displacement ratio for all the racks, for all isolation systems and for each earthquake are presented. To better visualize, a solid dashed line is drawn at 1.0 in each graph, to indicate a perfect estimate of equivalent linear modelling. Results below and above this line corresponds to conservative and unconservative estimates of the equivalent linear modelling, respectively.

To illustrate the earthquake-based change, nonlinear to equivalent linear floor displacement ratio graphs for the all floors of the rack models are presented for all isolation systems. As can be observed from Figure 4.33 and Figure 4.34, the peak displacement ratio is dependent on the type of earthquake loaded. The obtained peak floor ratio varies quantitatively for different earthquake as observed for floor acceleration before. For example, in the case of isolation system NL20 for RT02 at the top floor of the rack, the smallest ratio is 1.11 (Cape Mendocino Earthquake) and the highest ratio can go up to 3.37 (Kobe Earthquake). Similarly, for the case of NL30 for RT03 the smallest ratio is observed for the Cape Mendocino Earthquake (0.91) and the highest ratio San Fernando Earthquake (1.92).

The efficacy of the equivalent linear modelling also varies depending on the isolation system. For example, as can be seen in Figure 4.33 (c) in the case of Kobe earthquake for RT02 at the top floor of the rack, the smallest peak displacement ratio is observed at isolation system NL20 (2.37) while the highest ratio at NL30 (3.35). Similarly, as shown in Figure 4.34 (f) for the case of superstition hill earthquake for RT03 the smallest peak displacement ratio is observed at isolation system NL20 (1.13) and the highest peak displacement ratio observed at isolation system NL30 (1.48).

In Figure 4.35 the average peak displacement ratio of the isolation system per earthquake is presented. The dependence of the response ratio on the rack period can be observed. While the highest ratio for RT01 is 1.32 (Northridge), RT02 is 2.81 (Kobe) and RT03 is 1.69 (San Fernando). Additionally, in Figure 4.36 the average peak displacement ration of the earthquakes per isolation system is presented. It can be observed that the response depends on the rack type (rack period) with RT02 exhibiting highest ratio followed by RT03 and finally RT01 as observed before in floor acceleration analysis.

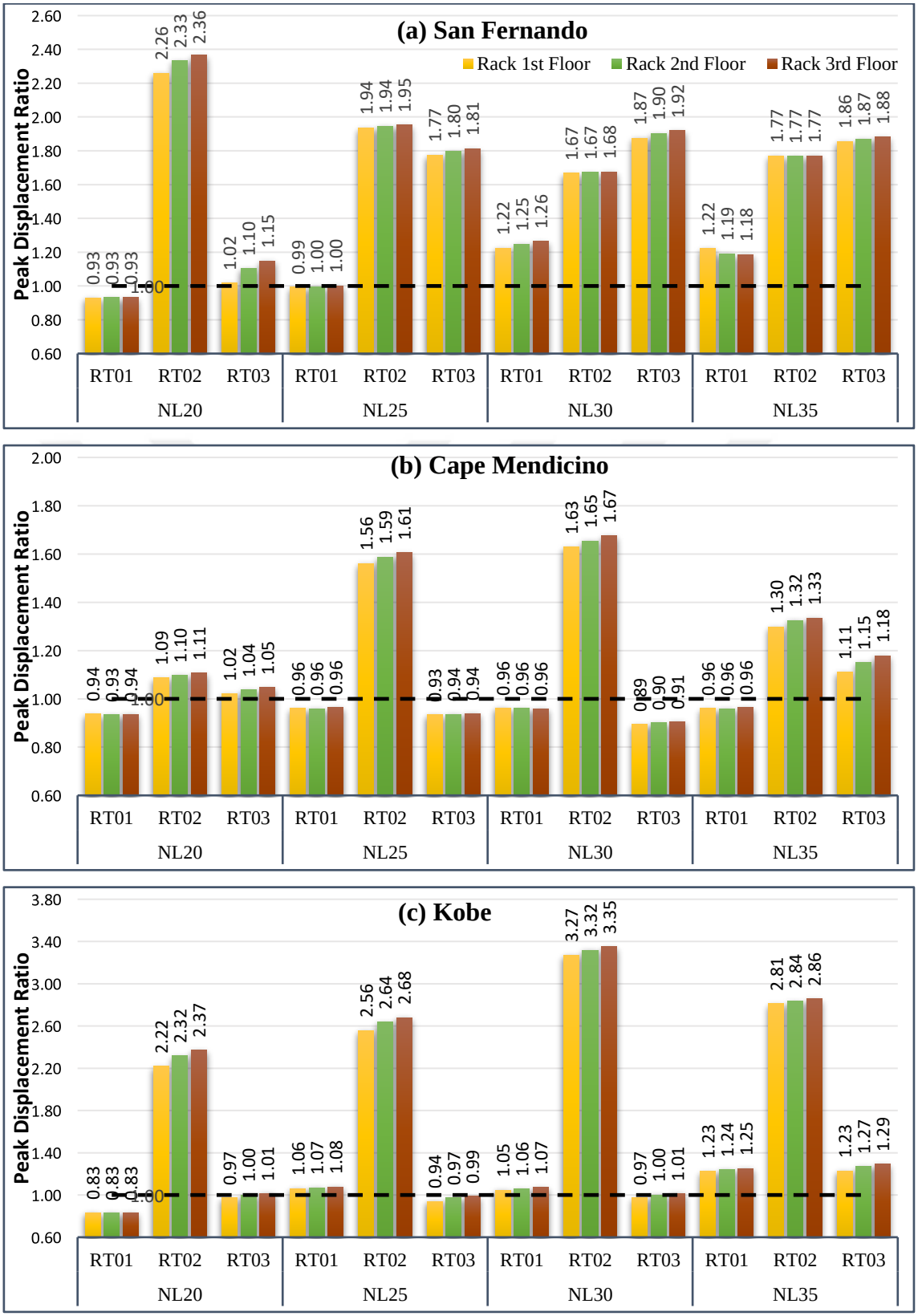

Figure 4.33: Peak displacement ratio for each earthquake per isolation system and per rack period

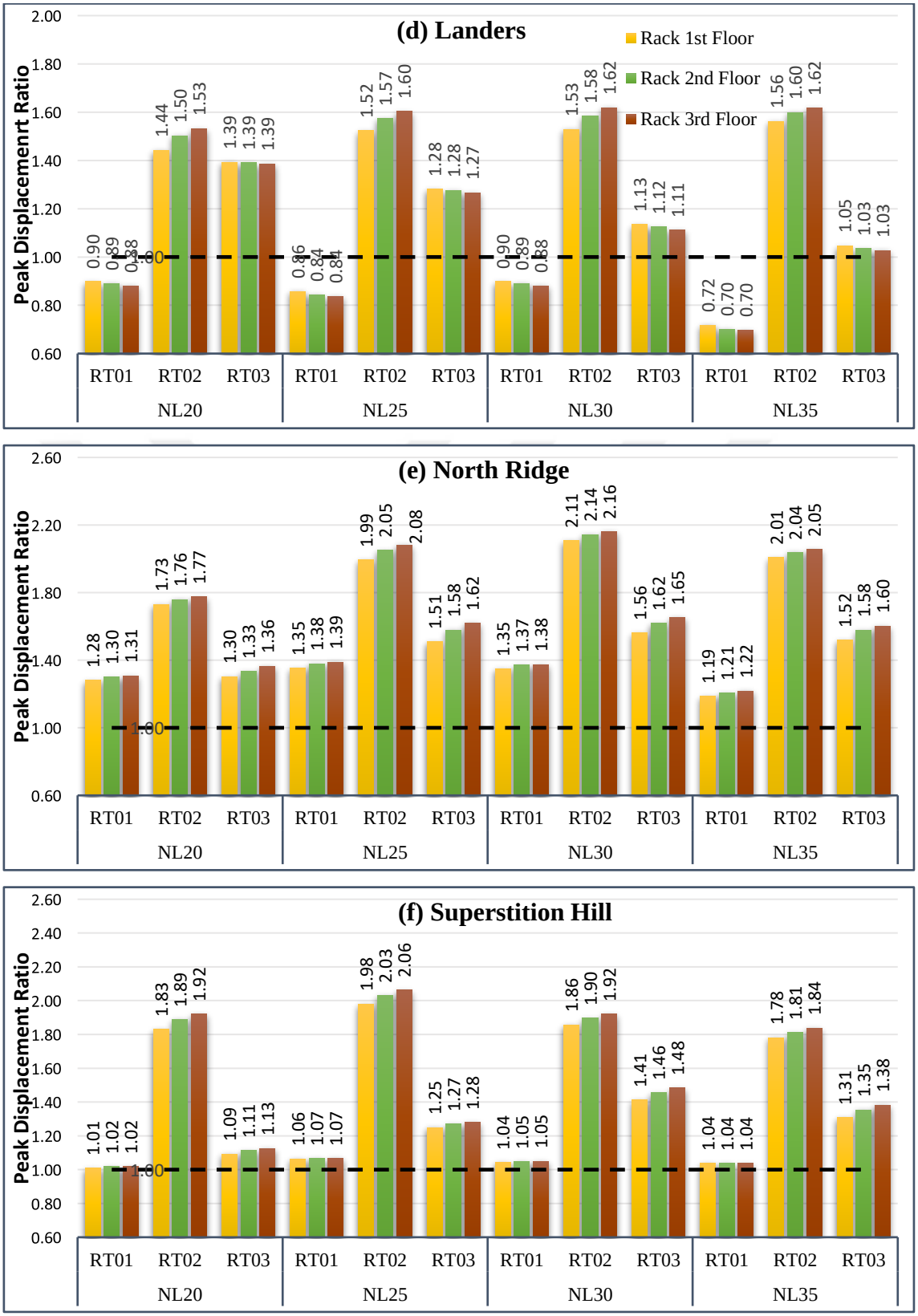

Figure 4.34: Peak displacement ratio for each earthquake per isolation system and per rack period

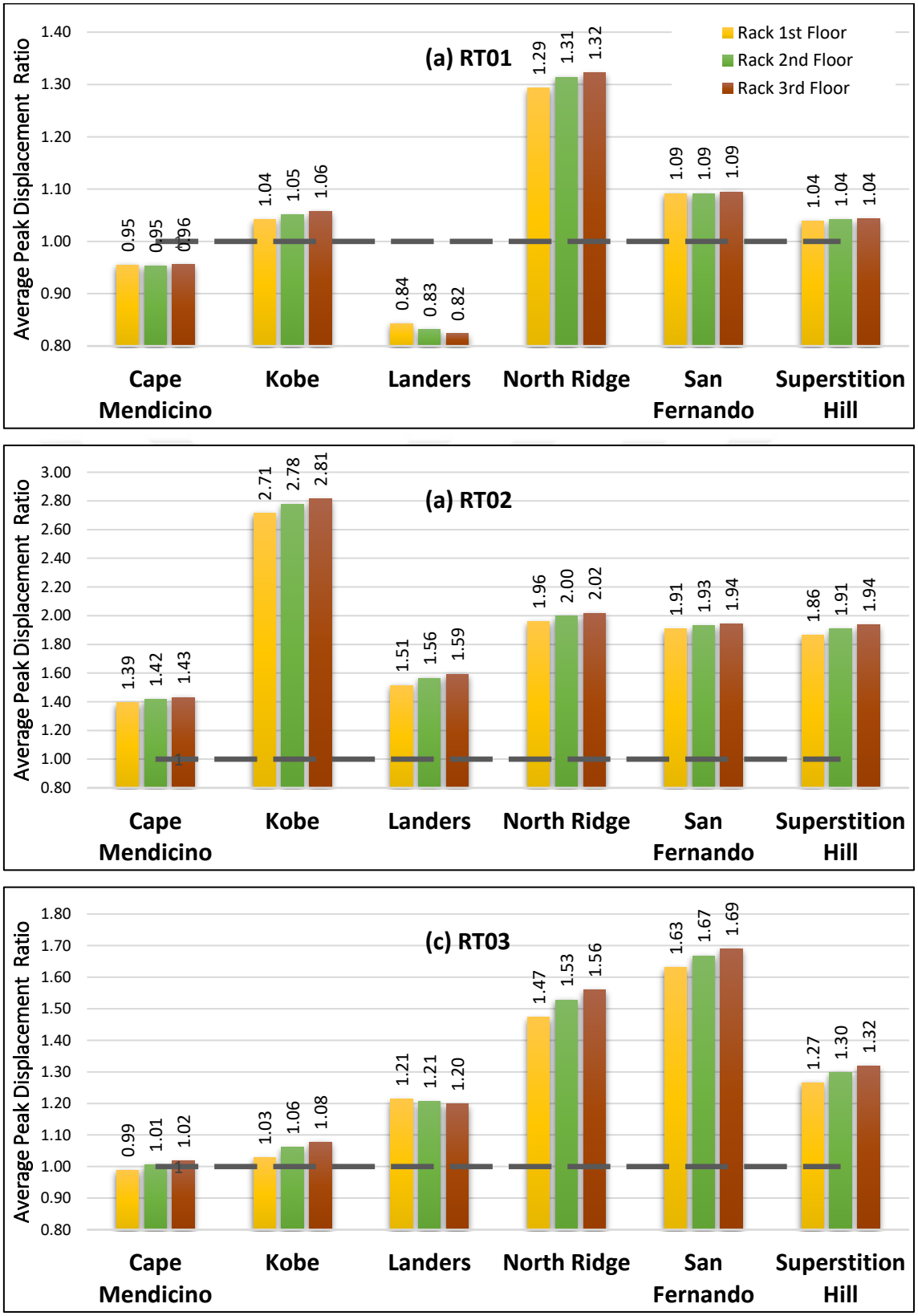

Figure 4.35: Average of peak displacement ratio for each earthquake per rack period

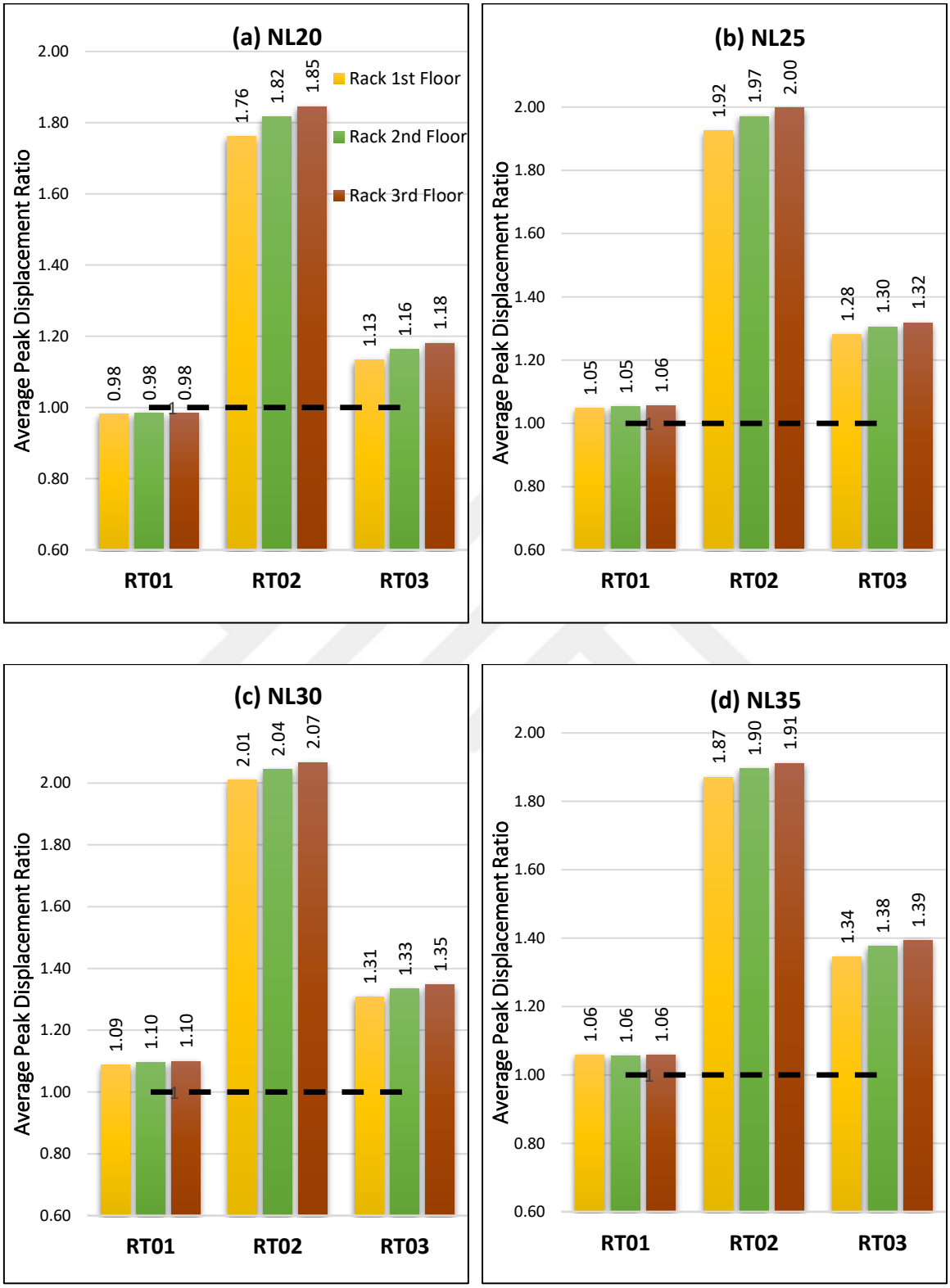

Figure 4.36: Average peak displacement ratio for each isolation system per rack period

4.2.3. RMS Rack Floor Displacement

In order to further understand the behaviour of floor displacement of the racks for both equivalent linear and nonlinear case, the nonlinear to equivalent linear RMS displacement ratio for all the racks under all isolation systems and for each earthquake is presented. To better visualize, a solid dashed line is drawn at 1.0 in each graph, to indicate a perfect estimate of equivalent linear modelling. Results below and above this line corresponds to conservative and unconservative estimates of the equivalent linear modelling, respectively.

To illustrate the earthquake-based change, nonlinear to equivalent linear floor displacement RMS ratio graphs for the all floors of the rack models are presented for all isolation systems. As can be observed from Figure 4.37 and Figure 4.38, the displacement RMS ratio is dependent on the type of earthquake loaded. The obtained displacement RMS ratio varies quantitatively for different earthquake. For example, in the case of isolation system NL30 for RT02 at the top floor of the rack, the smallest ratio is 1.78 (Cape Mendocino and Northridge earthquake) and the highest rate can go up to 3.46 (Kobe earthquake). Similarly, for the case of NL25 for RT03 the smallest ratio is observed for the superstition hill earthquake (1.06) and the highest ratio lander earthquake (1.70).

The efficacy of the equivalent linear modelling also varies depending on the isolation system. For example, as can be seen in Figure 4.37 (b) in the case of Cape Mendocino earthquake for RT02 at the top floor of the rack, the smallest displacement RMS ratio is observed at isolation system NL20 (1.35) while the highest ratio at NL30 (1.78). Similarly, as shown in Figure 4.38 (e) for the case of Northridge earthquake for RT03 the smallest displacement RMS ratio is observed at isolation system NL20 (1.06) and the highest displacement RMS ratio observed at isolation system NL30 and NL35 (1.52).

In Figure 4.39 the average displacement RMS ratio of the isolation system per earthquake is presented. The dependence of the response ratio on the rack period can be observed. While the highest ratio for RT01 and RT02 are Kobe (1.17 and 3.09 respectively) for RT03 is 1.53 (San Fernando). Additionally, in Figure 4.40 Figure 4.20 the average displacement RMS ratio of the earthquakes per isolation system is presented. It can be observed that the response depends on the rack type (rack period) with RT02 exhibiting highest ratio followed by RT03 and finally RT01.

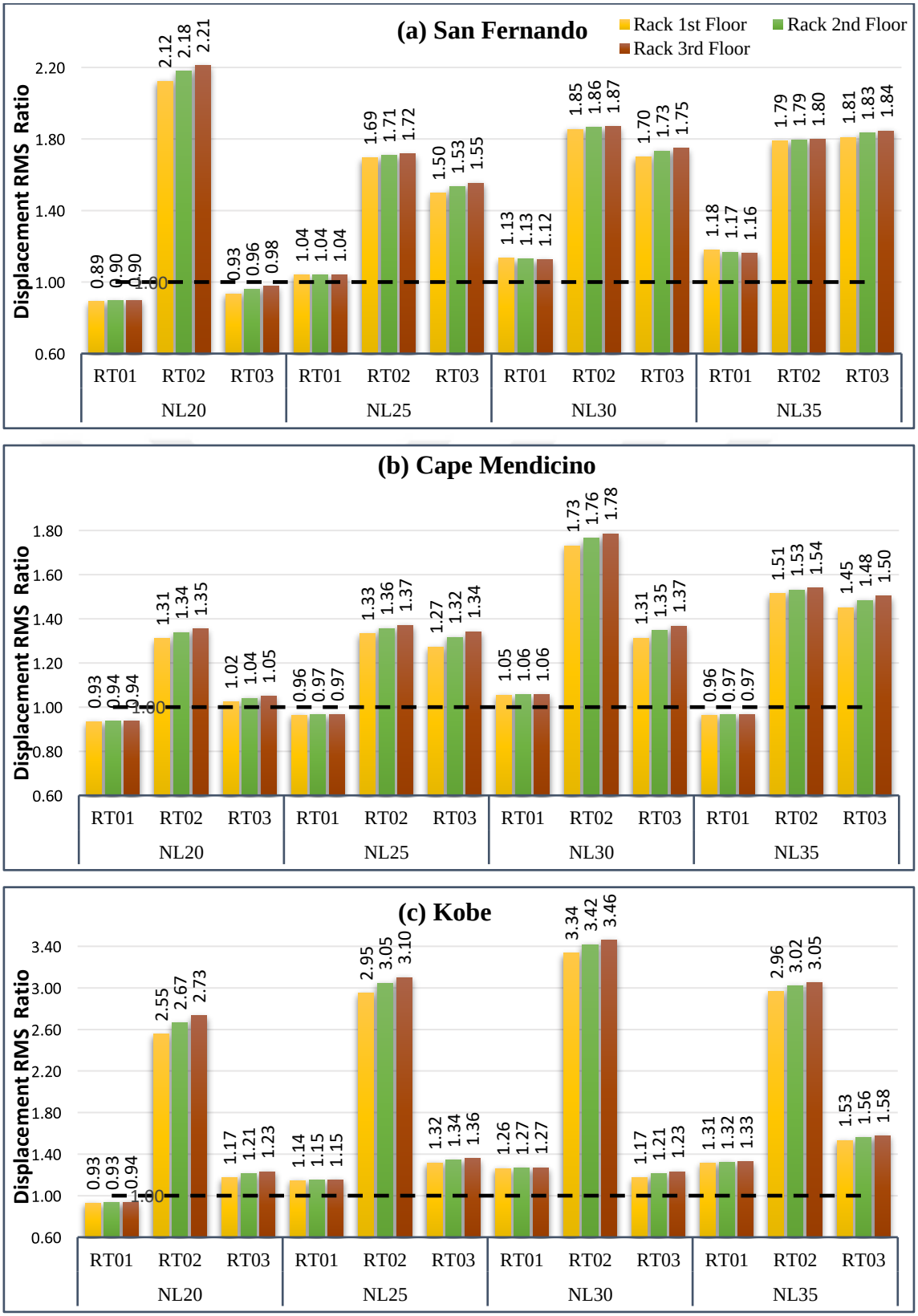

Figure 4.37: Displacement RMS ratio for each earthquake per isolation system and per rack period

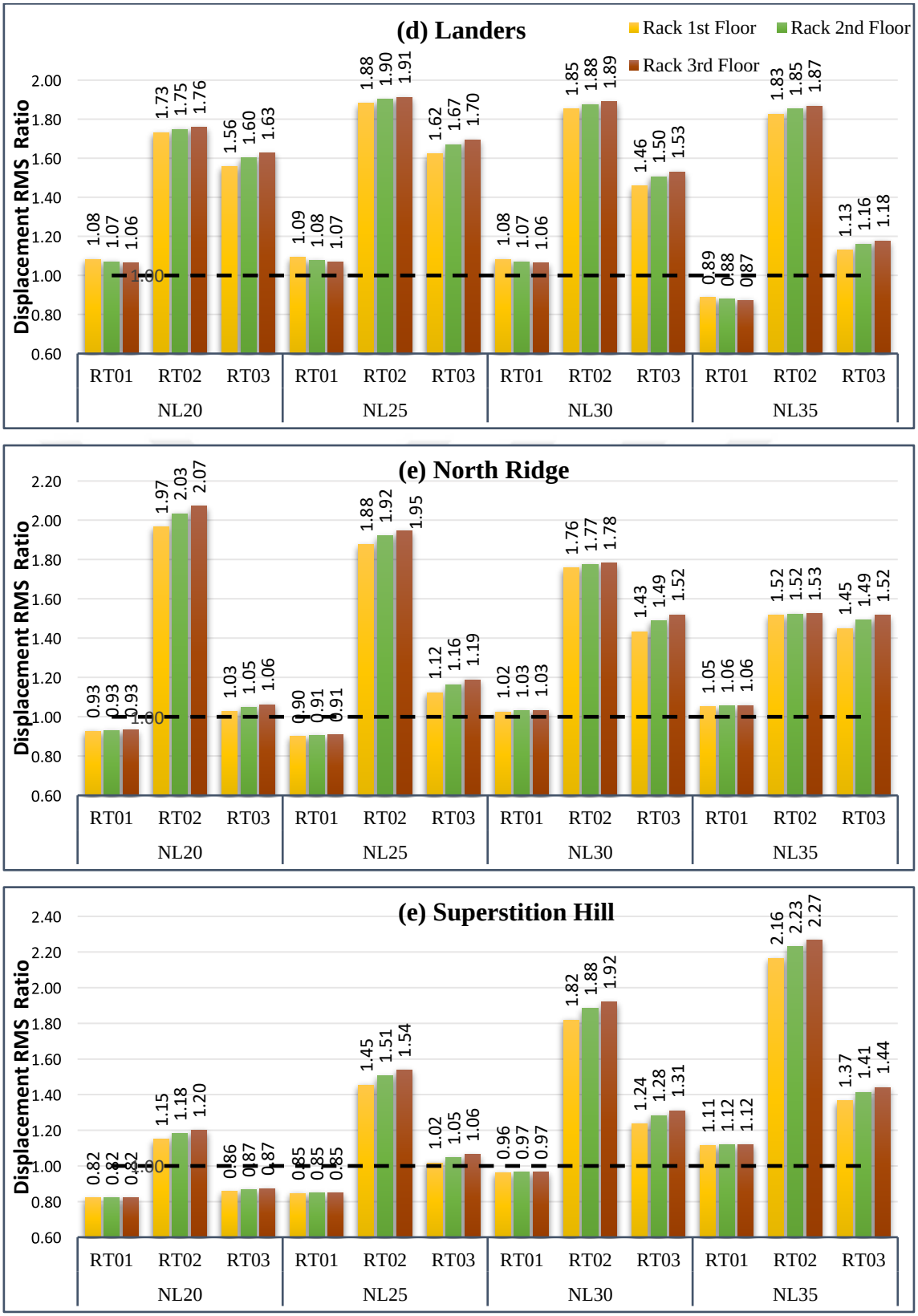

Figure 4.38: Displacement RMS ratio for each earthquake per isolation system and per rack period

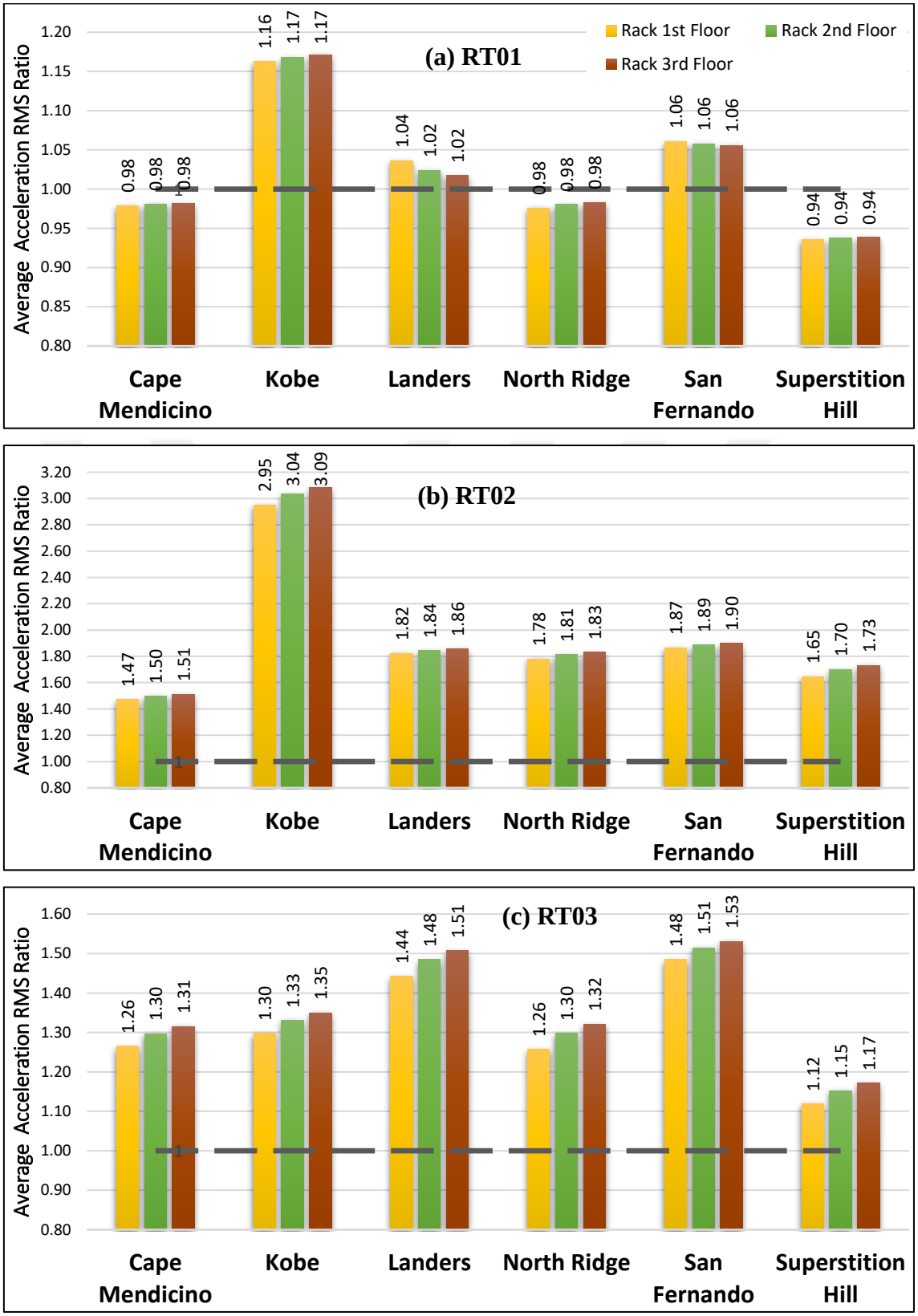

Figure 4.39: Average of displacement RMS ratio for each earthquake per rack period

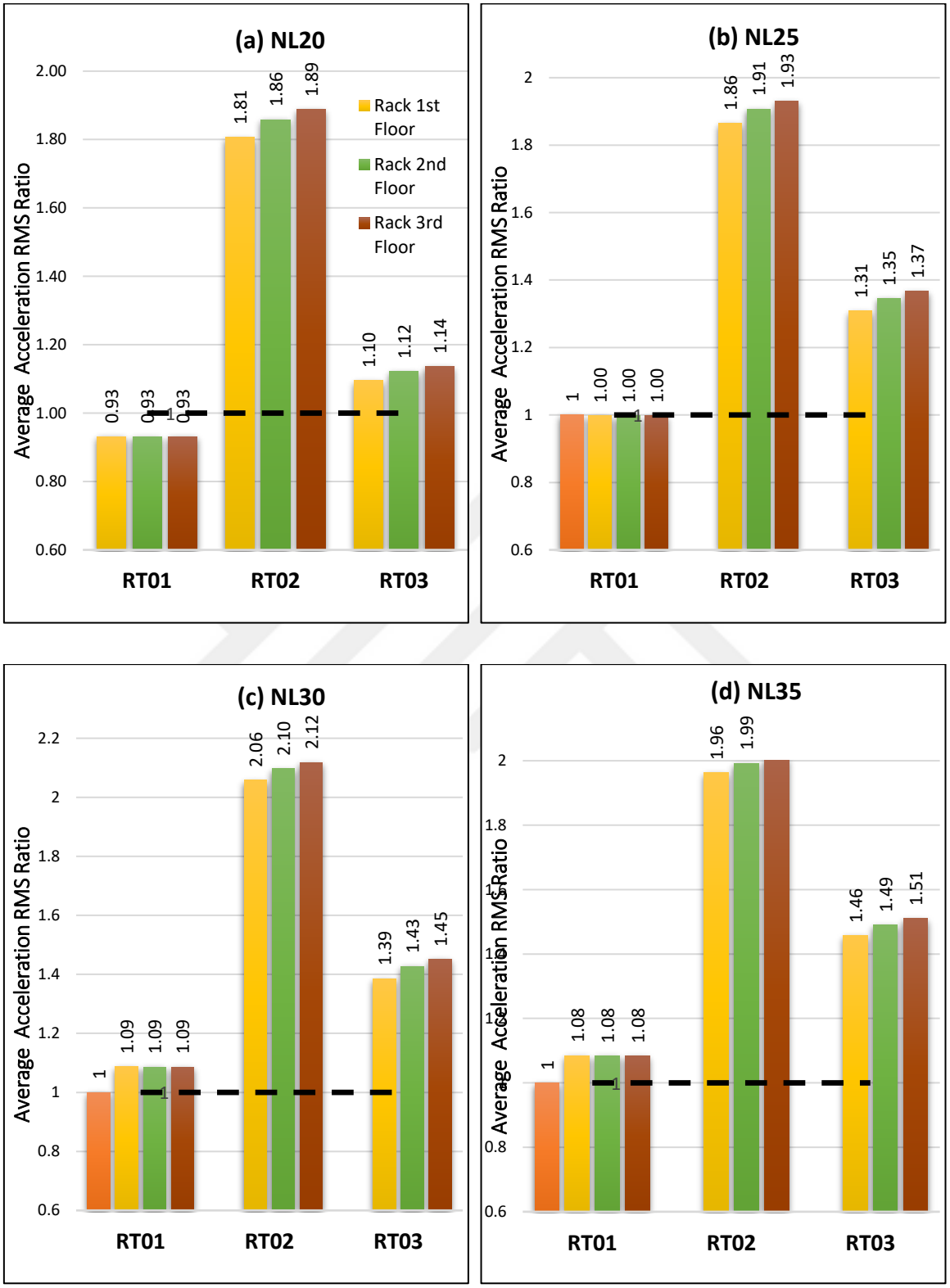

Figure 4.40: Average of displacement RMS ratio for each isolation system per rack period

4.3. AVERAGE OF ALL PARAMETERS

The average peak rack floor acceleration ratio, average RMS rack floor acceleration ratio, average peak rack floor displacement ratio and the average RMS rack floor displacement ratio for each rack floor is presented. The average values are calculated by averaging all results regardless of the isolation system type, earthquake record, or rack period. The aim is to understand how the equivalent linear modelling influence the response of the racks on average.

The base floor acceleration of the rack is the same as the floor acceleration of the isolated building on which the rack is placed. As can be seen from Figure 4.41 (a) while the ratio of the rack base is close to 1, the ratio of the second, third and fourth floors of the rack yield higher ratios of up to 1.44. This means equivalent linear modelling captures building response better and that there is little error, but for the response of the rack there is significantly high error. The same can be observed from the average RMS acceleration ratio as shown in Figure 4.41 (b) where the base of the rack ratio is 1.02 while the rack third floor ratio is as high as 1.58.

The plots discussed above give the average value of the peak floor acceleration ratio. This ratio can be higher depending on the type of earthquake, isolation system and rack period. In order to understand better we can refer to the peak floor acceleration ratio graphs of individual earthquakes and isolation systems discussed in previous sections. For instance, in Figure 4.13 (a) for racks placed on building with isolation system NL35 and under San Fernando earthquake it can be observed that the ratio increases depending on the floor of the rack and this ratio can be as high as 1.91.

The average displacement plots in Figure 4.41 (a) and (b) also shows similar behaviour. The displacement ratio again increases with increase in the floor of the rack. The higher rack floors have displacement of more than 1.40. As observed with acceleration, the displacement ratio also depends on the earthquake type, isolation type and the rack period. Figure 4.34 (e) shows how these parameters affect the displacement ratio. However, in general the rack base floor has a ratio of close to 1 while the higher floors show higher ratios that can go as high as 2.16 depending on the isolation type and the rack period.

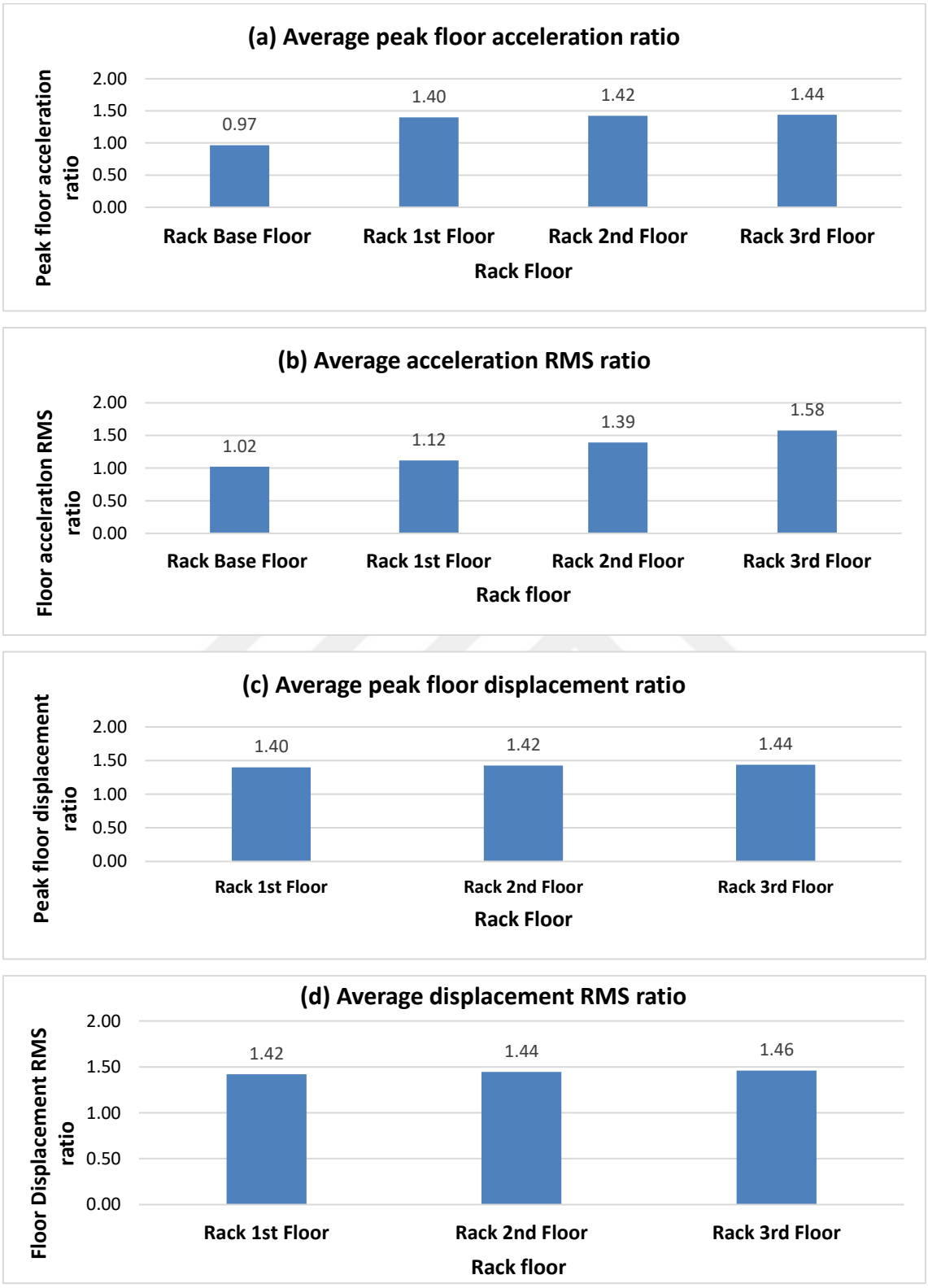

Figure 4.41: Average peak floor acceleration ratio, average rms acceleration ratio, average peak floor displacement ratio and the average rms floor displacement ratio of each rack floor.

5. CONCLUSION AND RECOMMENDATIONS

In this study the seismic response of critical equipment on a seismic isolated structure is investigated. The behaviour of isolators used in seismic isolation systems are nonlinear in nature. However, for the convenience of structural analysis, these isolators can be linearly modelled by obtaining equivalent linear properties with appropriate formulations. In previous studies it was observed that equivalent linear analysis underestimates the response of the structure. These studies focused on only the structure and not the content of the critical equipment located on racks housed in these structures. It was therefore necessary to investigate how the seismic responses of these rack floors change as a result of equivalent linear modelling of the isolators and equivalent linear analysis compared to nonlinear modelling and analysis.

For the purpose of this study, 6 historical near fault earthquakes obtained from PEER are used and time history analyses are conducted on a 3-story building with for 4 different isolation systems. The analyses are conducted using 3DBASIS and SAP2000. The time history response obtained at the top floor of the building is applied on racks of different periods and their responses are observed. Within the scope of the study, structural responses including rack floor acceleration and rack floor displacement are examined. Time history results, peak values and RMS values are included in the investigation.

Conclusions reached based on the results of the analyses conducted are summarized below:

1. The rack acceleration and displacement response results obtained for nonlinear modelling and analysis are generally higher than the results obtained for equivalent linear modelling and analysis. The degree of disparity varies and can be more than 3 times in some cases. Hence, equivalent linear analysis typically underestimates the rack response.
2. Although there is no clear tendency, the degree at which the equivalent linear analysis results defer from the nonlinear analysis depends on the earthquake characteristics as well as the type of isolation system.
3. The degree at which the equivalent linear analysis defers from the nonlinear analysis also depends on the rack period. When the rack period is low as it is for the case of RT01, the rack moves almost like a rigid body with the building itself, and the equivalent linear modelling is less erroneous. For the case of racks with higher periods (i.e. for more flexible racks) as for the case of RT02 and RT03 the discrepancy between equivalent linear analysis

and nonlinear analysis is higher. If the racks are fixed on the floor of the isolated building, they will be rigid and their response will be same with the building.

4. The effectiveness of equivalent linear analysis also depends on the rack floor. The higher floors of the rack typically exhibit higher disparity compared to the lower floors.
5. The displacement of a rack can be obtained with less error using equivalent linear modelling compared with acceleration which might contain more errors.
6. The equivalent linear modelling affects the contents (i.e. racks) of the isolated building more compared with the isolated building itself. Since the rack is placed on the floor of the isolated building, the rack base floor response is the same with the response of the building floor. Therefore, when the rack peak floor acceleration ratio and rack peak floor displacement ratio is compared for the base floor of the rack and other floors of the rack it is observed that the ratio is higher on upper floors of the rack while it is almost 1 for the rack base.
7. While equivalent linear modelling may be an appropriate tool for modelling and analysis of a building in the preliminary design stage, for the case of checking the rack response it may give highly erroneous results.

5.1. RECOMMENDATION FOR FUTURE WORK

This study should be repeated by taking care of friction-based isolation system because the change is more sudden. The high frequencies may affect the rack response even further.

REFERENCES

Alhan, C. and Ozgur, M. (2015) 'Seismic responses of base-isolated buildings: efficacy of equivalent linear modeling under near-fault earthquakes', *Smart Structures and Systems*, 15(6), pp. 1439–1461. doi: 10.12989/sss.2015.15.6.1439.

Alhan, C. and Özgür, M. (2015) 'Seismic responses of base-isolated buildings: Efficacy of equivalent linear modeling under near-fault earthquakes', *Smart Structures and Systems*. doi: 10.12989/sss.2015.15.6.1439.

Alhan, C. and Sürmeli, M. (2011) 'Shear building representations of seismically isolated buildings', *Bulletin of Earthquake Engineering*. doi: 10.1007/s10518-011-9293-z.

Cao, Y. *et al.* (2016) 'Effects of wave passage on torsional response of symmetric buildings subjected to near-fault pulse-like ground motions', *Soil Dynamics and Earthquake Engineering*. doi: 10.1016/j.soildyn.2016.04.001.

Chigira, M. *et al.* (2010) 'Landslides induced by the 2008 Wenchuan earthquake , Sichuan , China', *Geomorphology*. Elsevier B.V., 118(3–4), pp. 225–238. doi: 10.1016/j.geomorph.2010.01.003.

Chimamphant, S. and Kasai, K. (2016) 'Comparative response and performance of base-isolated and fixed-base structures', *Earthquake Engineering and Structural Dynamics*. doi: 10.1002/eqe.2612.

Clemente, P. and Martelli, A. (2019) 'Seismically isolated buildings in Italy: State-of-the-art review and applications', *Soil Dynamics and Earthquake Engineering*. doi: 10.1016/j.soildyn.2017.12.029.

Curadelli, O. (2013) 'Equivalent linear stochastic seismic analysis of cylindrical base-isolated liquid storage tanks', *Journal of Constructional Steel Research*. doi: 10.1016/j.jcsr.2012.12.022.

Dicleli, M. and Buddaram, S. (2007) 'Comprehensive evaluation of equivalent linear analysis method for seismic-isolated structures represented by sdof systems', *Engineering Structures*. doi: 10.1016/j.engstruct.2006.09.013.

Gandelli, E. *et al.* (2018) 'Seismic isolation retrofit of hospital buildings with focus on non-structural components', *Ingegneria Sismica*.

Garevski, M A (2012) ' Replacement of the Old Rubber Bearings of the First Base Isolated Building in the World', *15th World Conference on Earthquake Engineering (15WCEE)*.

Hu, J. W. (2015) 'Response of seismically isolated steel frame buildings with sustainable lead-rubber bearing (LRB) isolator devices subjected to near-fault (NF) ground motions', *Sustainability (Switzerland)*. doi: 10.3390/su7010111.

Kikuchi, M. and Aiken, I. D. (1997) 'An analytical hysteresis model for elastomeric seismic isolation bearings', *Earthquake Engineering and Structural Dynamics*. doi: 10.1002/(SICI)1096-9845(199702)26:2<215::AID-EQE640>3.0.CO;2-9.

Lee, J. H. and Song, J.-K. (2015) 'Comparison of Seismic Responses of Seismically Isolated NPP Containment Structures using Equivalent Linear- and Nonlinear-Lead-Rubber Bearing Modeling', *Journal of the Earthquake Engineering Society of Korea*. doi: 10.5000/eesk.2015.19.1.001.

Liu, T. *et al.* (2014) 'Evaluation of equivalent linearization analysis methods for seismically isolated buildings characterized by SDOF systems', *Engineering Structures*. doi: 10.1016/j.engstruct.2013.11.028.

Margesson, R. and Taft-Morales, M. (2011) 'Haiti earthquake: Crisis and response', in *Haiti: Earthquake and Response*.

Markou, A. A., Oliveto, G. and Athanasiou, A. (2016) 'Response simulation of hybrid base isolation systems under earthquake excitation', *Soil Dynamics and Earthquake Engineering*. doi: 10.1016/j.soildyn.2016.02.003.

Martelli, A. *et al.* (2014) 'Recent Development and Application of Seismic Isolation and Energy Dissipation and Conditions for Their Correct Use', *Geotechnical, Geological and Earthquake Engineering*. doi: 10.1007/978-3-319-07118-3_14.

Matsagar, V. A. and Jangid, R. S. (2004) 'Influence of isolator characteristics on the response of base-isolated structures', *Engineering Structures*, 26(12), pp. 1735–1749. doi:

10.1016/j.engstruct.2004.06.011.

Mavronicola, E. and Komodromos, P. (2011) 'Assessing the suitability of equivalent linear elastic analysis of seismically isolated multi-storey buildings', *Computers and Structures*. doi: 10.1016/j.compstruc.2011.05.010.

Mavronicola, E. and Komodromos, P. (2012) 'The effect of non-linear parameters on the modeling of multi-storey seismically isolated buildings', *the 15th World Conference on Earthquake Engineering Proceedings*.

Mayes, R. L., Brown, A. G. and Pietra, D. (2012) 'Using seismic isolation and energy dissipation to create earthquake-resilient buildings', in *Bulletin of the New Zealand Society for Earthquake Engineering*. doi: 10.5459/bnzsee.45.3.117-122.

Miranda, E. *et al.* (2012) 'Performance of nonstructural components during the 27 February 2010 Chile earthquake', *Earthquake Spectra*. doi: 10.1193/1.4000032.

Naeim, F. and Kelly, J. M. (1999) *Design of Seismic Isolated Structures, Design of Seismic Isolated Structures*. doi: 10.1002/9780470172742.

Nagarajaiah, S. and Erazo, K. (2016) 'Structural monitoring and identification of civil infrastructure in the United States', *Structural Monitoring and Maintenance*. doi: 10.12989/smm.2016.3.1.051.

Nagarajaiah, S., Reinhorn, A. M. and Constantinou, M. C. (1991) 'Nonlinear dynamic analysis of 3-D-base-isolated structures', *Journal of Structural Engineering (United States)*. doi: 10.1061/(ASCE)0733-9445(1991)117:7(2035).

Taghavi, S. and Miranda, E. (2003) *Response Assessment of Nonstructural Building Elements (PEER Report 2003/05), Report PEER 2003/05, Pacific Earthquake Engineering Research Center, University of California, Berkeley*.

Tena-Colunga, A. *et al.* (2015) 'Seismic isolation of buildings for power stations considering soil-structure interaction effects', *Journal of Building Engineering*. doi: 10.1016/j.jobe.2015.08.001.

Toopchi-Nezhad, H., Tait, M. J. and Drysdale, R. G. (2008) 'Lateral response evaluation of

fiber-reinforced neoprene seismic isolators utilized in an unbonded application', *Journal of Structural Engineering*. doi: 10.1061/(ASCE)0733-9445(2008)134:10(1627).

Turkington, D. H. *et al.* (1989) 'Seismic design of bridges on lead-rubber bearings', *Journal of Structural Engineering (United States)*. doi: 10.1061/(ASCE)0733-9445(1989)115:12(3000).

APPENDICES

Table 7.1: Peak point acceleration ratio of nonlinear to equivalent linear method for different isolation system period and rack models of different period

Earthquake Name	Isolation System Period	Rack Period	Rack Base Floor	Rack 1st Floor	Rack 2nd Floor	Rack 3rd Floor
Cape Mendocino	2	0.1	0.96	0.95	0.94	0.93
		0.2	0.96	0.93	1.05	1.21
		0.3	0.96	0.94	1.03	1.02
	2.5	0.1	0.95	0.97	0.96	0.95
		0.2	0.95	1.13	1.48	1.78
		0.3	0.95	0.94	0.94	0.97
	3	0.1	0.95	0.96	0.96	0.94
		0.2	0.95	1.14	1.54	1.87
		0.3	0.95	0.93	0.90	1.04
	3.5	0.1	0.90	0.91	0.91	0.91
		0.2	0.90	0.99	1.23	1.50
		0.3	0.90	0.93	1.10	1.30
Kobe	2	0.1	0.83	0.84	0.83	0.83
		0.2	0.83	1.06	1.97	3.01
		0.3	0.83	0.89	0.99	1.09
	2.5	0.1	0.92	1.01	1.07	1.10
		0.2	0.92	1.41	2.35	3.20
		0.3	0.92	0.90	0.97	1.09
	3	0.1	0.86	0.98	1.05	1.13
		0.2	0.86	1.66	3.00	3.59
		0.3	0.86	0.97	1.07	1.20
	3.5	0.1	0.97	1.14	1.24	1.30
		0.2	0.97	1.66	2.73	3.01
		0.3	0.97	1.01	1.25	1.39
Landers	2	0.1	1.06	0.98	0.89	0.85
		0.2	1.06	1.00	1.31	1.79
		0.3	1.06	1.35	1.42	1.37
	2.5	0.1	1.05	0.94	0.85	0.81
		0.2	1.05	1.05	1.37	1.72
		0.3	1.05	1.27	1.32	1.26
	3	0.1	0.97	0.86	0.77	0.72
		0.2	0.97	1.09	1.38	1.74
		0.3	0.97	1.11	1.17	1.07

	3.5	0.1	0.89	0.80	0.71	0.67
		0.2	0.89	1.07	1.46	1.73
		0.3	0.89	1.00	1.08	1.00
North Ridge	2	0.1	1.07	1.17	1.30	1.37
		0.2	1.07	1.27	1.64	2.07
		0.3	1.07	1.21	1.33	1.56
	2.5	0.1	1.10	1.22	1.37	1.46
		0.2	1.10	1.39	1.86	2.45
		0.3	1.10	1.28	1.51	1.82
	3	0.1	1.05	1.21	1.36	1.44
		0.2	1.05	1.45	2.00	2.36
		0.3	1.05	1.23	1.56	1.83
	3.5	0.1	0.90	1.05	1.20	1.27
		0.2	0.90	1.42	1.94	2.20
		0.3	0.90	1.13	1.63	1.71
San Fernando	2	0.1	0.89	0.92	0.93	0.95
		0.2	0.89	1.14	2.04	2.55
		0.3	0.89	0.90	1.08	1.41
	2.5	0.1	0.90	0.97	1.00	1.01
		0.2	0.90	1.21	1.89	2.01
		0.3	0.90	1.00	1.73	1.94
	3	0.1	0.91	1.05	1.24	1.19
		0.2	0.91	1.50	1.64	1.72
		0.3	0.91	1.43	1.86	2.01
	3.5	0.1	0.96	1.15	1.21	1.11
		0.2	0.96	1.64	1.78	1.78
		0.3	0.96	1.47	1.84	1.91
Superstition Hill	2	0.1	0.99	1.00	1.02	1.03
		0.2	0.99	1.21	1.70	2.32
		0.3	0.99	0.98	1.10	1.20
	2.5	0.1	1.04	1.05	1.07	1.07
		0.2	1.04	1.25	1.83	2.47
		0.3	1.04	1.10	1.27	1.40
	3	0.1	1.04	1.03	1.04	1.05
		0.2	1.04	1.26	1.74	2.22
		0.3	1.04	1.17	1.41	1.63
	3.5	0.1	1.05	1.05	1.04	1.03
		0.2	1.05	1.26	1.68	2.09
		0.3	1.05	1.10	1.30	1.51

Table 7.2: Average peak acceleration ratios per earthquake for different racks of periods 0.1, 0.2 and 0.3

Rack Period	Earthquake Name	Rack Base Floor	Rack 1st Floor	Rack 2nd Floor	Rack 3rd Floor
0.1	Cape Mendocino	0.94	0.95	0.94	0.93
	Kobe	0.90	0.99	1.05	1.09
	Landers	0.99	0.90	0.81	0.76
	North Ridge	1.03	1.16	1.31	1.38
	San Fernando	0.91	1.02	1.09	1.07
	Superstition Hill	1.03	1.03	1.04	1.05
0.2	Cape Mendocino	0.94	1.05	1.33	1.59
	Kobe	0.90	1.45	2.51	3.20
	Landers	0.99	1.05	1.38	1.75
	North Ridge	1.03	1.38	1.86	2.27
	San Fernando	0.91	1.37	1.84	2.01
	Superstition Hill	1.03	1.24	1.74	2.28
0.3	Cape Mendocino	0.94	0.93	0.99	1.08
	Kobe	0.90	0.94	1.07	1.19
	Landers	0.99	1.18	1.25	1.17
	North Ridge	1.03	1.21	1.51	1.73
	San Fernando	0.91	1.20	1.63	1.82
	Superstition Hill	1.03	1.09	1.27	1.43

Table 7.3: Average peak acceleration ratio per isolation system for different racks of periods 0.1, 0.2 and 0.3

Isolation System	Rack Period	Rack Base Floor	Rack 1st Floor	Rack 2nd Floor	Rack 3rd Floor
	0.1	0.97	0.98	0.98	0.99
2.00	0.2	0.97	1.10	1.62	2.16
	0.3	0.97	1.04	1.16	1.27
	0.1	0.99	1.03	1.05	1.07
2.50	0.2	0.99	1.24	1.80	2.27
	0.3	0.99	1.08	1.29	1.41
	0.1	0.96	1.02	1.07	1.08
3.00	0.2	0.96	1.35	1.88	2.25
	0.3	0.96	1.14	1.33	1.46
	0.1	0.94	1.01	1.05	1.05
3.50	0.2	0.94	1.34	1.80	2.05
	0.3	0.94	1.11	1.37	1.47

Table 7.4: Acceleration RMS ratio of nonlinear to equivalent linear method for different isolation system period and rack models of different period**.**

Earthquake Name	Isolation System Period		Rack Base Floor	Rack 1st Floor	Rack 2nd Floor	Rack 3rd Floor
Cape Mendocino	2	0.1	0.92	0.93	0.94	0.94
		0.2	0.92	0.98	1.24	1.53
		0.3	0.92	0.94	1.03	1.11
	2.5	0.1	0.94	0.95	0.97	0.98
		0.2	0.94	1.01	1.27	1.51
		0.3	0.94	1.03	1.30	1.49
	3	0.1	1.04	1.05	1.06	1.06
		0.2	1.04	1.16	1.63	1.98
		0.3	1.04	1.11	1.33	1.47
	3.5	0.1	1.13	1.13	1.12	1.11
		0.2	1.13	1.20	1.46	1.62
		0.3	1.13	1.22	1.47	1.60
Kobe	2	0.1	0.90	0.91	0.93	0.95
		0.2	0.90	1.14	2.25	3.48
		0.3	0.90	0.97	1.20	1.36
	2.5	0.1	1.10	1.12	1.15	1.17
		0.2	1.10	1.44	2.67	3.66
		0.3	1.10	1.15	1.33	1.44
	3	0.1	1.20	1.23	1.27	1.29
		0.2	1.20	1.72	3.09	3.89
		0.3	1.20	1.25	1.49	1.61
	3.5	0.1	1.25	1.28	1.32	1.35
		0.2	1.25	1.71	2.79	3.33
		0.3	1.25	1.30	1.55	1.66
Landers	2	0.1	1.15	1.14	1.07	1.03
		0.2	1.15	1.30	1.67	1.84
		0.3	1.15	1.24	1.57	1.71
	2.5	0.1	1.20	1.17	1.08	1.02
		0.2	1.20	1.39	1.82	2.00
		0.3	1.20	1.27	1.63	1.76
	3	0.1	1.07	1.05	0.99	0.94
		0.2	1.07	1.28	1.78	2.00
		0.3	1.07	1.13	1.46	1.61
	3.5	0.1	0.94	0.93	0.88	0.84
		0.2	0.94	1.18	1.74	2.00
		0.3	0.94	0.94	1.13	1.23

North Ridge	2	0.1	0.90	0.91	0.93	0.94
		0.2	0.90	1.06	1.78	2.48
		0.3	0.90	0.93	1.04	1.15
	2.5	0.1	0.86	0.87	0.90	0.93
		0.2	0.86	1.06	1.74	2.19
		0.3	0.86	0.91	1.15	1.33
	3	0.1	0.97	1.00	1.03	1.05
		0.2	0.97	1.24	1.70	1.86
		0.3	0.97	1.07	1.46	1.67
	3.5	0.1	1.01	1.03	1.05	1.07
		0.2	1.01	1.24	1.50	1.55
		0.3	1.01	1.11	1.47	1.62
San Fernando	2	0.1	0.84	0.86	0.89	0.91
		0.2	0.84	1.15	1.96	2.53
		0.3	0.84	0.83	0.95	1.07
	2.5	0.1	1.02	1.04	1.04	1.03
		0.2	1.02	1.26	1.65	1.78
		0.3	1.02	1.16	1.52	1.64
	3	0.1	1.14	1.15	1.13	1.10
		0.2	1.14	1.47	1.82	1.91
		0.3	1.14	1.33	1.71	1.81
	3.5	0.1	1.22	1.22	1.17	1.13
		0.2	1.22	1.52	1.77	1.82
		0.3	1.22	1.46	1.82	1.88
Superstition Hill	2	0.1	0.81	0.82	0.82	0.82
		0.2	0.81	0.85	1.07	1.45
		0.3	0.81	0.82	0.86	0.91
	2.5	0.1	0.84	0.84	0.85	0.85
		0.2	0.84	0.91	1.32	1.94
		0.3	0.84	0.88	1.03	1.18
	3	0.1	0.94	0.95	0.96	0.97
		0.2	0.94	1.07	1.64	2.37
		0.3	0.94	1.01	1.26	1.48
	3.5	0.1	1.08	1.10	1.12	1.13
		0.2	1.08	1.27	1.98	2.67
		0.3	1.08	1.14	1.39	1.61

Table 7.5: Average Acceleration RMS Ratios Per Earthquake for different Racks of Periods 0.1, 0.2 and 0.3

Rack Period	Earthquake Name	Rack Base Floor	Rack 1st Floor	Rack 2nd Floor	Rack 3rd Floor
0.1	Cape Mendocino	0.92	0.93	0.93	0.93
	Kobe	0.92	1.08	1.66	2.22
	Landers	0.92	0.95	1.11	1.22
	North Ridge	0.99	1.00	1.00	1.00
	San Fernando	0.99	1.18	1.74	2.18
	Superstition Hill	0.99	1.07	1.33	1.47
0.2	Cape Mendocino	1.06	1.07	1.07	1.07
	Kobe	1.06	1.32	1.94	2.33
	Landers	1.06	1.15	1.45	1.61
	North Ridge	1.10	1.12	1.11	1.10
	San Fernando	1.10	1.35	1.87	2.17
	Superstition Hill	1.10	1.19	1.47	1.60
0.3	Cape Mendocino	0.92	0.93	0.93	0.93
	Kobe	0.92	1.08	1.66	2.22
	Landers	0.92	0.95	1.11	1.22
	North Ridge	0.99	1.00	1.00	1.00
	San Fernando	0.99	1.18	1.74	2.18
	Superstition Hill	0.99	1.07	1.33	1.47

Table 7.6: Average acceleration RMS ratio per Isolation System for different Racks of Periods 0.1, 0.2 and 0.3

Isolation System	Rack Period	Rack Base Floor	Rack 1st Floor	Rack 2nd Floor	Rack 3rd Floor
	1.01	1.01	1.02	1.02	1.01
2.00	1.11	1.13	1.17	1.19	1.11
	1.09	1.07	1.01	0.96	1.09
	0.94	0.95	0.98	1.00	0.94
2.50	1.06	1.07	1.06	1.04	1.06
	0.92	0.93	0.94	0.95	0.92
	1.01	1.09	1.40	1.66	1.01
3.00	1.11	1.50	2.70	3.59	1.11
	1.09	1.29	1.75	1.96	1.09
	0.94	1.15	1.68	2.02	0.94
3.50	1.06	1.35	1.80	2.01	1.06
	0.92	1.02	1.50	2.11	0.92

Table 7.7: Average peak displacement ratios per earthquake for different racks of periods 0.1, 0.2 and 0.3

Rack Period	Earthquake Name	Rack 1st Floor	Rack 2nd Floor	Rack 3rd Floor
0.1	Cape Mendocino	0.95	0.95	0.96
	Kobe	1.04	1.05	1.06
	Landers	0.84	0.83	0.82
	North Ridge	1.29	1.31	1.32
	San Fernando	1.09	1.09	1.09
	Superstition Hill	1.04	1.04	1.04
0.2	Cape Mendocino	1.39	1.42	1.43
	Kobe	2.71	2.78	2.81
	Landers	1.51	1.56	1.59
	North Ridge	1.96	2.00	2.02
	San Fernando	1.91	1.93	1.94
	Superstition Hill	1.86	1.91	1.94
0.3	Cape Mendocino	0.99	1.01	1.02
	Kobe	1.03	1.06	1.08
	Landers	1.21	1.21	1.20
	North Ridge	1.47	1.53	1.56
	San Fernando	1.63	1.67	1.69
	Superstition Hill	1.27	1.30	1.32

Table 7.8: Average peak displacement ratio per Isolation system for different racks of Periods 0.1, 0.2 and 0.3

Isolation System	Rack Period	Rack 1st Floor	Rack 2nd Floor	Rack 3rd Floor
	0.1	0.98	0.98	0.98
2.00	0.2	1.76	1.82	1.85
	0.3	1.13	1.16	1.18
	0.1	1.05	1.05	1.06
2.50	0.2	1.92	1.97	2.00
	0.3	1.28	1.30	1.32
	0.1	1.09	1.10	1.10
3.00	0.2	2.01	2.04	2.07
	0.3	1.31	1.33	1.35
	0.1	1.06	1.06	1.06
3.50	0.2	1.87	1.90	1.91
	0.3	1.34	1.38	1.39

Table 7.9: Peak point displacement ratio of nonlinear to equivalent linear method for different isolation system period and rack models of different period

Earthquake Name	Isolation System Period	Rack Period	Rack 1st Floor	Rack 2nd Floor	Rack 3rd Floor
Cape Mendocino	2	0.1	0.94	0.93	0.94
		0.2	1.09	1.10	1.11
		0.3	1.02	1.04	1.05
	2.5	0.1	0.96	0.96	0.96
		0.2	1.56	1.59	1.61
		0.3	0.93	0.94	0.94
	3	0.1	0.96	0.96	0.96
		0.2	1.63	1.65	1.67
		0.3	0.89	0.90	0.91
	3.5	0.1	0.96	0.96	0.96
		0.2	1.30	1.32	1.33
		0.3	1.11	1.15	1.18
Kobe	2	0.1	0.83	0.83	0.83
		0.2	2.22	2.32	2.37
		0.3	0.97	1.00	1.01
	2.5	0.1	1.06	1.07	1.08
		0.2	2.56	2.64	2.68
		0.3	0.94	0.97	0.99
	3	0.1	1.05	1.06	1.07
		0.2	3.27	3.32	3.35
		0.3	0.97	1.00	1.01
	3.5	0.1	1.23	1.24	1.25
		0.2	2.81	2.84	2.86
		0.3	1.23	1.27	1.29
Landers	2	0.1	0.90	0.89	0.88
		0.2	1.44	1.50	1.53
		0.3	1.39	1.39	1.39
	2.5	0.1	0.86	0.84	0.84
		0.2	1.52	1.57	1.60
		0.3	1.28	1.28	1.27
	3	0.1	0.90	0.89	0.88
		0.2	1.53	1.58	1.62
		0.3	1.13	1.12	1.11
	3.5	0.1	0.72	0.70	0.70
		0.2	1.56	1.60	1.62
		0.3	1.05	1.03	1.03

North Ridge	2	0.1	1.28	1.30	1.31
		0.2	1.73	1.76	1.77
		0.3	1.30	1.33	1.36
	2.5	0.1	1.35	1.38	1.39
		0.2	1.99	2.05	2.08
		0.3	1.51	1.58	1.62
	3	0.1	1.35	1.37	1.38
		0.2	2.11	2.14	2.16
		0.3	1.56	1.62	1.65
	3.5	0.1	1.19	1.21	1.22
		0.2	2.01	2.04	2.05
		0.3	1.52	1.58	1.60
San Fernando	2	0.1	0.93	0.93	0.93
		0.2	2.26	2.33	2.36
		0.3	1.02	1.10	1.15
	2.5	0.1	0.99	1.00	1.00
		0.2	1.94	1.94	1.95
		0.3	1.77	1.80	1.81
	3	0.1	1.22	1.25	1.26
		0.2	1.67	1.67	1.68
		0.3	1.87	1.90	1.92
	3.5	0.1	1.22	1.19	1.18
		0.2	1.77	1.77	1.77
		0.3	1.86	1.87	1.88
Superstition Hill	2	0.1	1.01	1.02	1.02
		0.2	1.83	1.89	1.92
		0.3	1.09	1.11	1.13
	2.5	0.1	1.06	1.07	1.07
		0.2	1.98	2.03	2.06
		0.3	1.25	1.27	1.28
	3	0.1	1.04	1.05	1.05
		0.2	1.86	1.90	1.92
		0.3	1.41	1.46	1.48
	3.5	0.1	1.04	1.04	1.04
		0.2	1.78	1.81	1.84
		0.3	1.31	1.35	1.38

Table 7.10: Displacement RMS ratio of nonlinear to equivalent linear method for different isolation system period and rack models of different period

Earthquake Name	Isolation System Period	Rack Period	Rack 1st Floor	Rack 2nd Floor	Rack 3rd Floor
Cape Mendocino	2	0.1	0.93	0.94	0.94
		0.2	1.31	1.34	1.35
		0.3	1.02	1.04	1.05
	2.5	0.1	0.96	0.97	0.97
		0.2	1.33	1.36	1.37
		0.3	1.27	1.32	1.34
	3	0.1	1.05	1.06	1.06
		0.2	1.73	1.76	1.78
		0.3	1.31	1.35	1.37
	3.5	0.1	0.96	0.97	0.97
		0.2	1.51	1.53	1.54
		0.3	1.45	1.48	1.50
Kobe	2	0.1	0.93	0.93	0.94
		0.2	2.55	2.67	2.73
		0.3	1.17	1.21	1.23
	2.5	0.1	1.14	1.15	1.15
		0.2	2.95	3.05	3.10
		0.3	1.32	1.34	1.36
	3	0.1	1.26	1.27	1.27
		0.2	3.34	3.42	3.46
		0.3	1.17	1.21	1.23
	3.5	0.1	1.31	1.32	1.33
		0.2	2.96	3.02	3.05
		0.3	1.53	1.56	1.58
Landers	2	0.1	1.08	1.07	1.06
		0.2	1.73	1.75	1.76
		0.3	1.56	1.60	1.63
	2.5	0.1	1.09	1.08	1.07
		0.2	1.88	1.90	1.91
		0.3	1.62	1.67	1.70
	3	0.1	1.08	1.07	1.06
		0.2	1.85	1.88	1.89
		0.3	1.46	1.50	1.53
	3.5	0.1	0.89	0.88	0.87
		0.2	1.83	1.85	1.87
		0.3	1.13	1.16	1.18

North Ridge	2	0.1	0.93	0.93	0.93
		0.2	1.97	2.03	2.07
		0.3	1.03	1.05	1.06
	2.5	0.1	0.90	0.91	0.91
		0.2	1.88	1.92	1.95
		0.3	1.12	1.16	1.19
	3	0.1	1.02	1.03	1.03
		0.2	1.76	1.77	1.78
		0.3	1.43	1.49	1.52
	3.5	0.1	1.05	1.06	1.06
		0.2	1.52	1.52	1.53
		0.3	1.45	1.49	1.52
San Fernando	2	0.1	0.89	0.90	0.90
		0.2	2.12	2.18	2.21
		0.3	0.93	0.96	0.98
	2.5	0.1	1.04	1.04	1.04
		0.2	1.69	1.71	1.72
		0.3	1.50	1.53	1.55
	3	0.1	1.13	1.13	1.12
		0.2	1.85	1.86	1.87
		0.3	1.70	1.73	1.75
	3.5	0.1	1.18	1.17	1.16
		0.2	1.79	1.79	1.80
		0.3	1.81	1.83	1.84
Superstition Hill	2	0.1	0.82	0.82	0.82
		0.2	1.15	1.18	1.20
		0.3	0.86	0.87	0.87
	2.5	0.1	0.85	0.85	0.85
		0.2	1.45	1.51	1.54
		0.3	1.02	1.05	1.06
	3	0.1	0.96	0.97	0.97
		0.2	1.82	1.88	1.92
		0.3	1.24	1.28	1.31
	3.5	0.1	1.11	1.12	1.12
		0.2	2.16	2.23	2.27
		0.3	1.37	1.41	1.44